**NDOT Research Report**

**Report No: RDT06-005**

# Evaluation of Strategies to Control Erosion along U.S. Highway 50 between Carson City and Lake Tahoe

**February 2006**

Prepared by Research Division
Nevada Department of Transportation
1263 South Stewart Street
Carson City, Nevada 89712

This work was sponsored by the Nevada Department of Transportation. The contents of this report reflect the views of the authors, who are responsible for the facts and the accuracy of the data presented herein. The contents do not necessarily reflect the official views or policies of the State of Nevada at the time of publication. This report does not constitute a standard, specification, or regulation.

## ABSTRACT

Severe erosion is occurring at several locations in the Clear Creek watershed along U.S. Highway 50 between Carson City and Lake Tahoe. Surface water runoff from seasonal snowmelt or infrequent high intensity rain events has caused erosion and the transport of substantial quantities of soil and sediment. Erosion has caused problems related to slope stability along roadways and increased maintenance requirements, especially those associated with drainage structures. The physical characteristics of the upper Clear Creek watershed including steep slopes, thin soil sections, and highly weathered bedrock allows for erosion to proceed unchecked. The erosion has manifested itself in the form of deep gullies and rilled slopes.

Corrective action must be taken to limit the erosion of soil and transport of sediment during runoff events. The Hydraulics Section of the Nevada Department of Transportation (NDOT) has committed significant funding over the next several years to implement erosion control strategies. Numerous erosion control products are commercially available. However, the effectiveness and suitability of these products is often difficult to predict. This research project investigated just some of the many erosion control strategies for channel protection. A combination of laboratory flume studies and field studies were conducted to assess the performance of potential rolled erosion control products (RECPs).

In laboratory flume studies, several RECPs were found to be effective in reducing erosion over granular bare soil. The RECPs reduced the quantity of transported sediment compared to bare soil by a magnitude of three. The flume testing procedure utilized in this study varied from protocol used in other studies. RECPs with a stiffer netting, appeared to perform slightly better than the more flexible linings.

The most effective RECP products identified during the laboratory flume studies included Landlok 435, Landlok 450, NAG SC250, NAG P550, and Pyramat. Any of these products, or their equal, should perform well in channel applications within their published shear stress and velocity limitations. Each of these products, except NAG SC250, are fully UV resistant and are considered permanent linings. NAG SC250 has a degradable straw/coconut matrix and should primarily be used in locations where revegetation efforts will be successful.

To more fully evaluate the effectiveness of the RECPs tested in the laboratory flume studies, field plots were constructed and the conditions of the field plot sections were routinely monitored over the period from October 2003 to June 2005. Even though the RECPs were installed in channel sections with bed slopes that were slightly higher than those recommended by the product manufacturers, each of the products performed well. Each of the RECPs that was tested effectively minimized channel erosion and dramatically improved channel stability.

There is no evidence that any of the channel sections is experiencing severe erosion. Monitoring of the surface profiles within each field plot section indicated that some localized scour of 2 to 3 inches in depth was initially observed at the leading edges of the channel sections immediately downstream from the rip rap. Additional anchors were placed at the leading edges of each field plot section in order to minimize this scour. Some minor deposition of sediment was observed at the lower reaches of each field plot sections. Over time, the deposition and gradual accumulation of soil and sediment transported from the watershed and the roadway surface of Highway 50 is expected to further enhance the stability of the field plot sections. In addition, the gradual emergence of vegetation within each channel section will further enhance channel stability.

## TABLE OF CONTENTS

# LIST OF TABLES

## LIST OF FIGURES

# Chapter I

## INTRODUCTION AND BACKGROUND

Severe erosion is occurring at several locations in the Clear Creek watershed along U.S. Highway 50 between Carson City and Lake Tahoe. Surface water runoff from seasonal snowmelt or infrequent high intensity precipitation events has caused erosion resulting in the transport of substantial quantities of soil and sediment. Erosion has caused problems related to slope stability along roadways and increased maintenance requirements, especially those associated with drainage structures. During significant runoff events, erosion can also cause dramatic increases in turbidity and suspended solids entering surface streams. The subsequent deposition of suspended sediments in slower moving receiving waters can also negatively impact fish populations and may smother the benthic community (Dennison, 1996). The deposition of suspended solids within drop inlets and culverts can substantially reduce the hydraulic capacity of these drainage structures. This may lead to overtopping of curbing along the roadway shoulders resulting in surface flow across unstable, easily erodible slopes.

Corrective action must be taken to limit the erosion of soil and transport of sediment during runoff events. The Hydraulics Section of the Nevada Department of Transportation (NDOT) has committed significant funding over the next several years to implement erosion control strategies. Numerous erosion control products are commercially available. However, the effectiveness and suitability of these products is often difficult to predict. This research project investigated just some of the many erosion control strategies. A combination of laboratory tests and field studies were conducted in a relatively short timeframe to assess the performance of potential erosion control products. This research project will help identify some appropriate and cost effective strategies for mitigating erosion problems along U.S. Highway 50 in the Clear Creek watershed.

This research project evaluated the effectiveness and suitability of alternative, economical, long-term erosion control strategies designed to establish and maintain a cover of protective vegetation. The specific erosion control strategies that was evaluated during this study was the installation of rolled erosion control products (RECPs).

# Chapter II

## LITERATURE REVIEW

### Study Area

The Clear Creek watershed is located approximately two miles south of Carson City on the east slope of the Sierra Nevada mountains in the Carson Range near Lake Tahoe (Figure 2.1). The 16.5 square mile watershed is easily accessed from Clear Creek Road or U.S. Highway 50. Clear Creek is a tributary of the Carson River which drains into Lahontan Reservoir near Fallon, Nevada. Clear Creek has four main branches and many small tributary streams originating from seeps and springs.

The history of the Clear Creek watershed is similar to that of other watersheds in the western Sierra Nevada mountains. After the Comstock Lode was discovered in the 1860s, intensive logging almost depleted the forests. The basin was then overgrazed by sheep and cattle followed by repeated fires. In general, the vegetation and soil has been almost continuously disturbed from the 1860s to the present time (Fisher, 1978).

### Geology

The Clear Creek watershed ranges in elevation from 4700 feet to 9200 feet, with slopes varying from 2% in the lower valley areas to 2:1 (horizontal:vertical) in the higher elevations. Very steep slopes dominate a large portion of the watershed. The watershed lies within the Sierra Nevada batholith, which makes up a significant portion of the Sierra Nevada mountain range (Figure 2.2). The batholith was created from magma intrusions due to high temperatures and pressures associated with the subduction zone located between the Pacific and North American tectonic plates.

Individual intrusive masses of the granitic rocks are assumed to be large and homogeneous, resulting in uniform bedrock. Much of the basin is a complex range-front formed by down-warping and distributive faulting. Granitic rock in this broad warp is deeply weathered to over 100 feet, which indicates long-term weathering (Moore, 1969).

Granodiorite is the primary rock type within the batholith (Bateman, 1974). Per the United States Geological Survey (USGS) geologic map (Pease, 1980), the watershed is typically denoted “kgd”: hornblende-biotite granodiorite, which was formed in the Cretaceous period, some 80 to 90 million years ago. Granodiorite is generally composed of the minerals shown in Tables 2.1 and 2.2.

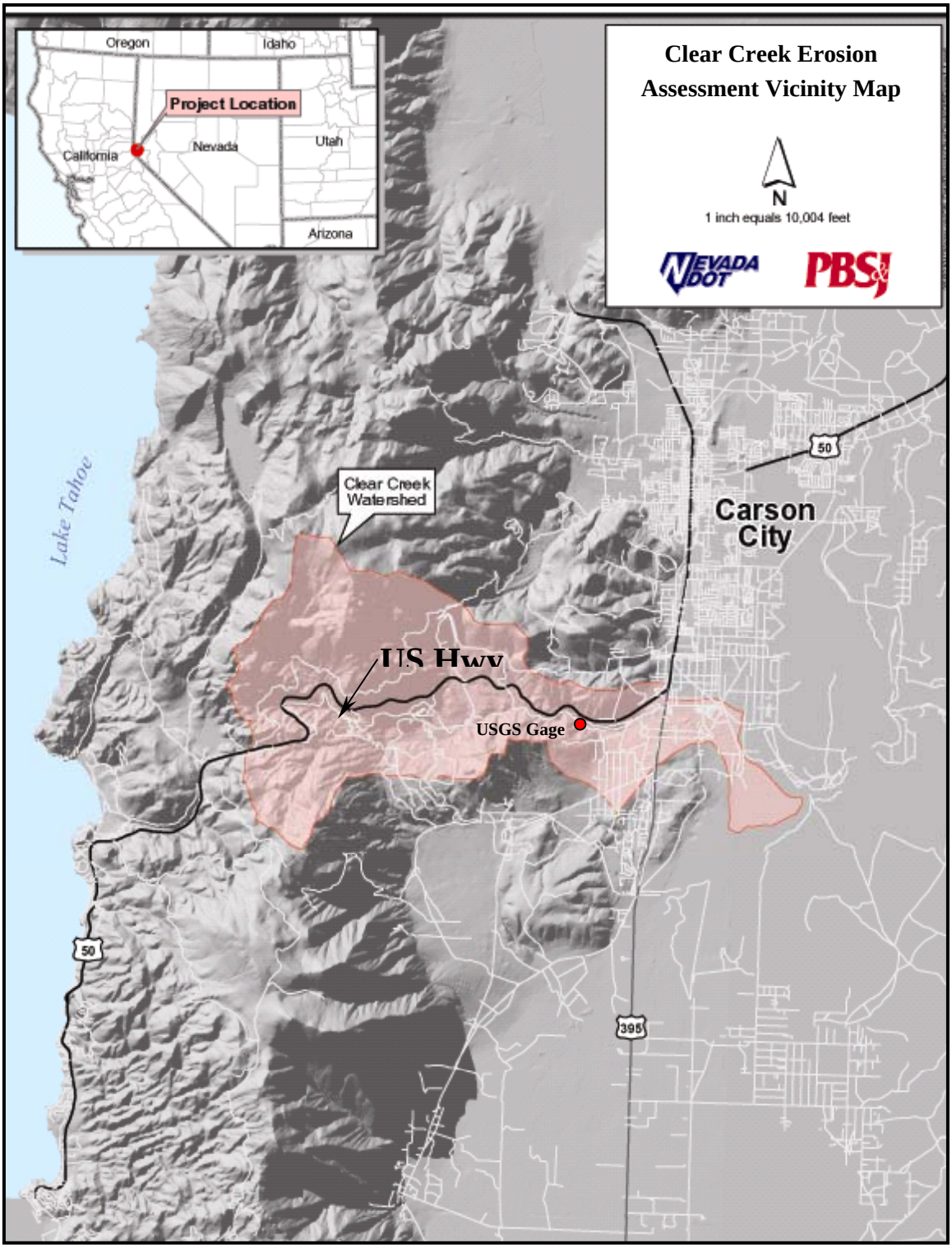


**Figure 2.1 Clear Creek watershed, NV (PBS&J, 2003).**

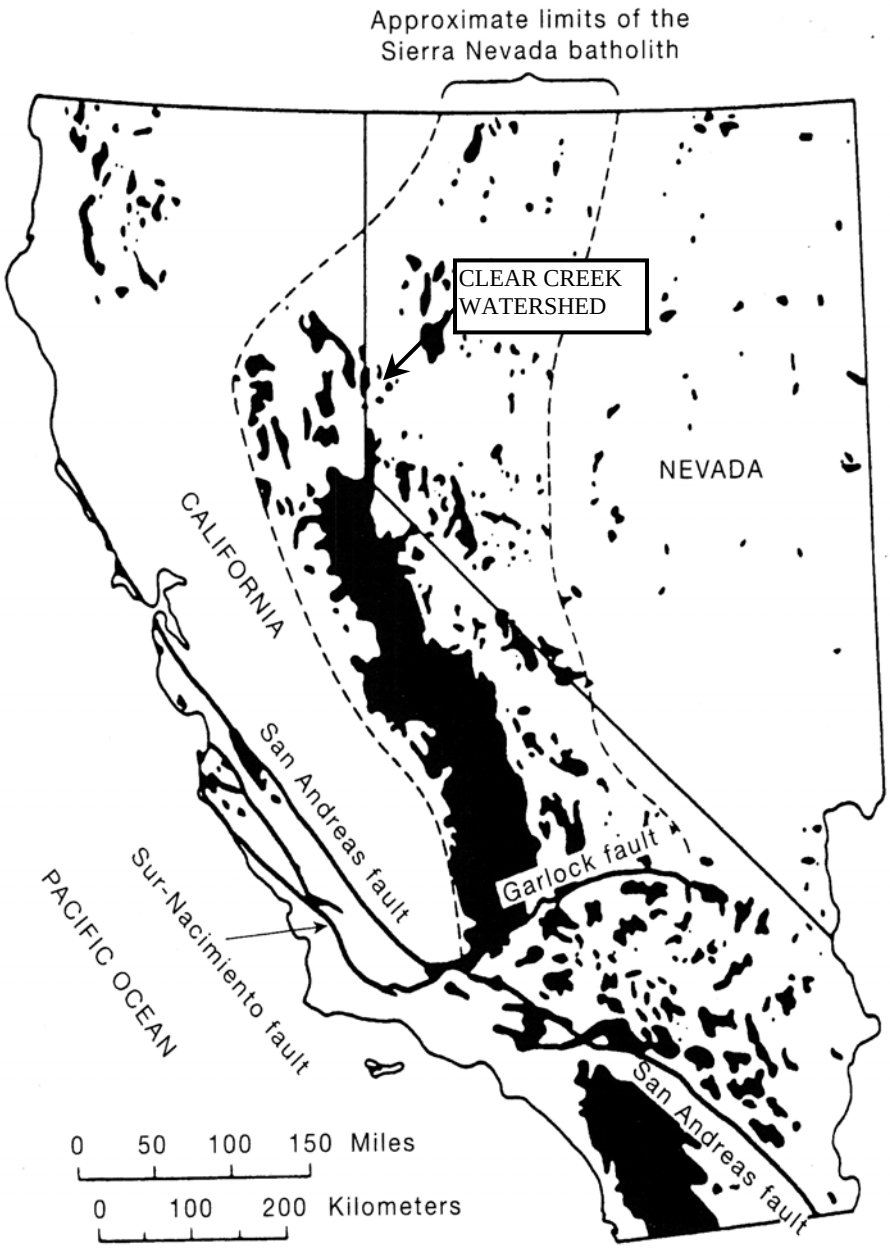


**Figure 2.2 Sierra Nevada batholith (Harden, 1998).**

**Table 2.1 Granodiorite Mineral Composition (% Weight)**

| Mineral | General (Hyndman, 1972) | Yosemite, CA (White et al., 1999a) | Sagehen Ck., CA (Rademacher, 2001) |
|---|---|---|---|
| Plagioclase | 15-85 | 36 | 40 |
| K- Feldspar | 5-70 | 15 | N/A |
| Quartz | 10-50 | N/A | 30 |
| Biotite | 0-30 | 8 | 10 |
| Hornblende | 5-20 | 5 | 20 |

**Table 2.2 Granodiorite Chemical Composition (% Weight)**

| Constituent | General (U.S.G.S., 1903) | Yosemite, CA (White et al., 1999a) |
|---|---|---|
| $SiO_2$ | 66-68.5 | 71 |
| $Al_2O_3$ | 15.5-16.5 | 14 |
| $Fe_2O_3$ | 1-2 | N/A |
| FeO | 1.5-2.5 | N/A |
| MgO | 1.25-1.75 | 1.4 |
| CaO | 3-4.5 | 3 |
| $Na_2O$ | 3.5-5 | 3.3 |
| $K_2O$ | 2-3.5 | N/A |

**General Soil and Vegetation Characteristics**

Soil Characteristics. Soils in the Clear Creek watershed are shallow to deep and are generally well drained to excessively well drained. They formed in residuum and colluvium from granitic and metavolcanic rock. Table 2.3 is a summary of soils information obtained from the Soil Conservation Soil survey (Candland, 1979), which lists the major types of soil within the watershed along with their percentages and associated characteristics. The basin soils are generally composed of sands, gravels, and rock outcrops (89%), with lesser amounts of loam (10.2%) and clay (0.7%). The rock outcrop complex soil type generally consists of a 1:2 ratio of rock outcrop to sands and gravels. Figure 2.3 is a graphical representation of the general soils in the basin and their approximate locations.

**Table 2.3 Soil Characteristics within Clear Creek Watershed (modified from Candland, 1979)**

| General Soil Type | | Predominant Soil Unit | | | | | | |
|---|---|---|---|---|---|---|---|---|
| Soil Class | % of Basin | Map Unit Name | % of Soil Type | Unified Soil Class* | Depth to Bedrock (in) | Bedrock Hardness | Erosion Factor K | Hydrologic Soil Group |
| Clay | 0.7 | Voltaire Silty Clay | 100.0 | CL | >60 | NA | NA | D |
| Loam | 10.2 | Surprise Sandy Loam | 35.9 | SM | >60 | NA | 0.20 | B |
| Sand | 39.0 | Corbett Gravelly Sand | 22.6 | SP - SM | 32 | Soft | 0.17 | B |
| Rock Outcrop | 50.0 | Toiyabe-Rock Outcrop | 48.7 | SP - SM | 15 | Soft | 0.10 | C |

*Reference Figure 2.11 for descriptions of the Unified Soil Classifications.

Percentages of the predominant soil units (based on area) for each soil type are listed along with selected soil properties. Incidentally, two of the predominant soils, the Corbett and Toiyabe units are located in areas of the watershed that are experiencing significant erosion.

All soil units, except for the Voltaire silty clay, are classified as sandy and gravelly soils in accordance with the Unified Soil Classification (ASTM, 2000b). This indicates that the majority of the soils are non-cohesive, with very little organic content.

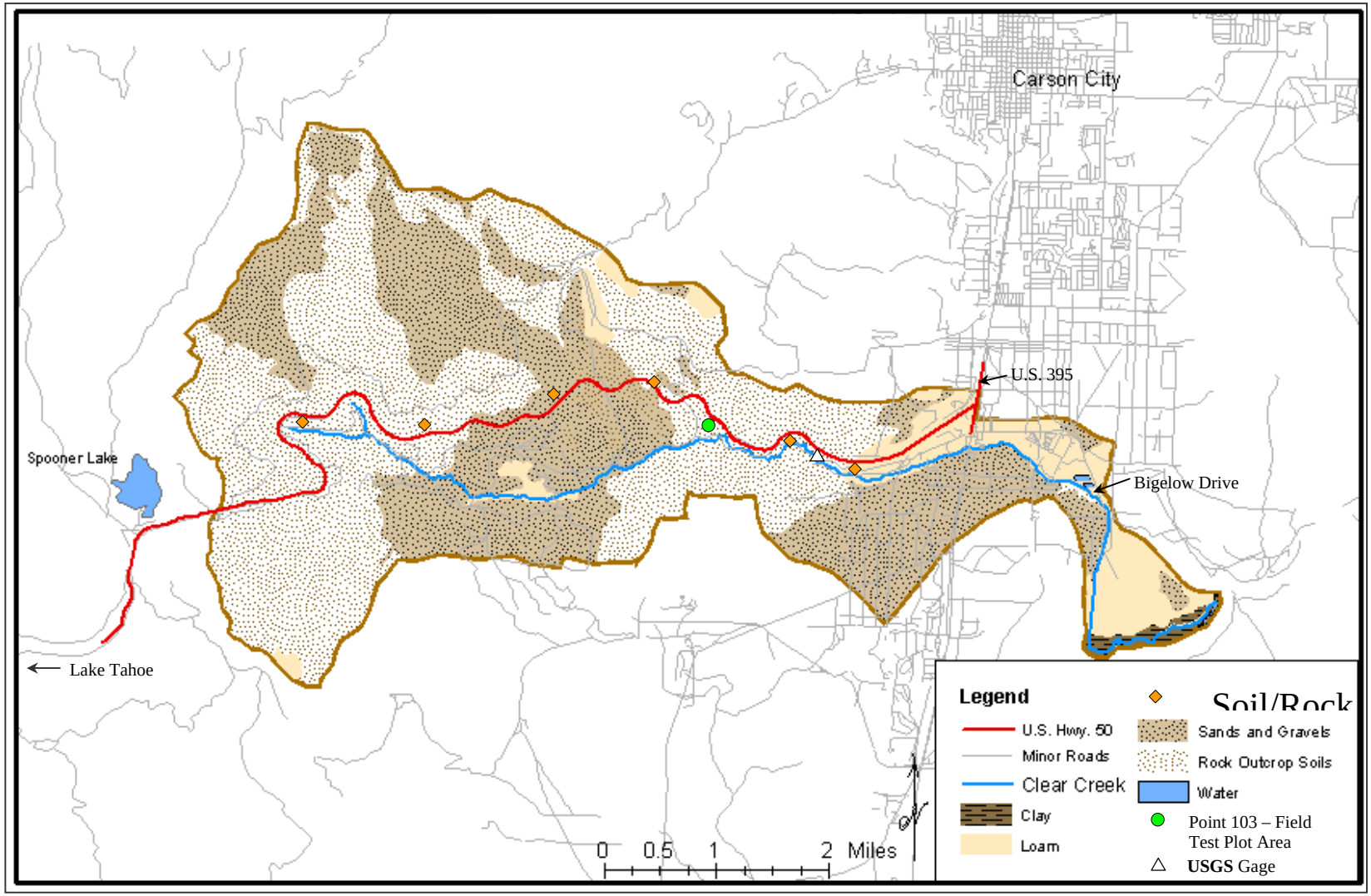


**Figure 2.3 Clear Creek watershed soils and water features (PBS&J, 2003).**

The column titled “Depth to Bedrock” indicates the soil depth. As shown, the depth to bedrock in the Corbett and Toiyabe units is very shallow, especially in the Toiyabe unit (15 in.). As discussed previously, the bedrock consists of weathered granitic rock. The bedrock hardness was estimated for the Corbett and Toiyabe units as soft and ripable, where excavations can be made with trenching equipment instead of blasting. This qualitatively indicates that the bedrock is indeed fractured and highly weathered.

The erosion factor *K* indicates the susceptibility of a soil to sheet and rill erosion by water (Candland, 1979). It is one of the six factors used in the Universal Soil Loss Equation (Wischmeier and Smith, 1965) to predict the average annual soil loss in tons per acre per year. The estimates are based primarily on percentage of silt, sand, and organic matter as well as soil structure and permeability. Values of *K* range from 0.05 to 0.69; the higher the value, the more susceptible the soil is to sheet and rill erosion by water. From Table 2.3, all predominant soil units in this watershed have relatively low erosion factors. However, this factor does not consider erosion due to concentrated flows in drainageways and from culvert outfalls.

The hydrologic soil groups are used to estimate runoff from precipitation and are an indication of the soil infiltration rate. There are four groups, A through D, arranged in order of decreasing infiltration capacity (Candland, 1979). Group A soils have high infiltration rates (low runoff potential) and high rates of water transmission. Group D soils, on the other hand, have very slow infiltration rates, typical of clays with high shrink-swell potentials. From Table 2.3, most of the soil is typically Group B or C which include soils with moderate to slow infiltration rates.

Vegetation Characteristics. Native vegetation in the higher elevations of the Clear Creek watershed is predominately red fir and Jeffery pine. Where the tree canopy is open, and in the lower elevations, the common ground cover consists of big sagebrush, antelope bitterbrush, pinemat manzanita, needlegrass and squirreltail. In the riparian zone adjacent to Clear Creek, vegetation consists of quaking aspen, white fir, mountain alder, and bitter cherry (Candland, 1979).

**Hydrology**

The climate in the Clear Creek watershed is characteristic of a semi-arid environment and experiences a ‘rain shadow’ effect from the Sierra Nevada mountains. Prevailing winds from the west carry storms from the Pacific Ocean to Nevada, which results in precipitation in the form of both rain and snow. Average annual precipitation in the basin ranges from 10 to 45 inches, most of which falls as snow during the winter months. The average annual air temperature ranges from 35 to 52 $^{o}$F. In the summer, maximum temperatures can reach 100 $^{o}$F and in the winter, the temperatures can drop to –30 $^{o}$F (Candland, 1979).

Clear Creek is a steeply incised perennial stream, which has its headwaters at Snow Valley Peak (elevation 9274 feet). It flows eastward into Eagle Valley where it enters the Carson River. Above U.S. Highway 50, a spring zone spreads and discharges into Clear Creek (Boone, 1983). All other tributaries to Clear Creek appear to be ephemeral. Clear Creek can be characterized as a first-order or headwater stream, which is forested with a narrow, steep gradient channel and a dense over-canopy of conifers or deciduous trees (PBS&J, 2003).

The average annual water yield from Clear Creek is approximately 3920 acre-feet per year (Arteaga and Durbin, 1978). Records from the United States Geologic Survey show that the annual mean streamflow varies from approximately 2 cubic feet per second (cfs) to 12 cfs (Figure 2.4). As shown in Figure 2.5, the monthly mean streamflow varies from a low of approximately 2.5 cfs in August to a high of 9.5 cfs in April. The maximum flow in April typically corresponds with the high normal snowmelt runoff characteristic of this watershed. In a recent watershed assessment, the 24- hour / 100-year storm peak discharge for the watershed was calculated at approximately 10,000 cubic feet per second (PBS&J, 2003). However, according to the USGS stream gage records shown in Figure 2.6, the maximum-recorded discharge in 42 years of record was 266 cfs in 1997. Note that no streamflow readings were obtained between 1979 and 1988.

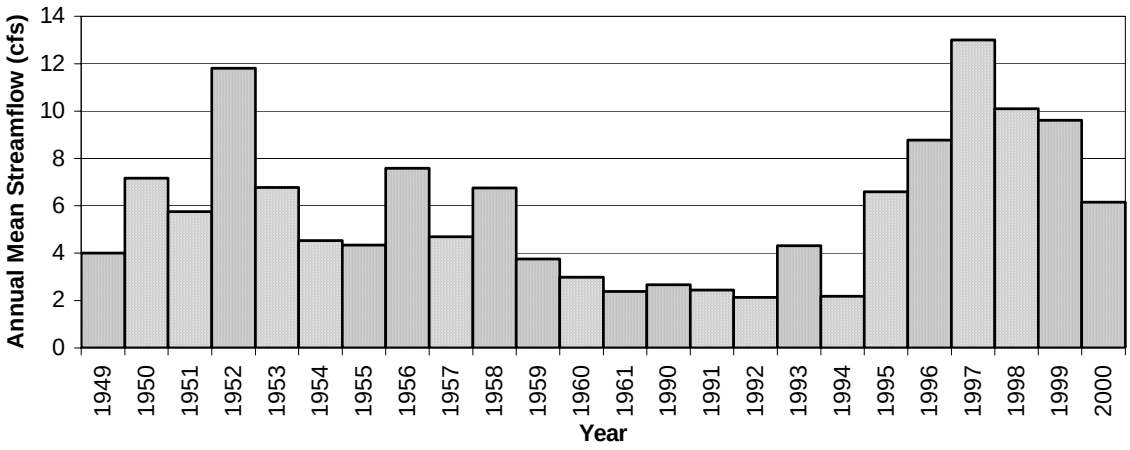


**Figure 2.4 Annual mean flows for Clear Creek, NV, USGS gage 10310500.**

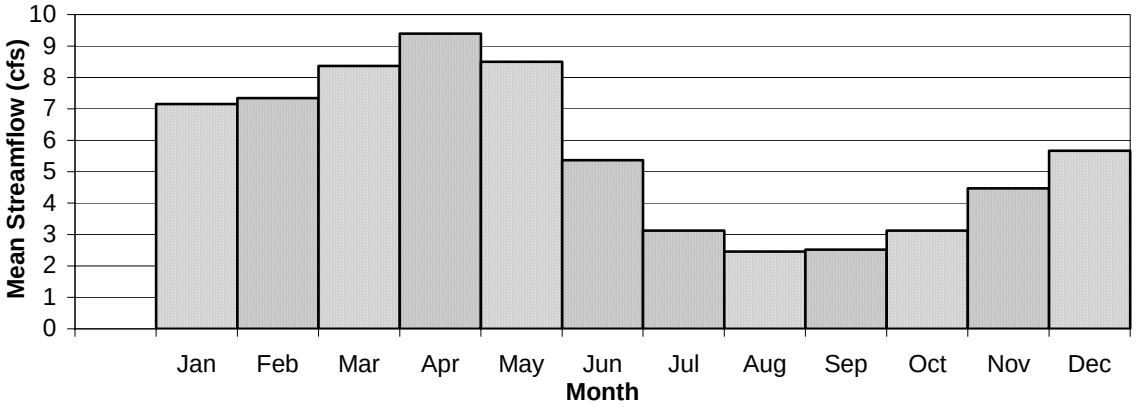


**Figure 2.5 Mean of monthly flows for Clear Creek, NV, USGS gage 10310500.**

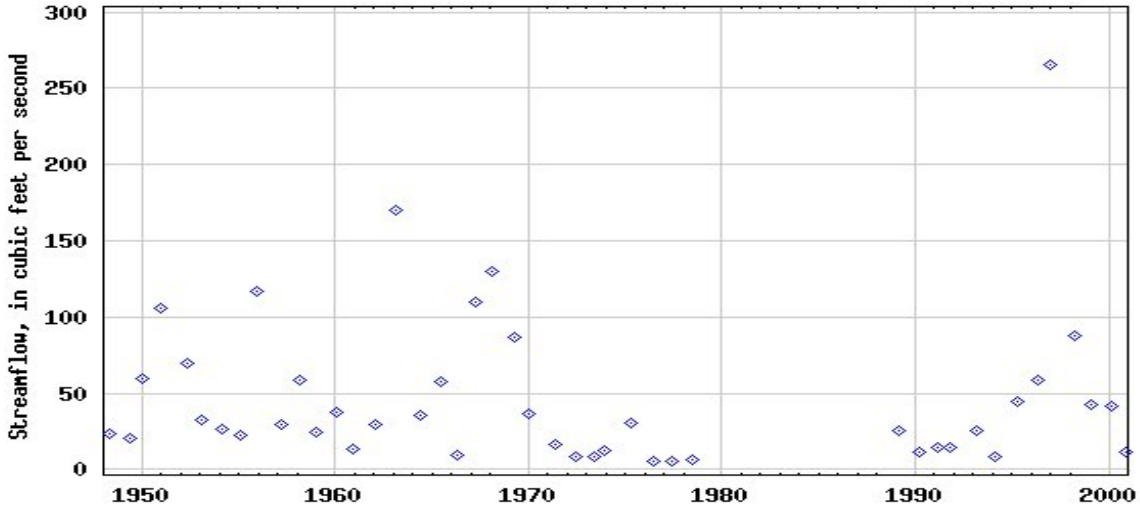


**Figure 2.6 Peak flows for Clear Creek, NV, USGS gage 10310500.**

## Weathering of Bedrock

Weathering of bedrock plays an important role in the erosion process by weakening or breaking the rock matrix. It may result from both physical and chemical processes due to changes in the equilibrium conditions in the natural environment (Krank, 1980).

Physical Weathering. Internal or external forces exerted on rock that exceed its cohesive strength results in a mechanical breakdown and subsequent physical weathering. Physical weathering may take the form of fracturing, jointing, and sheeting. Fractures and joints typically form perpendicular to the bedding planes and the ground surface.

Jointing is often a result of tectonic stresses and shrinkage from temperature and moisture changes. Sheeting, which is the formation of fractures parallel to the ground surface, is due to pressure relief from the removal of overburden (Krank, 1980).

Causes of physical weathering include frost action, expansion of minerals, insolation, physical action of water, recurrent wetting and drying of rocks, and abrasion from moving particles in wind, water, and glaciers (Krank, 1980).

Frost action in freeze-thaw environments plays a significant role in weathering. Water freezing to ice in confined joint spaces can produce pressures as much as 30,000 pounds per square inch (psi), exceeding the strength of most rocks (Ollier, 1969). However, thick snow pack in higher elevations may insulate the soils and prevent them from freezing during the winter months (Dahlgren et al., 1997).

Wedging action and development of grus may be produced by the hydration of biotite. As reported by Dahlgren et al. (1997), physical weathering of granitic bedrock to grus result, to a large part, from hydration of biotite (Wahrhaftig, 1965; Nettleton et al., 1968). Biotite swells by approximately 30% upon partial alteration and hydration creating many microfractures between larger grains that lead to shattering of the rock fabric. The occurrence of continuous moist conditions greatly enhances the grus-forming process (Wahrhaftig, 1965).

Temperature is the most significant factor influencing the mechanical breakdown of rock. It operates indirectly through its control on moisture movement and processes such as salt weathering and freeze/thaw and possibly through insolation weathering. Thermal expansion/contraction of salts has the theoretical potential to cause rock breakdown (Cooke and Smalley, 1968) and many common salts have coefficients of volumetric expansion greater than those of common rock types and their constituant minerals (Warke and Smith, 1998).

Insolation weathering describes direct heating of rock in which thermal properties control temperatures attained by rock as a whole and by individual mineral grains. The role of direct thermal or insolation weathering remains speculative, based primarily on theoretical arguments which suggest that stressing of rock occurs when a temperature gradient is established between surface and subsurface material and when differences exist in the coefficients of thermal expansion between adjacent mineral grains (Ollier, 1984; Yatsu, 1988; Lewin, 1990).

Chemical Weathering. Chemical weathering normally plays an important role in the erosion process. Low temperature reactions that occur between aqueous solutions and minerals in the soils and rocks are collectively called chemical weathering. These processes include both congruent (carbonate dissolution) and incongruent (silicate hydrolysis) reactions that supply solutes to groundwater and surface water systems, and produce secondary mineral products such as clays (Kehew, 2001).

Granitic rocks are primarily composed of silicate minerals with lesser amounts of carbonate minerals. Burkins et al. (1999) reported that due to the relatively homogeneous nature of the Sierra Nevada batholith, the bulk chemistry of soils in the region tend to be quite similar. Based on petrographic thin sections, all soil samples contain quartz, plagioclase feldspar, potassium feldspar, biotite/vermiculite, hornblende, sphene, and opaque minerals. Further, they reported that the clay mineralogy is dominated by kaolinite, gibbsite, and vermiculite, with lesser amounts of illite.

For the primary minerals, Goldich's stability series indicates the relative increasing resistance to weathering from bottom to top (Kehew, 2001). For granodiorite, the order is plagioclase, k-feldspar, hornblende, biotite, and quartz. About eighty percent of the rock-derived dissolved constituents found in Sierra Nevada watersheds could be accounted for by the breakdown of plagioclase (Garrels and MacKenzie, 1967).

There have been several studies involving silicate and carbonate dissolution from granitic bedrock. White et al. (1999a) studied the role of disseminated calcite in the chemical weathering of granitoid rocks. Their findings support other recent studies (e.g., Stauffer, 1990) which demonstrated that excess calcite typically occurs in the microfractures of the rocks. Their analyses indicated that trace amounts of calcite, originally proposed to be present based on mass balance calculations (Garrels and MacKenzie, 1967), are ubiquitous in the Sierra Nevada granitoids. Based on sodium/calcium ratios, disseminated calcium contributes between 57 and 98% of the total calcium released from granitoid rocks. This suggests that accessory calcite dissolution in granitoid rock can contribute a significant portion of the total calcium and alkalinity in watersheds and rivers. Over the duration of the 1.7-year study by White et al. (1999a), calcite dissolution progressively decreased and was superceded by steady-state dissolution of silicates.

In their field and laboratory studies of granitoid rocks, White et al. (1999b) found that climatic temperature variations significantly affected the concentrations of silicate and sodium in effluents. Concentrations from weathered granitoids were much lower than their fresh counterparts, but exhibited comparable temperature effects, increasing in concentration by an order of magnitude over a temperature range of 5 to 30 $^{o}$C. Potassium release was rapid, but less temperature sensitive. Concentrations of calcium, magnesium, and strontium were much less temperature dependent.

Mass balance calculations of weathering have been used successfully in estimating mineral compositions and dissolution processes. For example, Garrels and Mackenzie (1967) tested the conclusions of Feth (1964) in regards to weathering reactions by performing mass balance calculations on effluents from ephemeral and perennial springs in the Sierra Nevada mountains. The procedure consisted of reconstructing the primary minerals with the known quantities of the reaction products. For example, in the ephemeral springs, the dissolution of plagioclase and the precipitation of kaolinite accounted for the water chemistry. All of the sodium ($Na^{+}$) present in solution is contributed to rock weathering after subtracting concentrations in snow water:

$$1.23\ Al_2Si_2O_5(OH)_4 + 1.10\ Na^+ + 0.68\ Ca^{2+} + 2.44\ HCO_3^- + 2.20\ SiO_2 =$$
$$1.77\ Na_{0.62}Ca_{0.38}Al_{1.38}Si_{2.62}O_8 + 2.44\ CO_2 + 3.67\ H_2O \qquad \text{(moles/liter x } 10^4\text{)}$$

In this reaction, calcium ($Ca^{2+}$) is removed completely as well as 2.44 $HCO_3^-$ and 2.20 $SiO_2$. Then, by changing more kaolinite back into biotite, all of the magnesium ($Mg^{2+}$) is removed:

$$0.037\ Al_2Si_2O_5(OH)_4 + 0.073\ K^+ + 0.22\ Mg^{2+} + 0.15\ SiO_2 + 0.51\ HCO_3^- =$$
$$0.73\ KMg_3AlSi_3O_{10}(OH)_2 + 0.51\ CO_2 + 0.26\ H_2O$$

In addition to the magnesium ($Mg^{2+}$), this reaction also removes 0.73 $K^+$ and 0.15 $SiO_2$. The last step is to change the remaining kaolinite back into K-feldspar by removing the remaining 0.13 $K^+$:

$$0.065\ Al_2Si_2O_5(OH)_4 + 0.13\ K^+ + 0.13\ HCO_3^- + 0.26\ SiO_2 =$$
$$0.13\ KAlSi_3O_8 + 0.13\ CO_2 + 0.195\ H_2O$$

Not only does the reaction remove all of the potassium ($K^+$), it eliminates the bicarbonate ($HCO_3^-$), as well. Only a small portion of silica ($SiO_2$) remains (4%), so the mass balance is probably within the limits of error of the original values of concentration. From the calculations above, it can be concluded that the system is closed with respect to $CO_2$ and the weathering product is kaolinite, or a mineral very similar. If a balance of calcium ($Ca^{2+}$) and bicarbonate ($HCO_3^-$) were to remain after the silicate weathering reactions, it can be assumed that excess calcium carbonate ($CaCO_3$) is also being dissolved:

$$CaCO_3 + CO_2 + H_20 = Ca^{2+} + 2\ HCO_3^-$$

In deeper circulating perennial springs, it was found from ratios of sodium and silica ($Na^+/SiO_2$) in effluents that a solid other than kaolinite was being produced. The mass balances were successfully performed with the addition of montmorillonite as a second product, and the dissolution of calcite to account for the excess calcium ($Ca^{2+}$).

Weathering Classifications. The fracture characteristics of weathered granites play an important part in determining the erodibility of the rock mass. Several classifications for weathered granite have been proposed (e.g., Murphy, 1985; Dearman, 1974; Dearman et al., 1978; Selby, 1980; British Standards Institute, 1981). They are typically based on engineering properties and describe the condition and appearance of the rock. The classification proposed by Murphy (1985) is simpler than most and is more easily adapted to field use than most other classifications (Ehlen, 2002). Murphy's classification was modified to include the sound and feel of the square end of a 3-lb rock hammer hitting the rock as shown in Table 2.4. For visual reference, Figure 2.7 shows examples of the different weathering grades in granitic rocks.

**Table 2.4 Weathering Grade Classifications (modified from Murphy, 1985)**

| Weathering Grade | Description of Rock | Hammer Criteria |
|---|---|---|
| Fresh Rock (F) | No visible signs of weathering. Rock is fresh. Crystals are bright. | Hammer rings and bounces back. |
| Slightly Weathered (SW) | Discontinuities are stained or discolored and may contain a thin filling of altered material. Discoloration may extend into the rock from the discontinuity to a distance of 20% of the discontinuity spacing. | Hammer rings and bounces back. |
| Moderately Weathered (MW) | Slight discoloration extends from discontinuity planes for a distance of more than 20% of the discontinuity spacing. Discontinuities may contain filling of altered material. Partial opening of grain boundaries observed. | Hammer "thuds". |
| Highly Weathered (HW) | Discoloration extends throughout the rock, and the rock material is partly friable. The original texture of the rock has mainly been preserved, but separation of the grains has occurred. | Hammer "thuds" and fragments of rock can be easily broken off by hand. |
| Completely Weathered Rock (CW) | The rock is totally discolored and decomposed and in friable condition. The external appearance is that of a soil. Internally, the rock texture is partly preserved, but the grains have been completely separated. | The pick end of the hammer easily enters the rock. |

Fracture Characteristics of Weathered Granites. The weathering classifications previously mentioned do not address changes in frequency, length, and appearance of joints in the rock mass as weathering progresses. From studies on Asian granite (Ehlen, 2002), mean joint spacing appears to decrease from fresh, through slightly and moderately weathered granitic rock, then increases from moderately weathered rock, through highly and completely weathered granitic rock. The widest joint spacing occurs in either fresh or completely weathered rock, and the closest, in moderately weathered rock. The disappearance of the joints in more highly and completely weathered rocks is apparently due to filling of the joint by the crumbling rock mass (Ehlen, 2002).

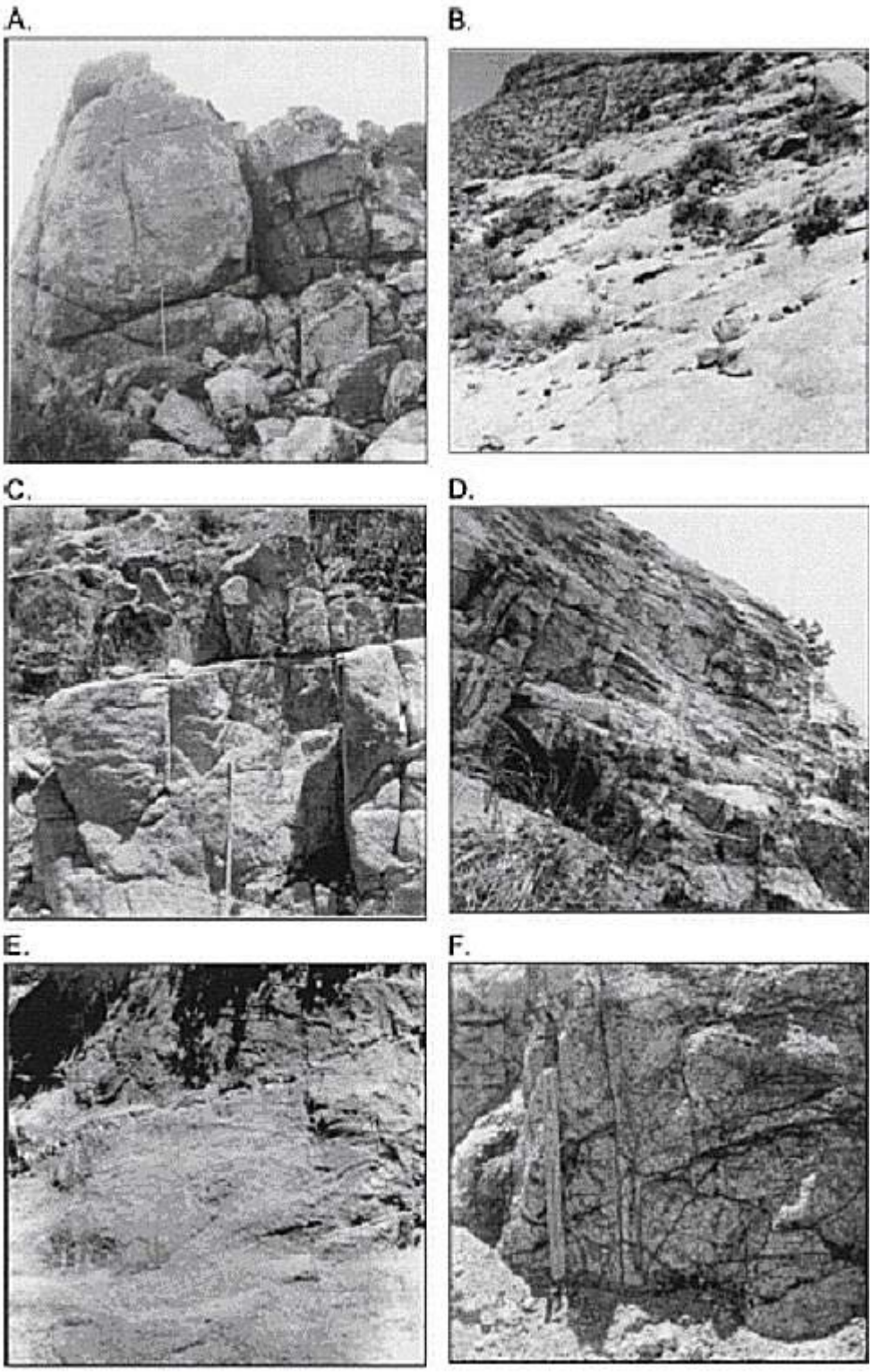


**Figure 2.7 Weathered granite examples (Ehlen, 2002).**
A – Fresh rock, B – Slightly weathered, C – Moderately weathered, D – Moderately weathered, E – Highly weathered, and F – Completely weathered.

Weathering Controls and Rates. Weathering rates of granitoid rocks can vary greatly depending on the site conditions and mineral properties. Site factors affecting the rates include water residence time, pH, $CO_2$ concentrations, climatic conditions (e.g., temperature and water volume), and geomorphic settings. Mineral properties that may control weathering rates include mineral composition, crystal size, and extent of fracturing. Soil cover has long been recognized as an important factor for chemical weathering of bedrock. Exposed bedrock remains dry most of the time and weathers slowly, whereas bedrock beneath a soil can remain perennially moist with soil solutions that promote mineral alteration (Granger et al., 2001). Dahlgren et al. (1997) reported in their study of soil development in the Sierra Nevada mountains that twice as much clay is produced per unit of weathering in the low-elevation soils as compared to high-elevation soils, primarily as a result of climatic differences.

The Clear Creek watershed, like most other environments, is heterogeneous in nature and has changing weathering controls with time and location. As an example, the exposed bedrock in the higher elevations will be subjected to less chemical weathering than the lower, wetter soil regions. Additionally, chemical weathering will proceed at faster rates during the wetter seasons. The rate of chemical weathering of rock in the vicinity of springs may be on the order of one meter in 9000 years (Garrels and MacKenzie, 1967). Conversely, the maximum mean bare-bedrock erosion rate can be as low as 7.6 meters $My^{-1}$, or approximately 0.07 meters in 9000 years (Small et al., 1997). Therefore, weathering in the vicinity of springs can be 2 orders of magnitude faster than bare-bedrock areas.

**Erosion Process**

Erosion involves the processes of particle detachment, transport, and deposition. Any site where soils are exposed to water, wind, and ice is susceptible to erosion (Dennison, 1996). For erosion caused by water, the specific forces that initiate the detachment of particles include the impact of raindrops and the shear stresses exerted by surface runoff (Lal and Elliot, 1994; Dennett, 1995). This section will review the types of soil erosion, factors affecting erosion, and erosion by rock scour.

Three recognized types of soil erosion that may occur along hillsides and steep slopes include: (1) surface erosion; (2) gully erosion; and (3) soil mass movement (Ffolliott et al., 1995).

Surface Erosion. Surface erosion occurs as a result of the collective action of the impact of raindrops, thin film surface flows, and concentrated surface runoff flows. Surface erosion may also be further classified as either interrill erosion or rill erosion (Lal and Elliot, 1994; Elliot and Ward, 1995) because it promotes the formation of rills and small gullies on the land surface. Figure 2.8 shows an example of rill erosion on a roadway embankment in the Clear Creek watershed. As shown in the photograph, rill erosion becomes more pronounced further down the slope.

As overland flow becomes concentrated and moves down slope, the velocity of the flow generally increases which increases the kinetic energy of the flow (Ffolliott et al., 1995). This subsequently increases the turbulence and ultimately the erosive potential of the flow, which varies with the square of the velocity (Goldman et al., 1986). In general, surface flows with velocities as low as approximately 0.5 feet per second (160 mm/s) are capable of eroding soil particles that are 0.3 mm in diameter (Bell, 1999). In order to reduce the erosive potential of flowing water, the channel velocity can be reduced by lining the channel bottom with a roughened surface such as vegetation and riprap or by increasing the width of the channel.

Gully Erosion. A gully is a relatively deep, recently formed eroding channel on hillslopes where no well-defined channels existed previously. Gullies usually result from uncontrolled, concentrated surface runoff down hillslopes that have very little vegetative cover and contain highly erodible soils (Ffolliott et al., 1995). Gullies are likely to form whenever concentrated surface flow passes over a point where an abrupt change in elevation or gradient of the land surface occurs. After gully erosion is initiated, it is very difficult and costly to control (Ffolliott et al., 1995). Figure 2.9 illustrates the potential magnitude of gully erosion. These photographs were taken in the Clear Creek watershed and show the dramatic depths of gullies that can exceed twenty feet.


**Figure 2.8 Rill erosion, U.S. Highway 50 roadway embankment, Clear Creek watershed.**

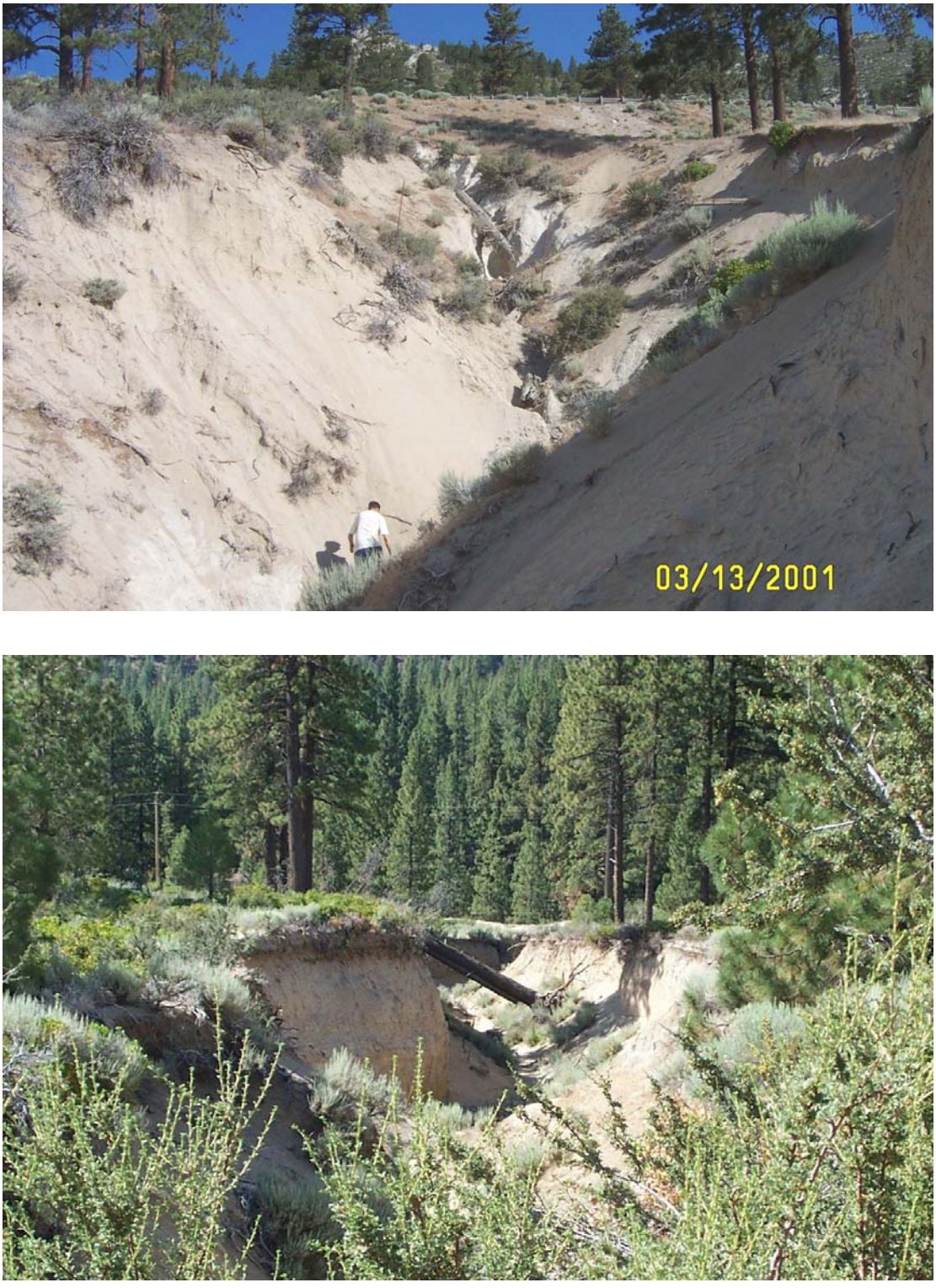


**Figure 2.9 Gully erosion in the Clear Creek watershed.**

Soil Mass Movement. Soil mass movement, commonly known as a landslide, is defined as the movement of a mass of rock, debris, or earth down a slope (Cruden, 1991). Landslides can be triggered by a variety of external stimuli, such as intense rainfall, earthquake shaking, water level change, storm waves, or rapid stream erosion that cause a rapid increase in shear stress or decrease in shear strength of slope-forming materials (Dai et al., 2002).

Precipitation is one of the major landslide triggers (Van Asch et al., 1999). The generation of surface runoff and high peak discharges in first-order alpine catchments is an important triggering mechanism for debris flows. Surface runoff supplies water to debris masses which accumulate in channels. This increases the pore pressure within the debris mass which may initiate debris flow. In such catchments thin soil mantles and bare rocks are present. Hortonian and saturation overland flow are the main processes producing runoff. The infiltration capacity of the soil and the steepness, shape, and roughness of the slopes determine the height of the peak discharge, and hence the maximum fluid pressure which will be generated in the debris. Other important factors are the sediment content, density, and viscosity of the overland flow, as well as the friction angle and porosity of the debris material.

Erosion Factors. The four principal factors that influence the erosion of soils are: (1) climate; (2) soil characteristics; (3) topography; and (4) groundcover (Goldman et al., 1986; Roberts, 1995). Four soil characteristics that are important in determining the erodibility of soils and sediments include texture, organic content, structure, and permeability (Goldman et al., 1986). These characteristics largely determine the infiltration capacity of soils. The steepness and length of slopes are important considerations related to topography. Long, continuous slopes tend to increase the momentum of flowing water, thereby increasing the erosive potential of the water.

Groundcover usually refers to vegetation but also includes other surface treatments such as mulches, wood chips, crushed rock, jute mesh or netting, and filter fabric (Goldman et al., 1986). Most of these surface treatments are considered as temporary erosion control measures until natural vegetation is established. In regions with harsh climates, it is usually difficult to establish vegetative cover. Thus, more permanent surface treatments such as geotextile blankets and mats are commonly used in these regions in order to allow more time for vegetation to become established.

Soil erosion can be accelerated by any activities that: (1) change natural drainage patterns; (2) alter undisturbed soil conditions; and (3) decrease the amount of permeable area for infiltration of water (Dennison, 1996). All of these activities tend to increase the quantity and the velocity of surface runoff. Areas that are most highly susceptible to erosion due to the increased quantity and rate of surface runoff include areas with steep slopes and areas with little or no vegetative cover (Dennison, 1996).

Rock Scour. The erosion of rock is a more complex process than the erosion of soil. Scour of jointed rock commences when the hydraulic forces interacting with earth

material exceeds the resistance offered by the earth (Annandale et al., 1996). Material properties that determine scour resistance of rock include intact material strength, block size, shear strength between the blocks of rock, and the relative shape and orientation of the rock blocks. A conceptual model of scour of jointed rock, viewed as a process of progressive dislodgement, can be characterized by three stages: (1) jacking; (2) dislodgement; and (3) displacement (Figure 2.10). Turbulence in the flowing water will cause fluctuations in pressure that progressively jack material units out of their positions of rest. Once jacked out, they are dislodged by the power of the flowing water, and finally displaced.

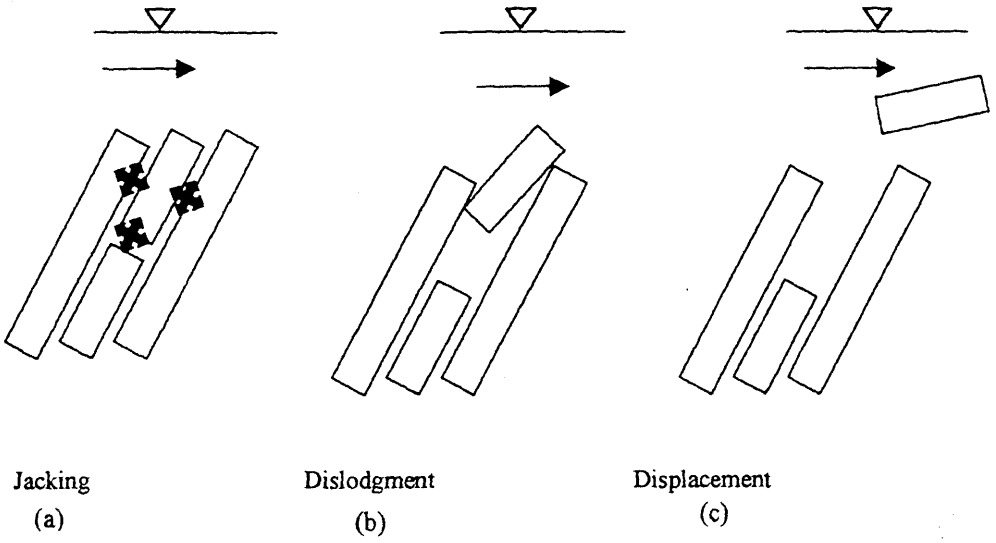


**Figure 2.10 Rock scour (Annandale, 1995).**

Erodibility of both soil and rock can be evaluated in terms of the rate of energy dissipation of flowing water and a classification of the erodibility of the materials. The correlation between the rate of energy dissipation (*P*) and the materials resistance of a material to erosion $K_h$ can be expressed as the function:

$$P = f(K_h) \tag{2-1}$$

at the erodibility threshold. If $P > f(K_h)$, the erodibility threshold is exceeded, and the material would be expected to erode. Conversely, if $P < f(K_h)$, the erodibility threshold is not exceeded, and erosion is not expected (Annandale, 1995).

In the development of Equation 2-1, the rate of energy dissipation was selected as the preferred parameter since it is related to turbulence and fluctuating pressures. Estimates of the rate of energy dissipation should represent the relative magnitude of fluctuating pressure, and thus, the erosive power of water. If the energy loss is $\Delta E$ and the unit discharge is *q*, the rate of energy dissipation per unit width of flow may be

expressed as:

$$P = \gamma q \Delta E \quad (2\text{-}2)$$

where $\gamma$ = unit weight of water (Annandale, 1995). Yang and Molinas (1982) derived a relationship between the rate of energy dissipation and the turbulence energy production rate, while Fiorotto and Rinaldo (1992) validated a relationship between rate of energy dissipation and pressure fluctuation.

The erodiblility index $(K_h)$ is based on Kirston's ripability index for which a rational relationship was established between flywheel power of excavation equipment and the ripability of any given earth material (Kirston, 1982 and 1988). It is a function of the earth mass strength $(M_s)$, particle/block size $(K_b)$, discontinuity or interparticle bond shear strength $(K_d)$, and the relative ground structure $(J_s)$:

$$K_h = M_s K_b K_d J_s \quad (2\text{-}3)$$

The mass strength $(M_s)$ represents the strength of intact material. The particle/block size $(K_b)$ refers to the mean grain size ($d_{50}$) for granular material and the mean size of blocks of intact rock material. The discontinuity or interparticle bond shear strength $(K_d)$ represents the strength of joint interfaces in rock masses or the shear strength of interparticle bonds in granular soils. The relative ground structure $(J_s)$ accounts for the structure of the ground with respect to the direction of stream flow. It is a complex function expressed in terms of the orientation and shape of individual blocks determined by joint set spacings, dip angles, and dip directions. Kirston (1982) provides standard tables for quantifying these geological parameters.

Utilizing the aforementioned relationships and parameters and 150 field observations, Annandale (1995) developed graphical relationships between the erodiblity index and the rate of energy dissipation across a broad range of materials. Further application and validation of the Erodibility Index Method was performed during additional studies on stream bank erosion (Annandale and Parkhill, 1995) and scour in fractured rock media (Annandale et al., 1998). The streambank erosion study showed that the method has the ability to predict the initiation of bank failure and the erodibility of slickensided clays, vegetated soils, and engineered protection such as riprap and bagwalls. The fractured rock study validated the applicability of the erodibility index in predicting rock scour.

**Sediment Transport Mechanics**

Sediment transport in watercourses starts with the process of erosion, whereby soil particles are detached from either rock or their soil mass. It continues with the movement of the soil by either entrainment into water or as bedload along the bottom of the watercourse. This section provides an overview of these processes and some of the parameters affecting sediment transport.

Physical Properties of Sediment. Generally, the solids present in natural soil formations have resulted from the disintegration of rocks and, therefore, are of mineral composition. Coarser soils contain mainly particles of the primary minerals, while clay particles are often composed of secondary minerals developed during soil formation (Hough, 1969).

The grain size distribution of sediments is important to engineers and geologists. From the size distribution, soil properties including strength, porosity, and erodibility may be estimated. Soil gradation is obtained from a mechanical sieve analysis in which the soil is passed through several sieves of varying size. The percent finer of each size can then be calculated and plotted to obtain a graphical representation of the distribution. With respect to sediment transport, the sediment size distribution is essentially a probabilistic approach in characterizing sediment properties (Simons and Senturk, 1977).

Particle size is customarily expressed in terms of a single diameter or the size of the smallest (square) hole, as in a sieve, through which the particle will pass. Standard sizes of sediments with limiting particle diameters are shown in Figure 2.11a. Sediments are roughly subdivided into four main size classes: clay, silt, sand, and gravel (Friedman and Sanders, 1978).

According to the ASTM sediment classifications shown in Figure 2.11b, cohesive sediments generally include both the clay and silt groups, while non-cohesive sediments are associated with the sands and gravels (Fetter, 2001). While particle size may be the primary defining characteristic, cohesiveness generally depends on other sediment properties including sediment composition, clay mineralogy, cation exchange capacity, organic matter content, and water content (Caywood, 1999; Parker, 1993).

In general, quartz particles with diameters greater than 400 microns behave in a cohesionless manner. Quartz particles between 40 and 400 microns will begin to exhibit apparent cohesive effects, but as with larger particles, erosion typically will occur particle by particle. Sediments composed of particles less than 40 microns generally behave in a fully cohesive manner and erode in flocs (Caywood, 1999; Miller et al., 1977).

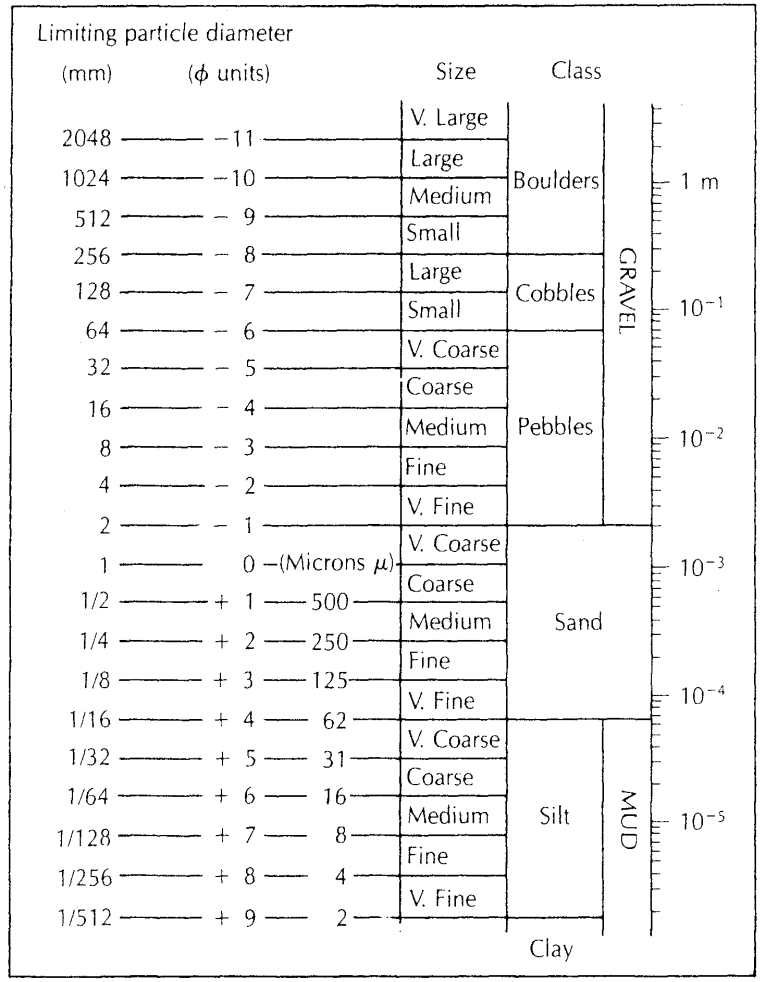


a) Standard sediment sizes (Friedman and Sanders, 1978).

**Cohesive Sediments**

| Size Fraction | Dry Strength | Toughness | Group Symbol |
|---|---|---|---|
| Clay | medium to high | medium | CL |
| Clay | high to very high | high | CH |
| Silt | none to low | none to low | ML |
| Silt | low to medium | low to medium | MH |
| Organic silt or clay | | | OL/OH |

**Coarse-Grained Sediments with fines ≤5%**

| Size Fraction | Grain-Size Sorting | Group Symbol |
|---|---|---|
| Gravel | well sorted | GP |
| Gravel | poorly sorted | GW |
| Sand | well sorted | SP |
| Sand | poorly sorted | SW |

**Coarse-Grained Sediments with fines between 5% and 15%**

| Size Fraction | Grain-Size Sorting | Type of Fines | Group Symbol |
|---|---|---|---|
| Gravel | well sorted | ML or MH | GP-GM |
| Gravel | well sorted | CL or CH | GP-GC |
| Gravel | poorly sorted | ML or MH | GW-GM |
| Gravel | poorly sorted | CL or CH | GW-GC |
| Sand | well sorted | ML or MH | SP-SM |
| Sand | well sorted | CL or CH | SP-SC |
| Sand | poorly sorted | ML or MH | SW-SM |
| Sand | poorly sorted | CL or CH | SW-SC |

**Coarse-Grained Sediments with fines ≥15%**

| Size Fraction | Type of Fines | |
|---|---|---|
| Gravel | ML or MH | GM |
| Gravel | CL or CH | GC |
| Sand | ML or MH | SM |
| Sand | CL or CH | SC |

b) Sediment descriptions, ASTM D 2488 (Fetter, 2001).

**Figure 2.11 Sediment classification charts.**

There are two general classifications of gradation based on the range of the particle sizes (Fetter, 2001). A good gradation (poorly sorted) has a wide range of particle sizes, while a poor gradation (well-sorted) has a relatively narrow range of particle sizes. The Hazen Uniformity Coefficient $C_u$ is a measure of whether sediment is well sorted or poorly sorted. $C_u$ is defined as the ratio of the grain size that is 60% finer by weight ($d_{60}$) to the grain size that is 10% finer by weight ($d_{10}$):

$$C_u = \frac{d_{60}}{d_{10}} \tag{2-4}$$

A soil with $\boldsymbol{C_u}$ less than 4 is generally well sorted; if $\boldsymbol{C_u}$ is less than 6 a soil is considered to be poorly sorted (Fetter, 2001).

An alternative way of classifying the gradation is by calculating the geometric standard deviation of the grain size distribution:

$$\sigma_g = \sqrt{\frac{d_{84.1}}{d_{15.9}}} \tag{2-5}$$

where:

$\sigma_g$ = geometric standard deviation
$d_{84.1}$ = grain size 84.1% finer by weight
$d_{15.9}$ = grain size 15.9% finer by weight

A sediment mixture with a geometric standard deviation less than 1.3 is often termed well sorted and can be treated as uniform material, while a value exceeding 1.6 is generally considered to be poorly sorted (Diplas and Sutherland, 1988).

Fall Velocity. The primary variable defining the interaction of sediment transport with the bed, banks, or suspended in the fluid is the fall velocity of suspended particles (Simons and Senturk, 1977). A particle falling at terminal velocity in a quiescent fluid is driven by the resulting force, which considers the particle buoyant weight and the resisting force resulting from fluid drag. Fluid drag is the result of either the tangential shear stress exerted by the fluid on the particle (skin drag), and/or a pressure difference on the particle (form drag). The general drag equation is:

$$F_D = C_D \rho_f A \left( \frac{\omega^2}{2} \right) \tag{2-6}$$

where:

$F_D$ = drag force
$C_D$ = drag coefficient
$\rho_f$ = density of the fluid
$A$ = projected area of the particle in the direction of fall
$\omega$ = fall velocity of the particle

The drag coefficient $C_D$ may be approximated from the following equation developed by Rubey (1933):

$$C_D = \frac{24}{\mathrm{Re}_p} + 2 \qquad (2\text{-}7)$$

where:

$\mathrm{Re}_p$ = particle Reynolds number

Equation 2-7 encompasses a wide range of particle Reynolds numbers. The following equation for the drag coefficient seems best suited for natural sands and gravels (Julien, 1995):

$$C_D = \frac{24}{\mathrm{Re}_p} + 1.5 \qquad (2\text{-}8)$$

Bed Shear Stress. In open channel flow, the movement of water creates a force on the channel bed which acts in the direction of flow. Chow (1959) identified this force as the tractive force. In a uniform flow, the tractive force is equal to the effective component of the gravity force acting in the body of water, parallel to the channel bottom and equal to $\gamma ALS$, where $\gamma$ is the unit weight of water, $A$ is the wetted area, $L$ is the length of the channel reach, and $S$ is the slope. The average value of the tractive force per unit area, or the unit tractive force per unit area (also known as bed shear stress $\tau_o$) is equal to $\gamma ALS/PL = \gamma RS$, where $P$ is the wetted perimeter and $R$ is the hydraulic radius; that is $\tau_o = \gamma RS$. In wide-open channels, the hydraulic radius is approximately equal to the depth of flow $y$; hence,

$$\tau_o = \gamma y S \qquad (2\text{-}9)$$

Incipient Motion. When the shear stress over a bed attains or exceeds its critical value, particle motion begins, and critical or threshold conditions are said to have been reached (Simons and Senturk, 1977). The problem of defining critical stress conditions associated with the inception of sediment transport is of fundamental importance to stable channel design and protection against erosion and scour.

A number of concepts of incipient motion of sediment particles have been put forward. Many early researchers including Jeffries (1929), Rubey (1938), White (1940), and Tison (1953) attempted to solve the problem of initiation of motion of sediment on plane beds using theoretical analyses with limited results (Law and Engel, 1999). Shields (1936) was more successful in using the empirical approach which resulted in the well known Shields diagram (Figure 2.14). His theory was based on the theory of the laminar sub-layer and that the critical shear stress varies with the particle Reynolds number. Since then, Yalin and Karahan (1979) refined the Shields diagram utilizing much more available data.

The following are other notable theories on incipient motion of sediment particles since Shields (1936). Kurihara (1948) extended the work of White (1940) and proposed empirical equations for the estimation of critical shear stress. Iwagaki (1956) developed a theory for the equilibrium of a single spherical particle placed on a rough sand surface

and found the conditions necessary for the beginning of particle motion. However, in practice, this case seldom occurs due to the existence of other particles. Egiazaroff (1965) presented another derivation for critical shear stress as a function of the particle Reynolds number. Mantz (1977) proposed an extended Shields diagram for flat sedimentary beds for the condition of maximum stability. Wieberg and Smith (1987) derived an expression for critical shear stress by balancing individual particles on the surface of the bed, which is also applicable to non-uniform particles. Recently, Ling (1995) studied the equilibrium of a solitary particle on a sedimentary bed, considering the spinning motion of the particle. Dey (1999) presented a model to compute the critical shear stress for non-cohesive sediments (uniform and non-uniform). The results of this model corresponded closely with the curve proposed by the modified Shields diagram (Figure 2.14) as developed by Yalin and Karahau (1979).

The tractive force acting on a sediment bed will move the soil particles if resisting forces are not sufficient. For coarse sediments (e.g., sands and gravels), the resisting forces are caused mainly by the weight of the particles. Finer grained particles, which consist mainly of silt or clay, generally tend to be more cohesive and resist movement by cohesive forces rather than by the weight of individual grains (ASCE, 1975).

Julien (1995) explained that for non-cohesive particles, the threshold at which the hydrodynamic moment of tractive forces is in balance with the resisting moment of force is the point of incipient motion. At incipient motion, if the tractive force is increased, motion of the particles will occur. As shown in Figure 2.12, the forces acting on a non-cohesive soil particle on a horizontal bed include the particle weight $F_W$, buoyancy force $F_B$, lift force $F_L$, drag force $F_D$, and the resisting force $F_R$. The submerged weight of the particle can be written $F_S = F_W - F_B$. The ratio of hydrodynamic forces $F_L \sim F_D \sim \tau_o d_s^2$ to the submerged weight $F_S \sim (\gamma_s - \gamma_m) d_s^3$ defines the dimensionless shear stress $\tau_*$, also called the Shields parameter:

$$\tau_* = \frac{\tau_o}{(\gamma_s - \gamma_m) d_s} \tag{2-10}$$

where:

$\tau_o$ = boundary shear stress or bed shear stress
$\gamma_s$ = specific weight of sediment particle
$\gamma_m$ = specific weight of fluid mixture (fluid and suspended particles)
$d_s$ = mean particle size (usually taken as $d_{50}$)

The critical value of the Shields parameter $\tau_{*c}$, corresponding to the initiation of particle motion ($\tau_o = \tau_c$) depends on whether laminar or turbulent flow conditions prevail around a particle. Besides the angle of repose, the ratio of the sediment size to the laminar sublayer thickness expressed as the grain shear Reynolds number $R_{e*} = u_* d_s / \nu_m$ is considered:

$$\tau_{*_c} = \frac{\tau_c}{(\gamma_s - \gamma_m) d_s} = f(R_{e*}, \tan\phi) \tag{2-11}$$

where:

$u_*$ = shear velocity
$v_m$ = kinematic viscosity
$\tau_c$ = critical shear stress
$\phi$ = angle of repose (Figure 2.13).

Shields laboratory experiments and those of Yalin and Karahan (1979) using the median grain size for $d_s$ led to the modified Shields diagram shown in Figure 2.14. The critical values of the Shields parameter $\tau_{*c}$ can be approximated as follows:

$\tau_{*c} = 0.5 \tan\phi$ when $d_* < 0.3$ (2-12a)
$\tau_{*c} = 0.25 d_*^{-0.6} \tan\phi$ when $0.3 < d_* < 19$ (2-12b)
$\tau_{*c} = 0.013 d_*^{0.4} \tan\phi$ when $19 < d_* < 50$ (2-12c)
$\tau_{*c} = 0.06 \tan\phi$ when $d_* > 50$ (2-12d)

where the dimensionless particle diameter $d_*$ is defined as:

$$d_* = d_s \left[ \frac{(G-1)g}{v_m^2} \right]^{\frac{1}{3}} \quad (2\text{-}13)$$

and where:

$G$ = specific gravity of the sediment
$g$ = acceleration due to gravity

To simplify the calculations, a graphical relationship between critical shear stress $\tau_c$ and median grain size $d_{50}$ on a flat horizontal surface has been developed (Figure 2.15). This chart is based on a comparison of data from the Highway Research Board (1970) and can be used for the design of channels. This graphical approximation provides reasonable results for the determination of median grain size if the shear stress is known, or the maximum permissible shear stress if the grain size is given.

The aforementioned equations were developed based on a horizontal bed and do not account for the decreased stability of a particle resting on a slope (e.g., sloping bed or channel bank). A sediment grain on a slope is less stable than one on a horizontal bed because the gravitational force tends to move it downward. As a result, particles on slopes will have lower associated critical shear stresses because it will take less force to cause particle motion. Lane (1955) gives the following relationship between the critical shear stress on a channel bank $\tau_{wc}$ to that of a similar particle on a horizontal bed $\tau_c$ as:

$$\tau_{wc} = \tau_c \cos\theta_1 \left[ 1 - \left( \frac{\tan\theta_1}{\tan\phi} \right)^2 \right]^{\frac{1}{2}} \quad (2\text{-}14)$$

where:

$\theta_1$ = slope of the channel bank

Similarly, the shear stress on a sloping bed $\tau_{c\theta}$ can be expressed as:

$$\tau_{c\theta} = \tau_c \cos\theta \left[ 1 - \left( \frac{\tan\theta}{\tan\phi} \right) \right] \qquad (2\text{-}15)$$

where:

$\theta$ = slope of the bed ($\theta$ is positive for downward sloping beds)

Sediment Transport Modes. The most common modes of sediment transport in streams and rivers are those of bedload and suspended load. In the former case, the particles roll, slide, or bounce over each other, never deviating too far above the bed. Turbulence can affect the entrainment of sediment particles in a number of ways (Raudkivi, 1990). Particles may be moved by the drag exerted by a passing eddy. Eddies may lower the local pressure and the particles may be ejected from the bed by hydrostatic pressure (Kirkbride, 1993). Entrained particles may be suspended into the flow rather than move along the channel bed surface.

Kirkbride (1993) observed two modes of sediment entrainment. Finer particles react dominantly to the upward forces due to eddying caused by roughness elements. Only downstream rushes of velocity entrained larger particles. The entrainment is related to the flow intermittency associated with turbulence structures.

Bedforms. Once sediment particles are in motion, the random patterns of erosion and sedimentation will generate small perturbations of the bed surface elevation. In subcritical flow, the upstream and downstream faces of these perturbations will experience differential bed shear stresses. The upstream face, under greater shear stress, will promote further erosion and sediment transport. Conversely, the decreased shear stress downstream induces sedimentation on the lee side of the perturbation. This mechanism causes amplification of the perturbation until large bedforms fully develop (e.g., dunes). Under supercritical flow conditions, however, the shear stress distribution is reversed, with the downstream face experiencing the higher boundary shear stress. Although the sediment particles are transported downstream, bedforms migrate upstream under supercritical flow conditions as sediment deposition occurs on the upstream face while erosion occurs on the downstream face (Julien, 1995).

Bedforms may have a significant effect on the flow structure. The nature of the flow field will change as bedforms modify the bed roughness and as suspended sediment is added to the flow. Though flow structure controls sediment motion, the structure itself is influenced by grain and form-roughness, and quantity and type of suspended load (Best, 1996).

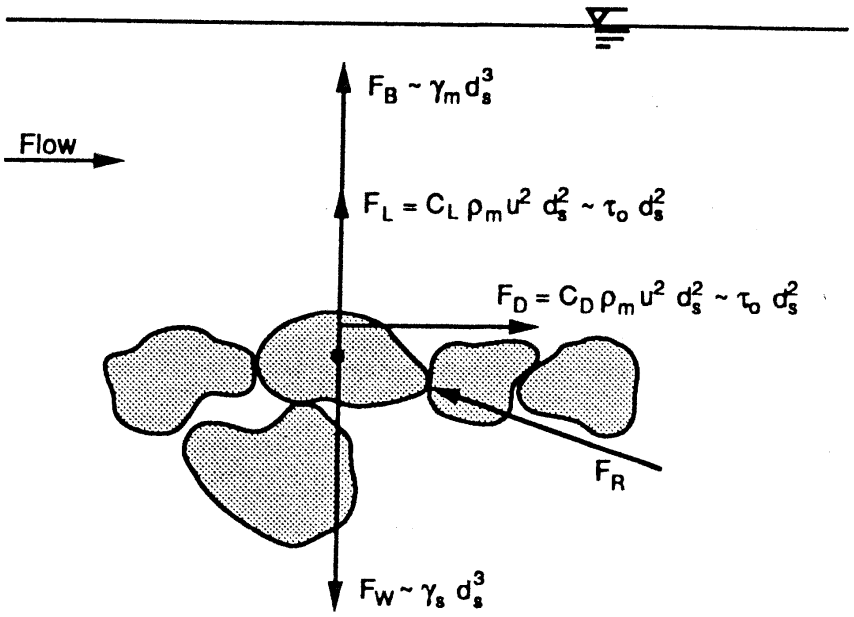


**Figure 2.12 Force diagram under steady uniform flow conditions (Julien, 1995).**

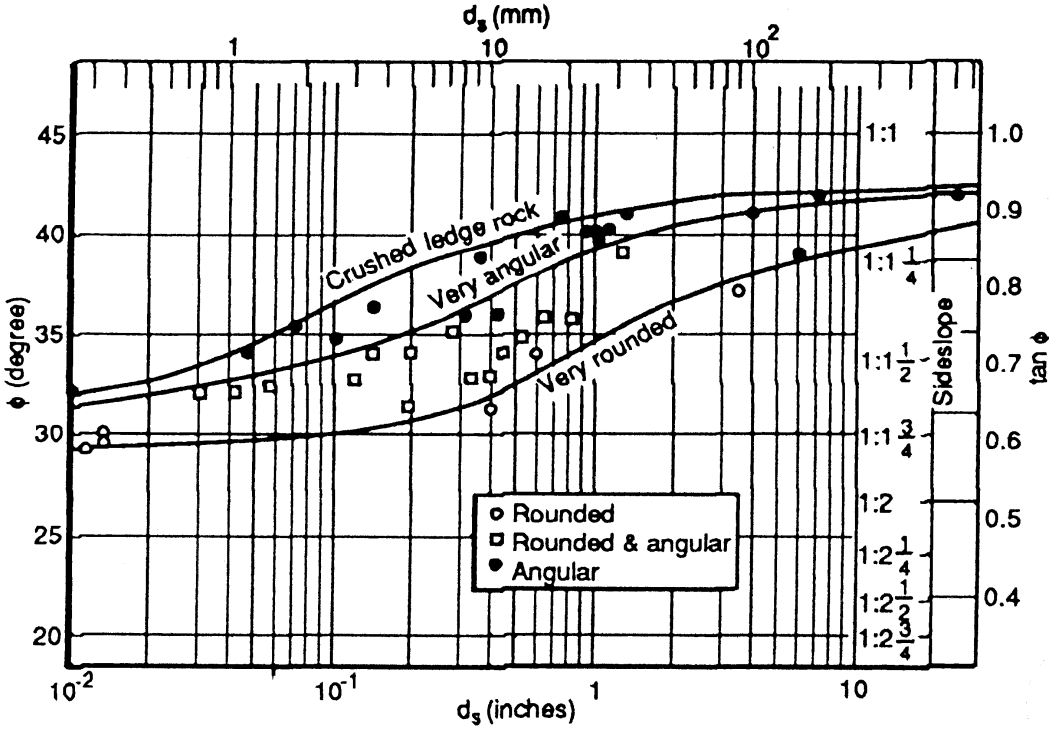


**Figure 2.13 Angle of repose for granular material (Simons, 1957).**

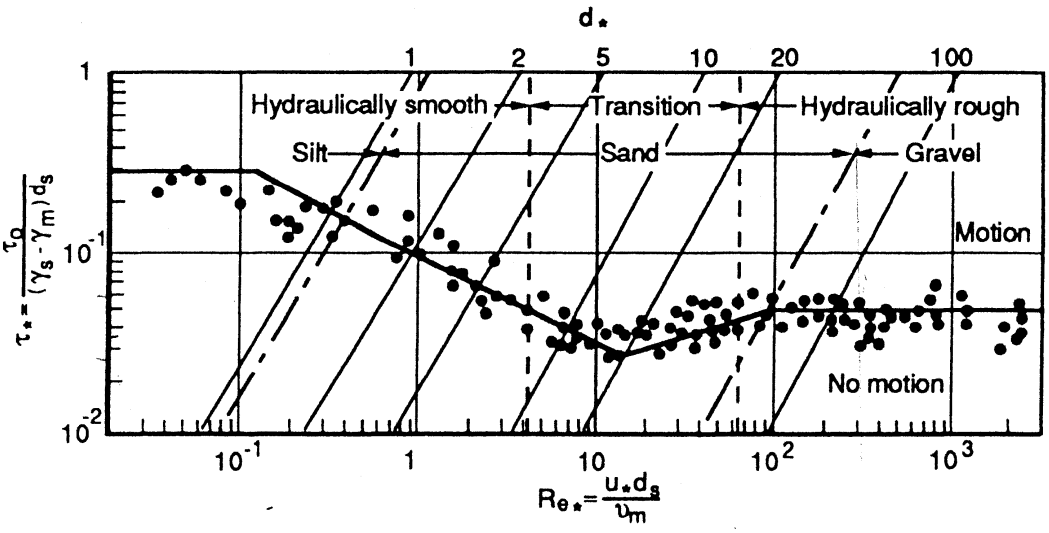


**Figure 2.14 Modified Shields diagram (Julien, 1995).**

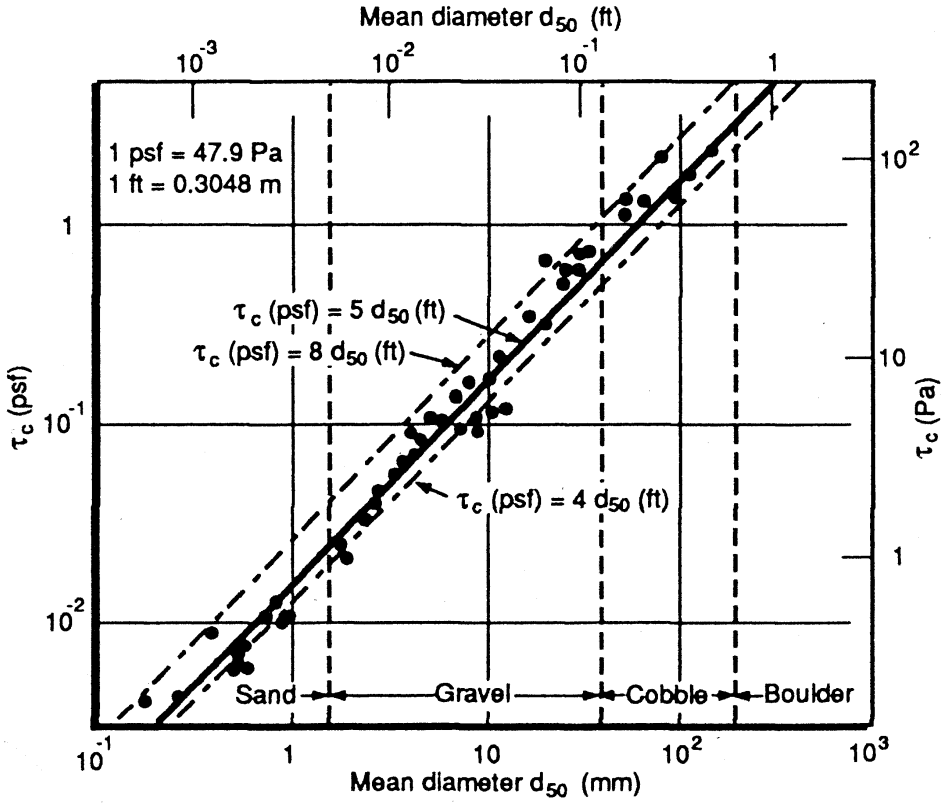


**Figure 2.15 Critical shear stress on a horizontal surface (Julien, 1995).**

As described below, a variety of sediment structures can form on the streambed or riverbed including ripples, dunes, antidunes, and alternate bars (Figure 2.16). These sediment structures can have a profound effect on the resistance to flow, thus affecting the depth of flow (ASCE, 1975). Since shear stress is proportional to flow depth (Equation 2-9), one would expect increased erosion with an increase in depth, and vise versa.

Bedforms may take on several different configurations depending on the slope of the energy grade line, flow depth, and the size and fall velocity of the sediment particles. Common bedforms shown in Figure 2.16 are arranged in order of increasing transport rate (Simons and Richardson, 1966).

Bedforms are associated with two flow regimes. The lower regime is characteristic of subcritical flow and begins with the onset of particle motion (Simons and Senturk, 1977). The resistance to flow is high due to the ripple or dune bedforms, and sediment transport is relatively small. The water surface undulations, if they exist, are out of phase with the bed surface, and there is a relatively large separation zone downstream from the crest of each ripple or dune (Figures 2.16 b and 2.16 c). The most common mode of bed material transport is either (1) individual sediment particles move up the backs of ripples or dunes and avalanche down the face, or (2) particles advance to the face of the ripple or dune from the downstream direction. The upper regime is characteristic of higher flow velocities where resistance to flow is relatively small and sediment transport is large. The usual bedforms are plane bed or anti-dunes (Figure 2.16 e and 2.16 f). The resistance to flow is the predominately the result of grain roughness. The mode of transport is for individual grains to roll almost continuously downstream in sheets, one to several grain diameters thick.

Ripples occur at lower transport rates and flow velocities and rarely occur in sediments coarser than approximately 0.6 mm (ASCE, 1966). They are small bedforms with wavelengths less than approximately 1 foot and heights less than approximately 2 inches. In longitudinal section, ripple profiles are approximately triangular with long gentle upstream slopes and short steep downstream slopes. Bars are bed forms having lengths of the same order as the channel width or greater, and heights comparable to the mean depth of the generating flow. Bars generated by high flows frequently appear as small islands during low flows (Simons and Senturk, 1977).

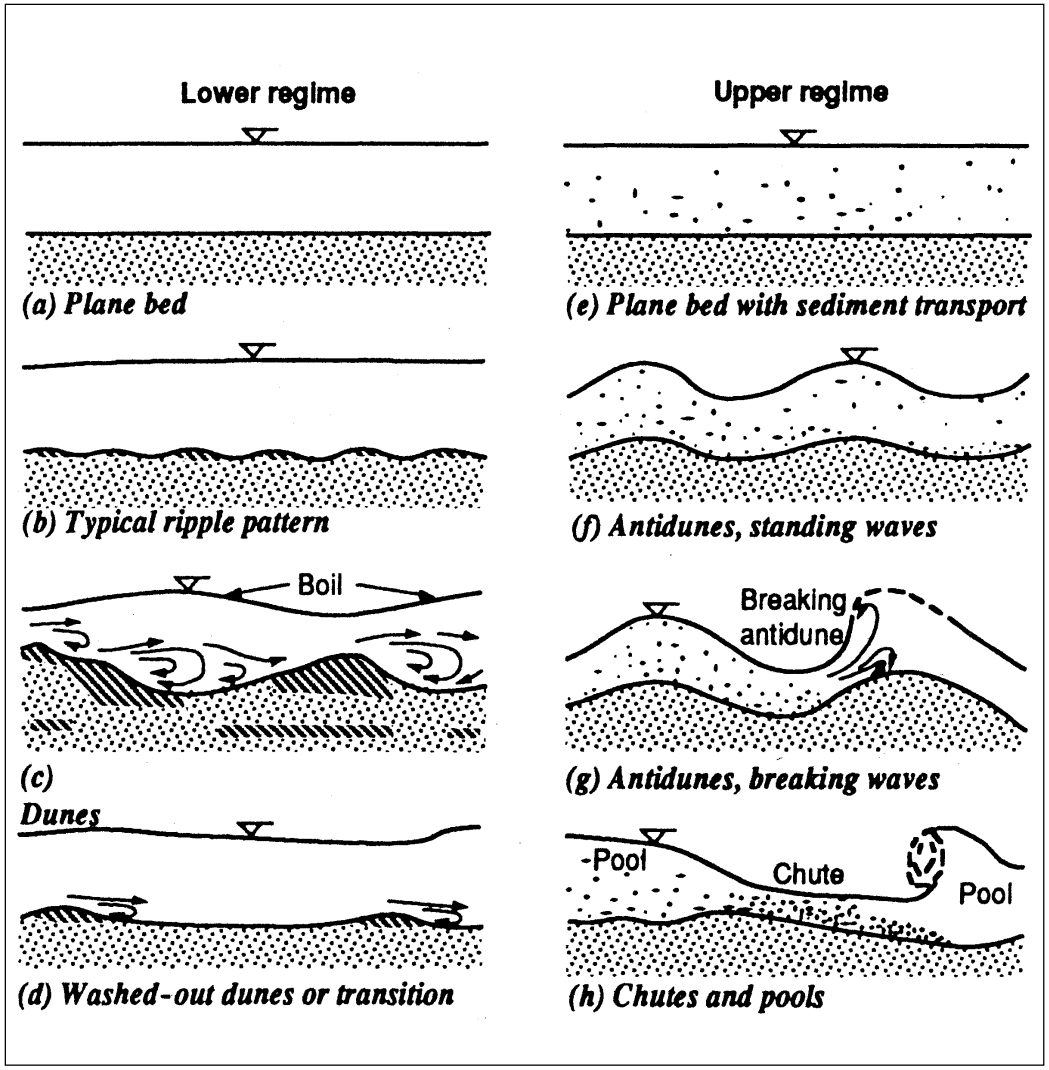


**Figure 2.16 Bedforms (Simons and Richardson, 1966).**

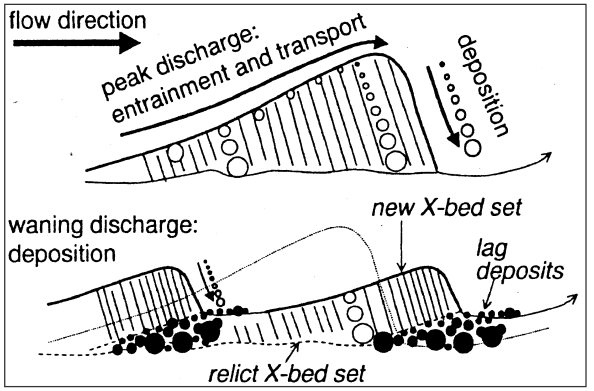


**Figure 2.17 Dune propagation (Kleinhans, 2001).**

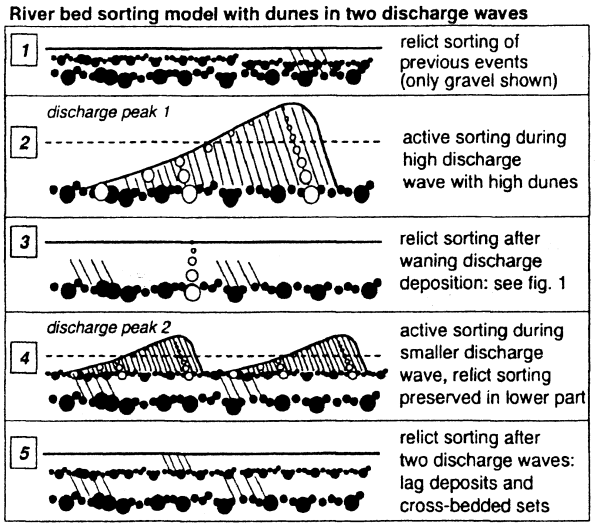


**Figure 2.18 Riverbed sorting model**

Dunes are larger than ripples, but smaller than bars. They generally occur at higher transport rates and are the most common bedform in all but very small streams. Their profile is typically out of phase with the water surface profile. Dunes have been observed to range in size from 0.2 feet high by 2 feet long in an 8-foot wide flume to 40 feet high by several hundred feet long in the Mississippi River (Carey and Keller, 1957).

A well-known feature of dunes in rivers is the cross-bedded deposit, resulting from avalanching of bedload sediment at the lee side of a dune during propagation. As shown in Figure 2.17, the sediment becomes sorted vertically; gravel is mainly deposited on the lower half of the lee slope, while finer particles are predominately deposited on the upper half. The result is an upward fining deposit with cross bedding. Figure 2.18 shows a conceptual model of sediment transport and deposition resulting in the formation of dunes (Kleinhans, 2001). This model, which is an extension of the work by Klaassen et al. (1987), consists of five steps including two discharge waves in order of decreasing magnitude, resulting in lag deposits and cross-bedded sets.

When certain flow conditions occur, dunes are washed out and a plane bed with sediment transport develops and the flow changes from a transitional state to an upper-stage plane bed or anti-dune state (Simons and Senturk, 1977). Upper-stage plane beds are generally associated with relatively large bedloads as well as large suspended load transport rates (Bennett et al., 1998). Studies in the transition from dune to upper-stage plane beds revealed that upper-stage plane beds exist only above a certain threshold of suspended sediment concentration at which bedform development is suppressed (Chakraborty and Bose, 1992; Allen, 1993; Oost and Baas, 1994; Sarker et al., 1999). Thus, upper-stage plane beds would not be expected in streams with a low suspended sediment load.

In coarse sands, dunes are replaced at higher flow velocity by anti-dunes instead of upper-stage plane beds (Williams, 1967; Southard and Boguchwal, 1990). In shallow flows over coarse sands, the Froude number required to generate antidunes is generally attained before the flow is able to suspend enough sediment to suppress turbulence for the generation of upper-stage plane beds (Best, 1996).

Chutes and pools occur in channels having relatively steep slopes with high flow velocities and high sediment discharges. These bedforms consist of large elongated mounds of sediment. The flow is supercritical within the chutes; pools form between subsequent chutes (Simons and Senturk, 1977).

There are a large number of variables affecting the formation of bedforms (e.g., flow velocity, depth, energy gradeline, sediment properties, etc.)(Simons and Senturk, 1977). Some of the variables change with the flow conditions and alter their roles from dependant to independent. This interdependency among the variables makes the analysis of flow extremely complex. Simons and Richardson (1965) reported a comprehensive study of variables affecting bedforms and flow characteristics and the conditions in which a dependent variable changes into an independent one, or vise versa.

Turbulent Boundary Layer. Most flows that transport sediment are turbulent boundary layer flows, and the forces exerted on sediment grains, both those resting on the bed and those in transport, are governed by the characteristics of the turbulence (Middleton and Southard, 1984). A boundary layer is the zone of flow in the immediate vicinity of a solid surface (e.g., channel wall or bed) in which the motion of the fluid is affected by the frictional resistance of the boundary (e.g., particle size and bedforms). Flow in boundaries may be either laminar or turbulent. Since fluid does not slip at solid boundaries, all turbulent components must vanish at the walls and remain very small in their immediate neighborhood (Julien, 1995).

In turbulent flows, laminar motion must persist in a very thin layer next to the wall. This is known as the laminar sublayer. Two types of boundary conditions are recognized depending on the relative magnitude of the grain size $d_s$ and the laminar sublayer thickness $\delta$. Conceptually, the boundary is said to be hydraulically smooth when $\delta >> d_s$ and, conversely, hydraulically rough when $\delta << d_s$. A transition zone is also recognized, as shown in Figure 2.19. In all turbulent flows, the laminar sublayer thickness $\delta$, can be determined by the following equation (Julien, 1995):

$$\delta = \frac{11.6 v_m}{u_*} \tag{2-16}$$

where:

$v_m$ = kinematic viscosity
$u_*$ = shear velocity

Grain and form roughness may greatly modify the turbulent boundary layer (TBL) structure and introduce many complexities when considering the entrainment of sediment (Clifford et al., 1993). For example, viscous drag forces acting on particles in a smooth boundary (grains enclosed in the laminar sublayer) are a major component of the total drag. Lift forces due to unequal pressure distribution are probably small. The resultant force acts along a line well above the particle center of gravity. In contrast, in rough boundary conditions, the particles are more exposed, which produces a turbulent wake behind the particle. This reduces the viscous drag force; however, lift forces approach 0.8 times the magnitude of the drag forces. The resultant force acts through, or close to, the center of gravity of the soil particle (Middleton and Southard, 1984).

Turbulence – Particle Interaction. Turbulent Boundary Layer (TBL) research has provided valuable insights into particle fluid interactions, which have enhanced our understanding of the mechanisms of sediment transport and bedform genesis. However, there are still significant gaps in our understanding such as quantitative data on bedform dynamics and the influence of the concentration of suspended particles on turbulence structure and bedform morphology (Mazumder, 2000).

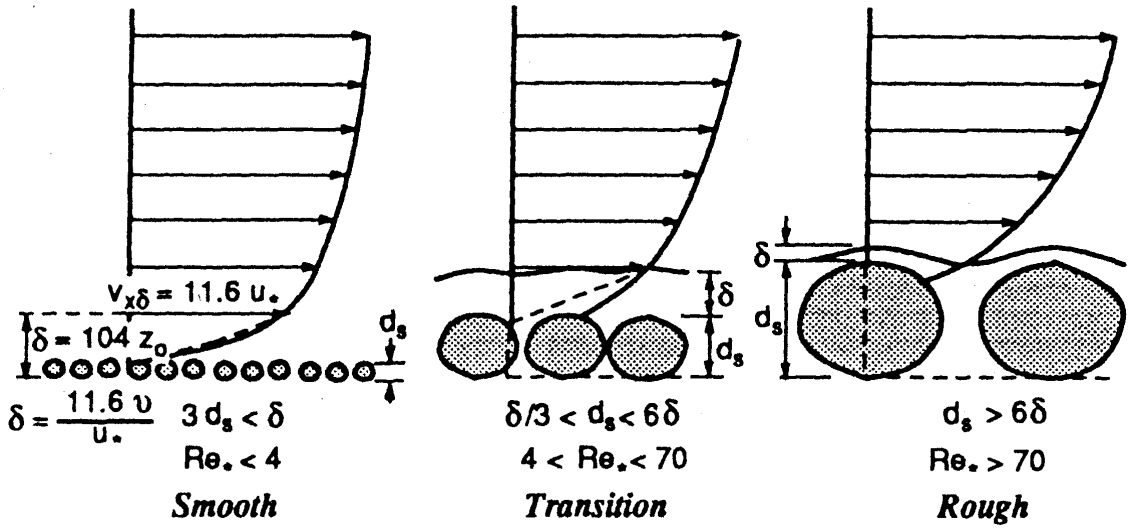


**Figure 2.19 Hydraulically smooth and rough boundaries (Julien, 1995).**

The behavior of solid particles and their interaction with coherent flow structures (e.g., eddies and vortices) in the TBL is of considerable importance for gaining insights into the mechanisms of sediment transport. A vortex developing over a sediment particle that is at rest can lift it and entrain it. Particle transport may proceed in several ways depending on proper combination of density ratio, trajectory, and inertia and kinetic energy of the particle and fluid (Kaftori et al., 1995). Three categories of coherent flow structures have been reported (Kaftori et al., 1995): (1) persistent streamwise corkscrew vortices in counter-rotating pairs very close to the wall (Figure 2.20); (2) periodic disruption and lifting of the fluid from the inner region into the outer parts as steeply inclined hairpins or horseshoe vortices (Figure 2.21); and (3) large eddies that grow over a significant period by combination of hairpin vortices to a scale comparable to the TBL thickness. The corkscrew vortices periodically experience sudden disruption (bursting) during which low momentum fluid is drawn outward from the inner region to the high-velocity regions of the TBL in the form of a hairpin vortex (Mazumder, 2000).

Kaftori et al. (1994) suggested that various coherent structures are manifestations of one underlying large-scale structure, a funnel-shaped streamwise vortex that expands sidewise and outward from the wall in the form of a spiral facing in the downstream direction (Figure 2.22). Particles spend more time inside the funnel vortices than elsewhere and if there is a net downward movement of the particles inside the vortices, there are chances of deposition. The role of funnel vortices has been confirmed by several researchers (McLaughin, 1989; Brooke et al., 1992; Kaftori et al., 1995).

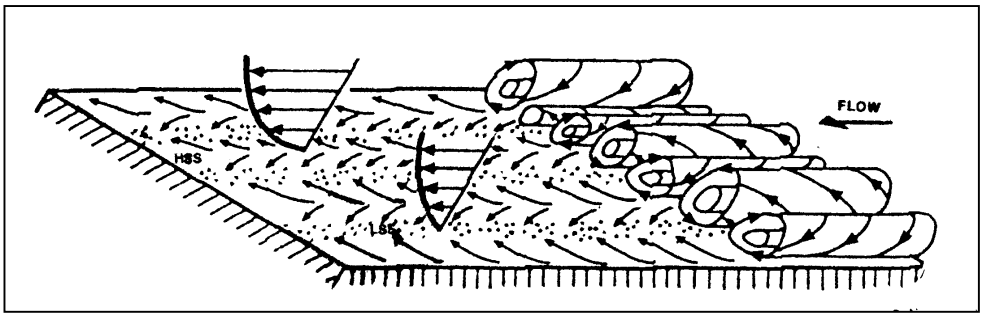


**Figure 2.20 Vortices in the turbulent boundary layer (Mazumder, 2000; Allen, 1994).**

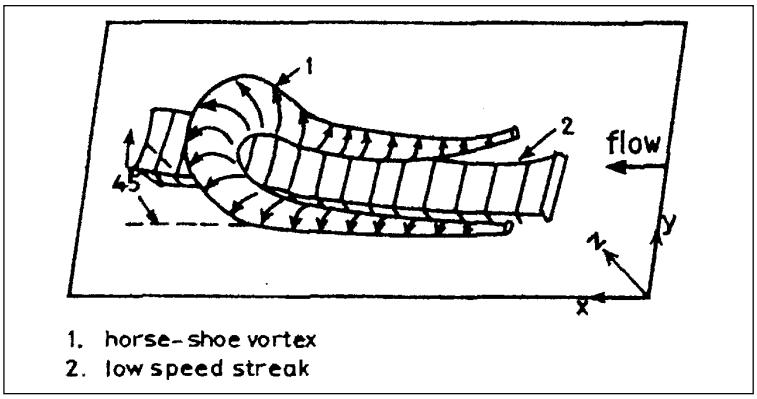


**Figure 2.21 Horseshoe vortex (Mazumder, 2000; Banerjee, 1992).**

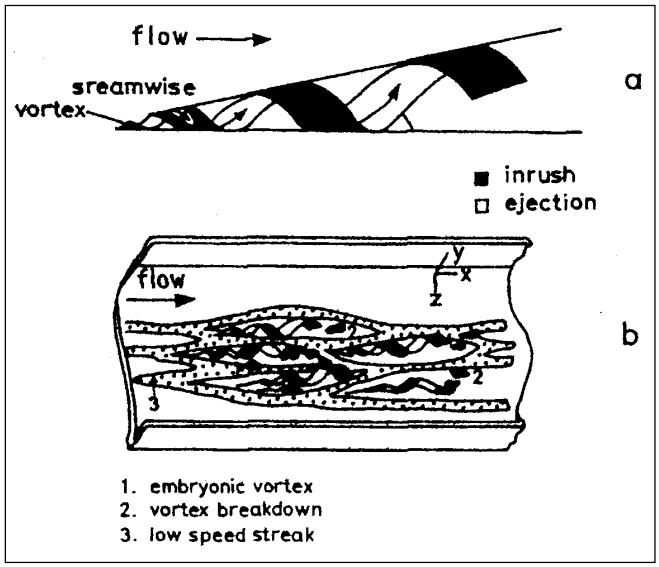


**Figure 2.22 Funnel vortex (Mazumder, 2000; Kaftori et al., 1995).**

**Erosion Mitigation**

Because of the negative impacts that erosion can have on water quality, slope stability, and maintenance costs, strategies to limit erosion need to be implemented. This section provides an overview of current erosion control technology, examines erosion mitigation within the Clear Creek watershed, and summarizes the performance evaluation of rolled erosion control products (RECPs).

Erosion Mitigation Techniques. Ffolliott et al. (1995) summarized a number of actions that can be taken to limit the progression of surface erosion. These include: (1) protecting the soil surface against the impact of raindrops; (2) increasing the roughness of the soil surface in order to reduce the velocities of surface flows; (3) reducing the inclination of slopes; (4) increasing the infiltration capacity of soils in order to reduce the quantity of surface runoff; and (5) preventing the concentration of overland flow. In most cases, significant surface erosion can be prevented or minimized using appropriate vegetative management practices (Ffolliott et al., 1995). Thus, the implementation of erosion control strategies that improve the infiltration of water into a soil will generally improve the opportunity for plant growth that can eventually lead to the development of a protective vegetative cover.

The selection of appropriate strategies to prevent and/or control erosion of soils and the transport of sediments must consider site-specific conditions such as land use, existing structures, hydrology, climate, soil type, and topography (Dennison, 1996). In locations where significant surface erosion has already occurred, structural and/or mechanical erosion control strategies must typically be employed in order to reduce surface erosion until a protective vegetative cover can be established (Ffolliott *et al.*, 1995).

Structural and mechanical controls are typically designed to reduce the erosive energy of flowing water. Examples of structural erosion control strategies include the construction of pipe slope drains, energy dissipaters, check dams, and terraces as well as the installation of gabions and channel linings such as rip rap. Examples of mechanical controls include contour furrows, contour trenches, pitting, and basins. The main disadvantage of structural and mechanical erosion control strategies is their relatively high cost.

As mentioned previously, the most effective long-term methods for controlling surface erosion are based on establishing and maintaining a cover of protective vegetation (Ffolliott et al., 1995). A variety of erosion control strategies involve the application of temporary or permanent surface materials or treatments that are designed to promote the establishment of a protective vegetative cover over time. Examples of these surface treatments include topsoiling, mulching, chemical stabilization, and erosion control blankets and mats.

Topsoiling may be used when the existing soil is not suitable for establishing vegetation because of acidity, low nutrient content, poor texture, or other conditions

(Roberts, 1995). In general, topsoiling is not recommended on slopes steeper than 2 horizontal to 1 vertical (Roberts, 1995).

Mulching is typically a temporary erosion control method that protects soil from the impact of rainfall and overland flow. Mulching also promotes retention of moisture within the soil horizon, which encourages the growth of vegetation. The materials commonly used for mulching may be organic or synthetic and include hay, straw, fiber mulch, and soil binders (Roberts, 1995).

Chemical stabilization techniques can also be used to stabilize and protect the soil surface (Roberts, 1995) or promote the aggregation of soil particles within the soil horizon (Haigh, 2000). Chemical stabilization involves the application of soil binders or tackifiers such as emulsified asphalt, nonasphaltic emulsions, polyvinyl acetate, and acrylic copolymers. These soil binders may be used alone or in conjunction with mulches. The application of soil binders is only a temporary method for controlling erosion since they typically decompose within 90 days (Roberts, 1995). In addition, commercially available soil binders are relatively expensive, are usually designed for agricultural use, and do not work reliably on all soils (Haigh, 2000).

Erosion control blankets (ECBs) may be used to control erosion while providing time for vegetation to become established. The primary function of an ECB is to control temporary erosion until vegetation is established. A secondary function is to promote germination of the seed by maintaining moisture and temperature, which is critical for seed germination (Chirbas and Urroz, 1999). ECBs provide important protection against periodic, highly erosive overland flows that are common in drought prone regions where vegetation is typically slow to develop (Bhandari et al., 1998). Erosion control blankets may be organic or synthetic. Organic blankets may be composed of wood fibers (excelsior), jute net, or coconut coir fiber (Roberts, 1995; Bhandari et al., 1998). The typical life expectancy of an ECB is between 10 months and 3 years, depending on the degradable component (Chirbas and Urroz, 1999). However, coconut coir blankets are relatively resistant to decay and may last for as long as five to ten years in arid regions.

Synthetic ECBs or mats (e.g., gabions, mattresses, geogrids, geomats, geocells, and geowebs) are typically constructed of non-biodegradable materials and will last for many years (Bhandari et al., 1998; Rickson, 1995). The two main categories of synthetic ECBs include turf reinforcement mats (TRMs) and erosion control and revegetation mats (Roberts, 1995). These mats are typically permanently installed and allow vegetation to grow through surface of the mats.

TRMs typically consist of a variety of three-dimensional matrices composed of synthetic fibers and filaments. These fibers and filaments consist mainly of polyamides (nylon), polyolefins (propylene and ethylene), and polyvinyl chloride (PVC). The primary function of a TRM is to provide permanent reinforcement for the vegetation during higher hydraulic flow events where velocities and shear stresses exceed the limits of mature, natural vegetation. A secondary, and more temporary, function is to collect

sediments during the hydraulic flows prior to, and while, vegetation is being established (Chirbus and Urroz, 1999). TRM and ECB erosion control products are collectively referred to as Rolled Erosion Control Products (RECPs).

Erosion Mitigation within the Clear Creek Watershed. The most severe erosion along U.S. Highway 50 typically occurs at the discharge of culverts. In some locations, the free discharge of culverts onto unstable hillslopes has resulted in the formation of gullies as shown in Figures 2.23 and 2.24. In a number of other locations, there is evidence of additional surface erosion due to overtopping of the curb and gutter along the outer edge of the roadway shoulder.

Steep slopes, shallow soil profiles with low permeability, a lack of nutrients and organic matter in the soils, and limited vegetative cover exacerbate erosion along Highway 50. Also, the cold and dry climate in the higher elevations of the Sierra Nevada mountains is not very favorable for growth of natural vegetation. Thus, the soils in this region are highly susceptible to erosion.

In order to prevent or effectively control the formation of gullies, the gradient of hillslopes must be stabilized and abrupt changes in elevation must be eliminated. Check dams are often an effective structural erosion control strategy for controlling gully erosion (Ffolliott et al., 1995). Another alternative that has been used at some culverts along Highway 50, as shown in Figure 2.25, is a pipe slope drain that conveys water from the top to the bottom of the slope. Pipe slope drains are commonly used in conjunction with diversion dikes or swales constructed at the top of a slope (Goldman et al., 1986). The installation of channel linings such as riprap has also been effective at some locations along Highway 50 as shown in Figure 2.26. Each of these strategies for mitigating gully erosion is relatively expensive and difficult to construct and/or install.

**Figure 2.23 Culvert with free discharge.**

**Figure 2.24 Gully erosion from culvert.**

**Figure 2.25 Culvert slope drain.**

**Figure 2.26 Riprap channel protection.**

Performance Evaluation of RECPs. Since the 1940s, many laboratory and field experiments have been conducted by a number of researchers to determine the permissible shear stress of flexible channel lining systems. These tests typically compared the soil loss from a channel that had been covered to that of a bare soil control. Tests were performed, both in non-vegetated and in vegetated conditions, on a variety of different soil types and flow conditions. Testing various products under similar conditions provided a means of comparison between products; however, as yet, government, academia, and industry have not adopted a standard method for testing the performance of channel lining systems (Gharabaghi et al., 1994; Clopper and Byars, 1998).

The lack of performance standards for RECPs have led manufacturers, in many cases, to develop their own tests, procedures, and failure criteria in order to evaluate their products' performance (Chirbas and Urroz, 1999). Manufacturers use a number of organizations (e.g., trade associations, academic institutions, as well as government and private laboratories) to develop protocols for testing their products. These tests generally fall into two categories: 1) index properties and 2) performance properties. Index properties typically refer to inherent physical/mechanical characteristics, such as mass per unit area, thickness, and tensile strength. Performance properties generally refer to product characteristics such as maximum permissible shear stress.

Manufacturers typically use index testing as a measure of quality control (Chirbas and Urroz, 1999). Index tests have been, or are in the process of being, standardized through independent organizations such as the American Society for Testing Materials (ASTM) and the Erosion Control Technology Council (ECTC). Performance testing is much more complicated and sometimes controversial.

Efforts are underway by the ECTC to establish erosion control industry standards for terminology, index tests, and performance criteria (Allen, 1996). Subsequent work on Index Property Standards has led to the Technical Guidance Manual for RECPs. Table 2.5 summarizes the current recommended standards based on index properties.

**Table 2.5 Index Test Matrix for RECPs (Allen, 2001)**

| Parameter | Method Test Based On | |
|---|---|---|
| | ECBs | TRMs |
| Thickness (Wet & Dry) | ASTM D6525 | ASTM D6525 |
| Mass per unit area | ASTM D6475 | ASTM D6566 |
| Stiffness | ASTM D6575 | ASTM D6575 |
| Water Absorption | ASTM D1117/Allen, 2001 | ASTM D1117/Allen, 2001 |
| Swell | Allen, 2001 | - |
| Resiliency | ASTM D6524 | ASTM D6524 |
| Tensile Properties | ASTM D5035/Allen, 2001 | ASTM D5035/Allen, 2001 |
| Smolder resistance | Allen, 2001 | - |
| Light penetration | ASTM D6567 | ASTM D6567 |
| Porosity and open volume | Allen, 2001 | Allen, 2001 |
| Specific Gravity and Density | ASTM D792 | ASTM D792 |
| Compression | - | ASTM D6454 |

The preferred criterion for selection of RECPs is performance in lieu of index properties (Chirbas and Urroz, 1999). While different products may have widely different index properties, these products may exhibit very similar performance. Since index property testing is more standardized, some efforts have been made to correlate relationships between index properties and performance (Fifield and Manor, 1990; Fifield, 1992). Presently, however, there is no consensus on whether such correlations exist. In the meantime, the most prudent method for determining field performance is to conduct performance testing.

Experiments by Gharabaghi et al. (1999) have shown that the most influential RECP index properties with respect to erosion control performance are permittivity (ASTM D4491) and initial tensile modulus (ASTM D4595). Permittivity is a measure of the ability of water to pass through an RECP, directly influencing their role as turbidity curtains in erosion control. Less permeable liners can prevent eroded sediments from entraining in the higher velocity flow above the liner. Liners with higher tensile strength and flexural rigidity can have less deformation due to hydrodynamic shear-drag and uplift forces of flow and can remain in close contact with the soil surface.

Normally, performance tests are performed for two common site conditions: slope and channel protection (Chirbas and Urroz, 1999). Testing alternatives include both vegetated and non-vegetated conditions. Slope protection tests may be conducted at varying slope angles, with or without simulated rainfall. Channel testing is usually performed in flumes of either rectangular or trapezoidal section.

During channel testing, the bed shear stress applied to the soil and sediment samples placed in a channel can be adjusted by varying the depth of the flow, the approach velocity of the flow, and the bed slope of the channel. The critical shear stress is the bed shear stress required to initiate the erosion and/or resuspension of particles. When the bed shear stress is below the critical shear stress, no erosion or resuspension will occur. When the bed shear stress is exceeded, particles will be eroded and transported (Dennett, 1995; Dennett et al., 1998; and Ravisangar et al., 2001).

The evaluation of the performance of RECPs has usually been based on one or more of the following criteria: (1) average soil loss (failure due to sediment transport); (2) RECP deformation (failure due to ripples, sags, and tears); (3) vegetation growth (density over one growing season); and (4) durability (degradation due to photodegradation or biodegradation) (Gharabaghi et al., 1999).

Generally, RECPs are made of highly flexible, permeable, and buoyant materials. Particularly prior to the establishment of vegetation, buoyant forces along with hydrodynamic shear-drag and uplift forces can cause RECPs to float above the bed and separate from the soil surface, allowing a portion of the flow to 'pipe' between the bed and the liner and to generate a wavy-geometry liner (Figure 2.27). Vertical oscillation of the liner can cause significant turbulence below the liner, resulting in additional erosion. Therefore, flow in an open channel lined with a RECP can be classified as turbulent, free-surface, shear flow over a wavy, permeable, and moveable boundary (Gharabaghi et al., 1999). This flow 'piping' effect can result in the erosion and transport of large quantities of soil at the bed surface. The Erosion Control Industry has defined a new concept called 'soil failure' which occurs when the top 1.0-centimeter of soil is washed away during a single 30-minute flow event (Gharabaghi et al., 1999).

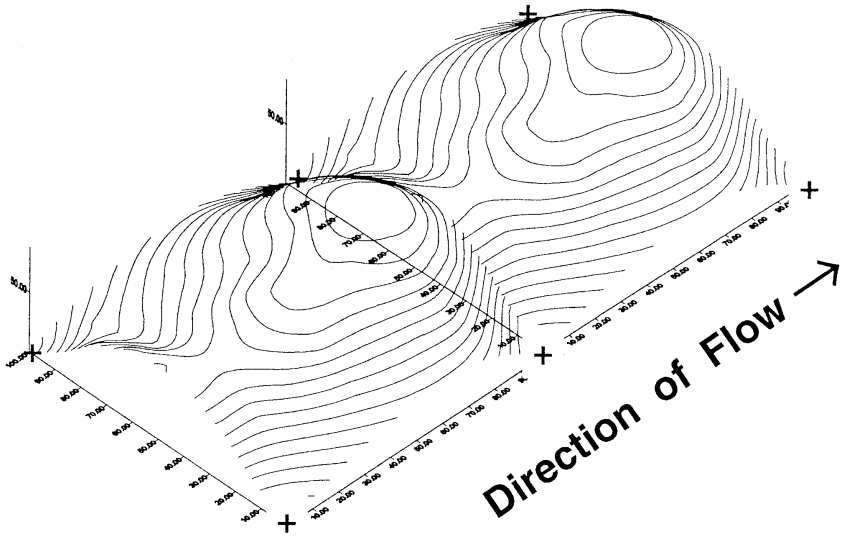


**Figure 2.27 Floated geometry of RECPs (Gharabaghi et al., 1999).**

As previously mentioned, several organizations have developed performance-testing protocol for the evaluation of RECPs. Below are some examples showing the variance in testing procedures for channel applications.

ASTM has developed a standard performance test method (D 6460) for the evaluation of ECBs (ASTM, 2000a). The method provides a comparative evaluation of an ECB to baseline soil conditions under controlled and documented conditions. This method employs a straight 80-foot long trapezoidal flume set a 10% maximum slope. A flow up to 30 cfs is recommended to reach the targeted shear stresses of 1.0, 2.0, 3.0, and 4.0 lbs/sf. The test duration for each targeted shear stress is 30 minutes or until catastrophic channel erosion is observed. The lining material is not removed between subsequent test runs at the target shear stresses. The recommended soil gradation has a median particle diameter of approximately 0.6 mm.

Channel liner testing at Utah State University (USU) has been performed in a rectangular, 4-foot wide by 48-foot long flume with velocities ranging from 2 to 20 fps (Chirbas and Urroz, 1999). The soil bed consisted of either sandy-loam or clay-loam compacted to 90% Proctor density. RECPs were subjected to a series of short duration runs (30 minutes) and a long duration run (50 hours). Failure criteria used to terminate the long duration run typically included excessive material damage, excessive soil exposure, or excessive soil erosion. Tests were run for both vegetated and non-vegetated conditions. It was found that the factors affecting the performance of the RECP were quality of the vegetation, initial soil moisture, type of soil, and bed slope (Chirbas and Urroz, 1999).

Some state governmental agencies have developed testing programs and protocol for testing of RECPs. For example, the Texas Department of Transportation (TxDOT) has shifted from a “material type” specification into an “approved product” type specification for flexible channel liner applications. Products must meet minimum performance standards through controlled field-testing at the TxDOT/Texas Transportation Institute (TTI) Hydraulics and Erosion Control Laboratory.

For channel applications, the testing at TTI is conducted in a 3% or 7% gradient channel with flows exerting shear stresses up to 8 lbs/sf. The channels are rectangular, 30 feet long by 1.5 feet wide by 4 feet deep, with soil contained in vegetated trays. Each test begins at a shear stress of 2 lbs/sf and continues at 1 lb/sf increments up to a shear stress greater than 6 lbs/sf. Each increment of shear stress is tested for 20 minutes. After each incremental run, 3 profiles are taken with a computerized tracing wheel. Sediment loss is calculated from the profiles as well as measuring the gross sediment deposited and lost (TxDOT/TTI, 2001).

The TxDOT minimum performance standards are based on maximum sediment loss and minimum vegetation density. The products must meet or exceed the standards as shown in Table 2.6.

**Table 2.6 TxDOT Minimum Performance Standards (TxDOT/TTI, 2001)**

| Specification Pay Item | Class | Type | Site Conditions | Maximum Sediment Loss | Minimum Vegetation Density |
|---|---|---|---|---|---|
| 169 "Soil Retention Blanket" | 1 "Slope Protection" | A | Slopes 1:3 or Flatter - Clay Soil | 0.34 | 80% |
| | | B | Slopes 1:3 or Flatter - Sand Soil | 12.20 | 70% |
| | | C | Slopes Steeper than 1:3 - Clay Soil | 0.34 | 80% |
| | | D | Slopes Steeper than 1:3 - Sand Soil | 26.84 | 70% |
| | | | | | |
| 169 "Soil Retention Blanket" | 2 "Flexible Channel Liner" | E | Shear Stress Range 0 - 96 Pa | 1.15 | 70% |
| | | F | Shear Stress Range 0 - 192 Pa | 1.00 | 70% |
| | | G | Shear Stress Range 0 - 287 Pa | 1.00 | 70% |
| | | H | Shear Stress Range 0 - 383 Pa | 0.80 | 70% |
| | | | | | |
| 164 "Seeding for Erosion Control" | "Cellulose Fiber Mulch" | N/A | Clay or Tight Soil | N/A | 70% |
| | | N/A | Sand or Loose Soil | N/A | 60% |
| | | | | | |

Effective Date: March 1, 1997
Maximum Sediment Loss – Class 1 = Kilograms of Sediment per 10 Square Meters
Maximum Sediment Loss – Class 2 = Average Centimeters of Soil Displacement
Minimum Vegetative Density = Average Percentage of Vegetative Cover at Final Measurement Round

## Previous Erosion Studies in the Clear Creek Watershed

Only a few erosion studies have been conducted in the Clear Creek watershed, and include two erosion and sedimentation studies and one watershed assessment as summarized below.

A bedload erosion and sedimentation study on Clear Creek was completed in order to determine the amount of bedload in Clear Creek (Fisher, 1978). Sediment source areas or areas with erosion potential were also evaluated. The study utilized a V-type, wooden flume to collect bedload sediment near the USGS gaging station. Several geometric design alternatives were evaluated before selecting V-type flume geometry, which was found to minimize changes in flow conditions and successfully separate bedload from suspended load. Bedload sediment was collected by means of a transverse slot and discharged through a pipe system. Suspended sediment samples were also collected to determine total sediment load.

The estimated average total sediment load over the 30-month study period was 2200 grams/minute (g/min); however, during high flow events a significant increase in total load was observed. As shown in Figure 2.28, bedload accounts for a majority of the transported sediment (78%). The low amount of clay and silt in the basin is the major reason for the high percentage of bedload in relation to suspended load.

As part of the same study, a stream survey was conducted to identify areas of erosion and various land uses. This survey concluded there is a potential for erosion because of steep slopes, fragile vegetation and deeply weathered granite rock, but there is little evidence of erosion in the basin (Fisher, 1978). However, areas of significant sediment sources were identified:

- The lowest segment of Clear Creek contributes a large percentage of the bedload because of the concentration of water by the highway pavements.
- The meadows area where active gullies with banks 10 to 15 feet in height and active downcutting below highway culverts are major sources of sediment.
- Irrigation diversions with downcuts below the structures are major sources of suspended sediment during thunderstorms.

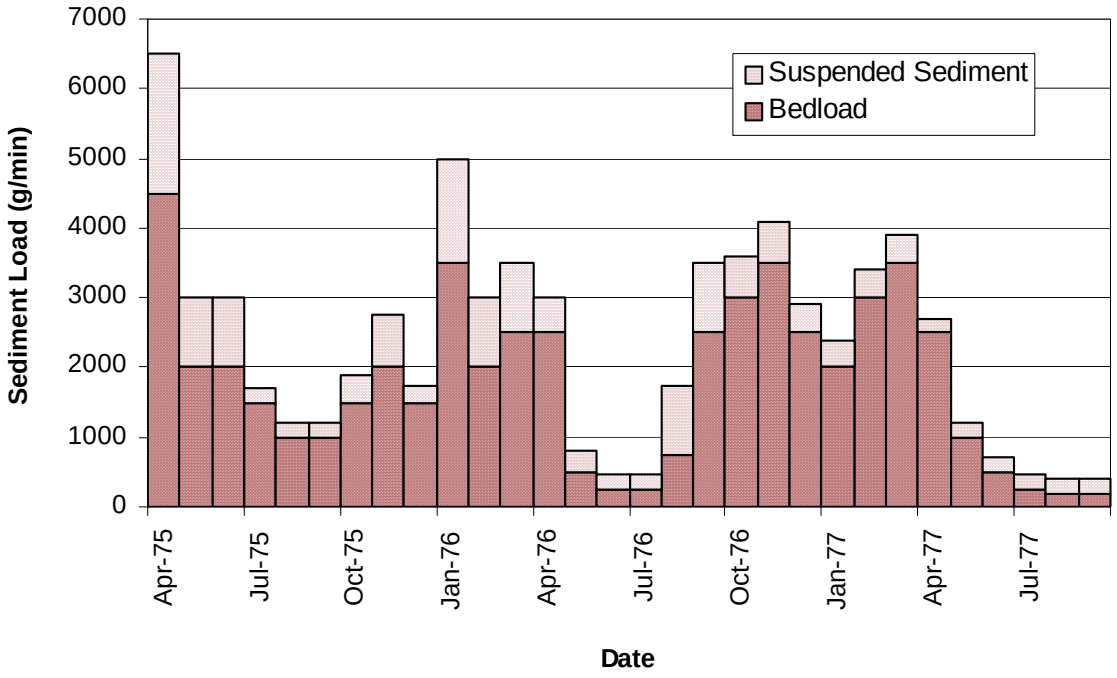


**Figure 2.28 Estimated monthly average sediment load in Clear Creek (Fisher, 1978).**

The National Resources Conservation Service (NRCS), previously the Soil Conservation Service, conducted a study of the Clear Creek watershed in July 1989 to evaluate areas of erosion and to quantify erosion and sedimentation (Stevenson, 1989). The most severe areas of erosion were associated with road banks (cut and fill slopes) and gullies downstream from the roadway culverts. The highly erodible granite and steep topography are the most significant factors contributing to sediment yield by sheet and rill erosion. Snow removed from the road is piled in large masses at the top of unprotected fill slopes. Melt water from these snow banks contributes to extreme rilling

and gulleying on the fill slopes below Highway 50. Concentrated runoff from culverts is discharged onto largely unprotected fill slopes and large gulleys have formed. These gulleys often exceed 10 feet in depth and in many cases headcutting threatens to undercut the culvert and highway.

The Direct Volume Method was used by (Stevenson, 1989) to quantify erosion from road banks and gullies. The Pacific Southwest Interagency Committee Procedure (PSIAC) was used to estimate sheet and rill erosion. Table 2.7 illustrates the magnitude of the erosion, showing a total of approximately 18,000 tons per year (8.3 ac-ft/yr) transported out of the watershed. This is equivalent to about 670 twenty-yard trucks each year (1.8 trucks per day). As shown in Table 2.7, the total annual sediment load of 18,000 tons converts to approximately 31,000 g/min, which is significantly higher than the average of 2,200 g/min estimated by Fisher (1978).

**Table 2.7 Clear Creek Erosion-Sediment Quantities (Stevenson, 1989)**

| Area | Total Erosion (tons/yr) | Sediment Delivered* (tons/yr) | Delivered % of Total |
|---|---|---|---|
| Sheet/Rill | 7330 | 1466 | 8.1 |
| Streams | 630 | 567 | 3.1 |
| Gullies | 6420 | 3852 | 21.2 |
| Roads | 35,160 | 12298 | 67.6 |
| Total | 49,540 | 18,183 | 100.0 |

*Sediment delivered at the low-end of the watershed near the intersection of Clear Creek and Highway 395.

Recently, NDOT funded a Clear Creek watershed assessment to identify areas of erosion and to develop mitigation techniques and associated construction cost estimates (PBS&J, 2003). Watershed information was collected through field investigations and was used to conduct hydrologic, hydraulic, erosion and sedimentation, and environmental analyses. The erosion and sedimentation areas were prioritized and mitigation alternatives were proposed.

The environmental analyses completed for the main channel of Clear Creek were inconclusive because sufficient historical data was not available for comparison. Without historical data on a reference stream, it is difficult to establish impacts of sediment loading and land use modifications to the Clear Creek watershed. However, PBS&J (2003) estimated that, based on an inventory of drainage structures and drainage corridors, approximately 10 percent of these areas are experiencing relatively high rates of erosion, 15 percent relatively moderate rates of erosion, and 75 percent have low rates of erosion. While it is evident that sediment loading is occurring, impacts to the aquatic biota are difficult to establish. Human influence has accelerated erosion in many areas, but to what extent is not clear.

Bottom sediment composition varies from cobbles to large gravels to fine materials. Sediments being loaded by these tributaries appears to be small to medium gravel (predominately decomposed granite) that is not carried as a suspended solid for any measurable distance, but is more likely to be transported as bed load during larger flood events (PBS&J, 2003).

PBS&J (2003) generally concurs with Fisher (1978) regarding sediment sources; however, PBS&J (2003) concludes that the major erosion areas down gradient from US Highway 50 may not have been present in 1978.

**Clear Creek Water Quality**

Results of recent water quality testing for Clear Creek were obtained from the Nevada Division of Environmental Protection (NDEP) (Table 2.8). Water samples were obtained at the USGS gaging station and at Bigelow Drive, which is at the lower end of the watershed (Figure 2.3). Table 2.8 includes test results over the past 4 years and lists typical stream and river values (Maidment, 1993), as well as the maximum contaminant levels (MCL) for drinking water as regulated by the Environmental Protection Agency (EPA). Parameters that were routinely monitored include flow, temperature, dissolved oxygen, specific conductivity, pH, turbidity, total dissolved solids, total suspended solids, chloride, sulfate, and *E. coli*.

Comparing the sample results with the MCL, the creek water typically meets the drinking water standards except for turbidity. The average measured turbidity of 6.1 NTU exceeds typical stream and river values of 0 to 3 NTU (Maidment, 1993) and the drinking water standards of 0.3 NTU. As shown in Figure 2.29, there does not appear to be a consistent trend in the variation of turbidity over time. However, the turbidity is typically lower at Bigelow Drive than at the USGS gaging station. This suggests that some suspended solids are settling between the two sampling stations.

The concentration of total dissolved solids (TDS) is an important indicator of the suitability of water for drinking, irrigation, and industrial use. The concentration of TDS of 96 – 150 mg/L are slightly higher than the typical stream and river values of 73 – 89 mg/L (Maidment, 1993), but well below the secondary drinking water standard of 500 mg/L. This may be an indication of some minor, active mineral dissolution and/or the presence of desorbed minerals or other environmental contaminants entering the watercourse. Water contact time with soils and rocks from which material is dissolved is an important determinant of the dissolved concentrations and the mixture of ions present. As the contact time increases (as in groundwater systems), the concentrations of dissolved solids typically increase. Dissolved solids in streams typically increase downstream due to both evaporation and inflow from groundwater (Maidment, 1993). The TDS concentrations shown in Figure 2.30 indicate that there is a slight increase in TDS concentrations as flow progresses from the USGS gaging station to Bigelow Drive.

## Table 2.8 Clear Creek Surface Water Quality Data (NDEP, 2003)

| Water Quality Parameter | Unit | USGS Gaging Station 10310500 (sampling by Nevada Division of Environmental Protection) | | | | | | | | | | | | | Bigelow Dr. | | MCL[1] | Typical Values[2] |
|---|---|---|---|---|---|---|---|---|---|---|---|---|---|---|---|---|---|---|
| | | 1 | 2 | 3 | 4 | 5 | 6 | 7 | 8 | 9 | 10 | 11 | 12 | 13 | 14 | 15 | | |
| **Sample Date** | | 3-99 | 6-99 | 11-99 | 4-00 | 10-00 | 1-01 | 4-01 | 6-01 | 9-01 | 12-01 | 4-02 | 7-02 | 10-02 | 7-02 | 10-02 | | |
| **Temp** | $^{o}$C | 4.75 | 10.3 | 5 | 7.5 | 7 | 0 | 3 | 6.5 | 10 | 3 | 6 | 13.5 | 5 | 15.5 | 3 | | |
| **DO** | (mg/L) | 9.3 | 9.05 | 10.3 | 10.2 | 10.6 | 13.8 | 11 | 9.7 | 9.4 | 10.3 | 10.2 | 8.1 | 11.4 | 8.4 | 10.7 | | 3 to 9 |
| **Elec. Cond.** | (us/cm) | 233 | 147 | 154 | 173 | 177 | 157 | 164 | 163 | 297 | 190 | 250 | 170 | 160 | 200 | 170 | | 70 |
| **Lab pH** | | 7.57 | 7.59 | 7.57 | 8.11 | 8.18 | 8.08 | 8.09 | 8.11 | 8.54 | 7.95 | 8.02 | 8.02 | 8.16 | 7.95 | 7.94 | 6.5 - 8.6 | 4.5 to 8.6 |
| **Field pH** | | 8.2 | 8.12 | 7.12 | 8.53 | 8.1 | 7.6 | 7.15 | 6.87 | 8.86 | 8.34 | 8.57 | 8.04 | 8.3 | 7.55 | 7.1 | 6.5 - 8.5 | 4.5 to 8.5 |
| **Turbidity** | (NTU) | 13.5 | 10.2 | 6.8 | 7.7 | 4.3 | 3.9 | 6.5 | 2.8 | 4.6 | 6 | 16 | 8 | 4 | 3 | 1.7 | 0.3 | 0 to 3 |
| **TDS** | (mg/L) | 123 | 89 | 97 | 109 | 108 | 108 | 106 | 96 | 174 | 130 | 150 | 104 | 96 | 119 | 102 | 500.0 | 73 to 89 |
| **TSS** | (mg/L) | 23 | 22 | 6 | 16 | 4 | 3 | 12 | 4 | 5 | 1 | 12 | 7 | 6 | 1 | 2 | | 10 to 110 |
| **$HCO_3^-$** | (mg/L) | 63 | 63 | 73 | 71 | 88 | 76 | 73 | 85 | 110 | 81 | 68 | 93 | 93 | 98 | 95 | | 58.4 |
| **ALK ($CaCO_3$)** | (mg/L) | 52 | 52 | 60 | 58 | 72 | 62 | 60 | 70 | 94 | 66 | 56 | 76 | 76 | 80 | 78 | | 150 |
| **$NO_3^-$+$NO_2^-$** | (mg/L) | 0.05 | 0.11 | 0.01 | 0.03 | 0.01 | 0.01 | 0.01 | 0.01 | 0.01 | 0.11 | 0.03 | 0.05 | 0.06 | < 0.10 | < 010 | 10 + 1 | 0.1 to 0.5 |
| **TKN** | (mg/L) | 0.66 | 0.42 | 0.43 | 0.45 | 0.19 | 0.11 | 0.25 | 0.14 | 0.18 | 0.2 | 0.32 | 0.27 | 0.16 | 0.25 | 0.2 | | 0.1 to 10 |
| **Total N** | (mg/L) | 0.71 | 0.53 | 0.44 | 0.48 | 0.2 | 0.12 | 0.26 | 0.15 | 0.19 | 0.31 | 0.35 | 0.32 | 0.22 | 0.30 | 0.20 | | |
| **Total P** | (mg/L) | 0.07 | 0.08 | 0.04 | 0.06 | 0.03 | 0.03 | 0.03 | 0.03 | 0.04 | 0.03 | 0.08 | 0.05 | 0.06 | 0.07 | 0.04 | | 0.02 to 6 |
| **$Cl^-$** | (mg/L) | 28 | 9 | 12 | 15 | 8 | 8 | 11 | 6 | 19 | 13 | 39 | 5 | 4 | 7 | 5 | 250.0 | 8 |
| **$SO_4^{2-}$** | (mg/L) | 1 | 2 | 5 | 1 | 1 | 1 | 1 | 1 | 16 | 1 | 1 | 1 | 1 | 1 | 1 | 250.0 | 8.3 to 11.2 |
| **E-Coli** | #/100mL | < 10 | 1013 | 10 | 53 | 20 | < 10 | < 10 | 10 | 42 | < 10 | < 10 | 111 | 20 | 1091 | 254 | 5%[3] | |

1. MCL = Maximum Contaminant Level – Primary or Secondary Drinking Water Standards (EPA, 2002).
2. Typical values in streams and rivers (Maidment, 1993).
3. More than 5.0% samples total coliform-positive in a month.

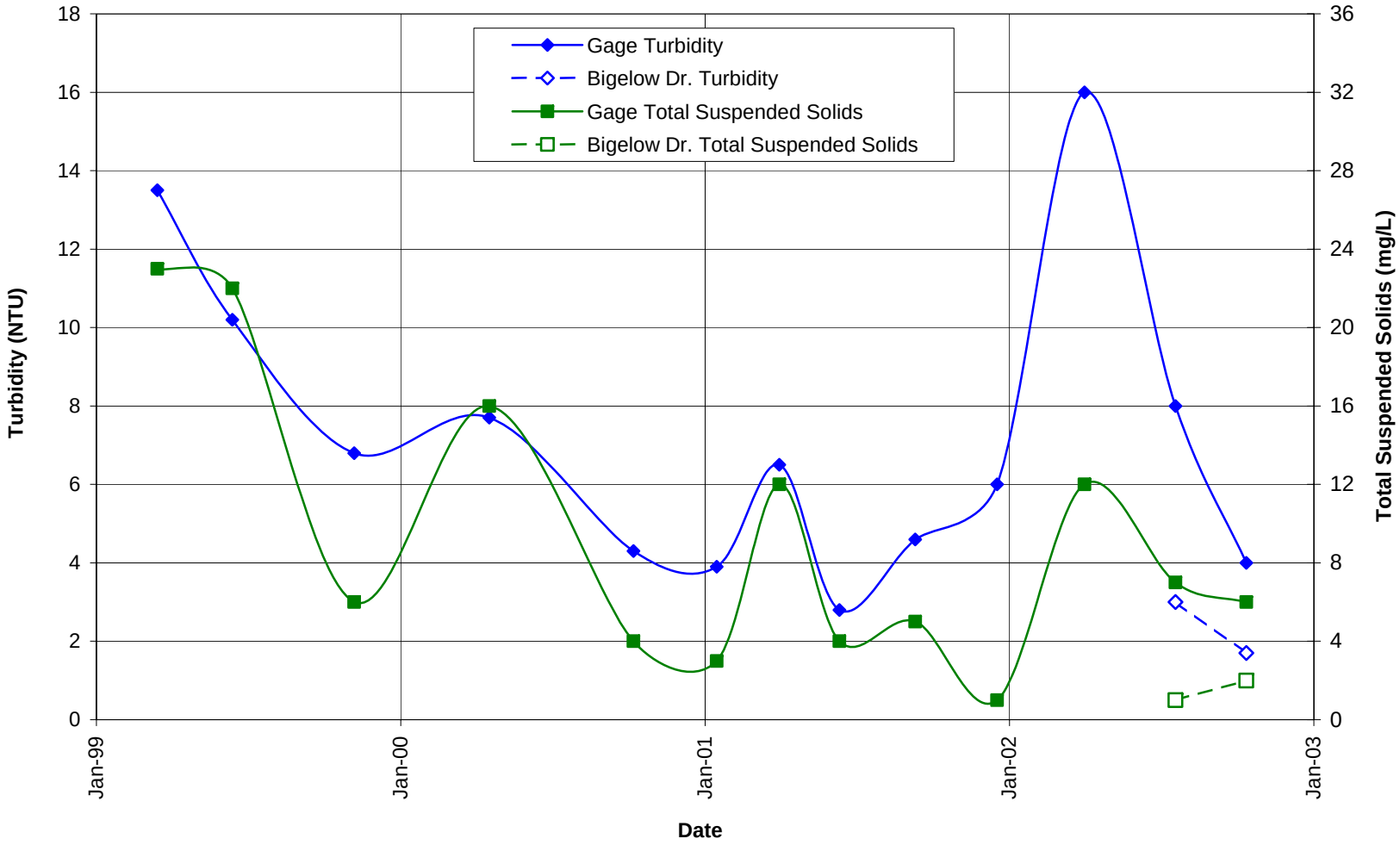


**Figure 2.29 Variations in turbidity and total suspended solids concentrations in Clear Creek (data from NDEP, 2003).**

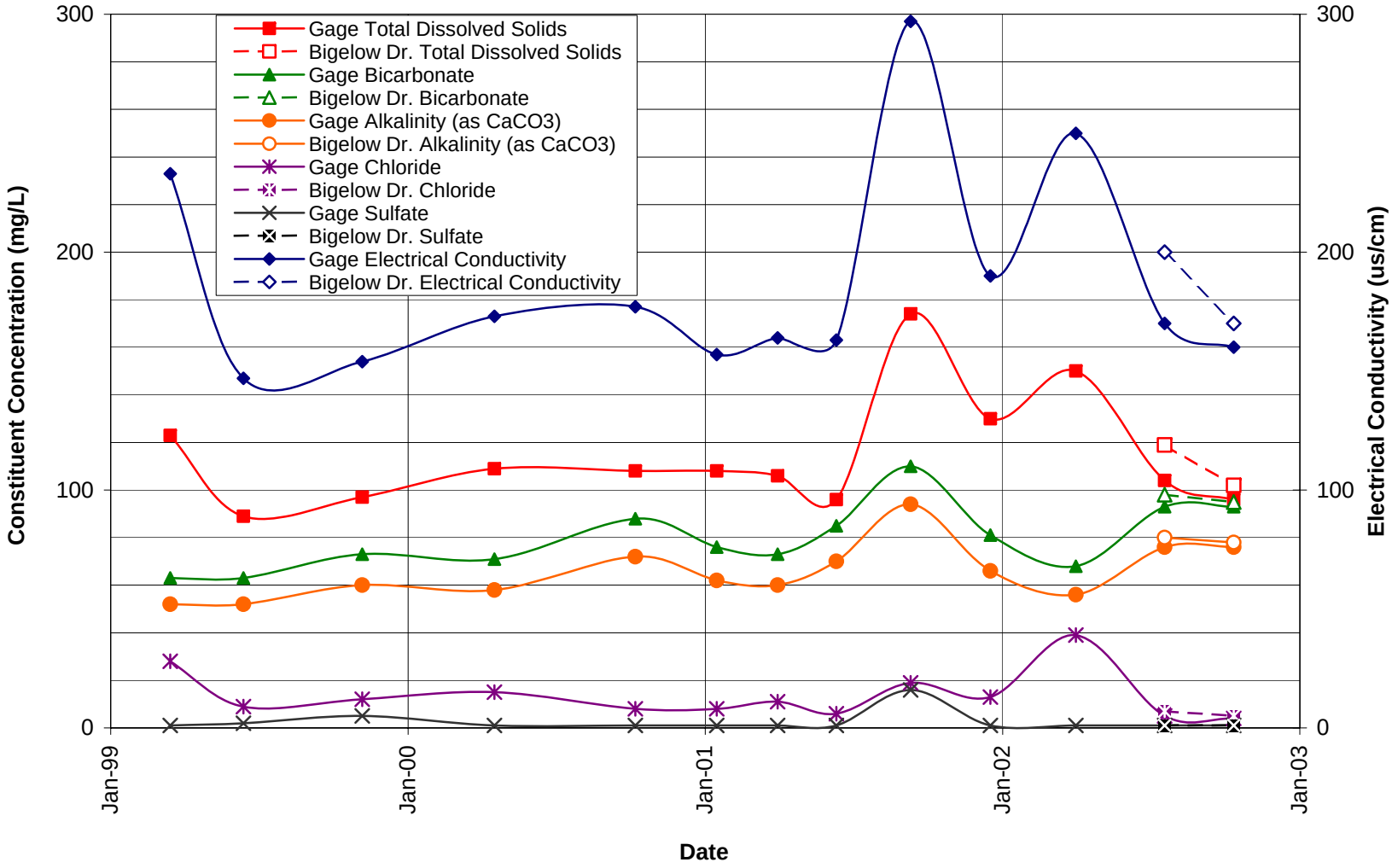


**Figure 2.30 Variations in surface water constituent concentrations in Clear Creek (data from NDEP, 2003).**

The concentration of dissolved oxygen (DO) is an indirect measure of the ability of a surface water to support aquatic life. DO concentrations may be decreased by eutrophication which often results from excessive nutrient concentrations in the watershed. As nutrient concentrations increase, the rate of aquatic plant growth exceeds the normal growth rate in a stream, resulting in excess bacterial decay of biomass and a subsequent reduction in DO concentrations. As shown in Figure 2.31, the DO concentrations are relatively high in Clear Creek, which corresponds with the observed low concentrations of the nutrients nitrogen and phosphorus, suggesting that eutrophication is not currently a problem in this watershed.

Alkalinity is the measure of the capacity of water to neutralize acid and measures the net effect of cations and anions (Maidment, 1993). As shown in Table 2.8, the alkalinity of water in Clear Creek is approximately one half of the typical values observed in stream and river waters. The calcium in the watershed may be attributed to either mineral dissolution or anthropogenic sources such as roadway de-icing salts. Figure 2.30 indicates that there is a slight increase in alkalinity between the USGS gaging station and Bigelow Drive.

Bicarbonate ($HCO_3^-$) is important to stream water quality because it provides buffering capacity against changes in pH produced when dissolved carbon dioxide is consumed faster than it can be replaced by atmospheric gas exchange or bacterial decomposition (Maidment, 1993). The concentrations of $HCO_3^-$ in Clear Creek are slightly higher than average bicarbonate concentrations in typical streams and rivers (83.8 mg/L vs. 58.4 mg/L) (Maidiment, 1993). Bicarbonate concentrations were also observed to increase slightly from the USGS gaging station to Bigelow Drive (Figure 2.30).

Fecal coliform and *E. coli* are bacteria whose presence indicates that the water may be contaminated with human or animal wastes. Disease-causing microbes (pathogens) in these wastes can cause diarrhea, cramps, nausea, headaches, or other symptoms. These pathogens may pose a special risk for infants, young children, and people with severely compromised immune systems (EPA, 2002). The amounts of *E. coli* detected in Clear Creek (Table 2.8) indicate that there are levels of *E. coli* above the MCL. Levels appear to increase at the low end of the watershed. This may be a result of activities such as ranching below the USGS gaging station.

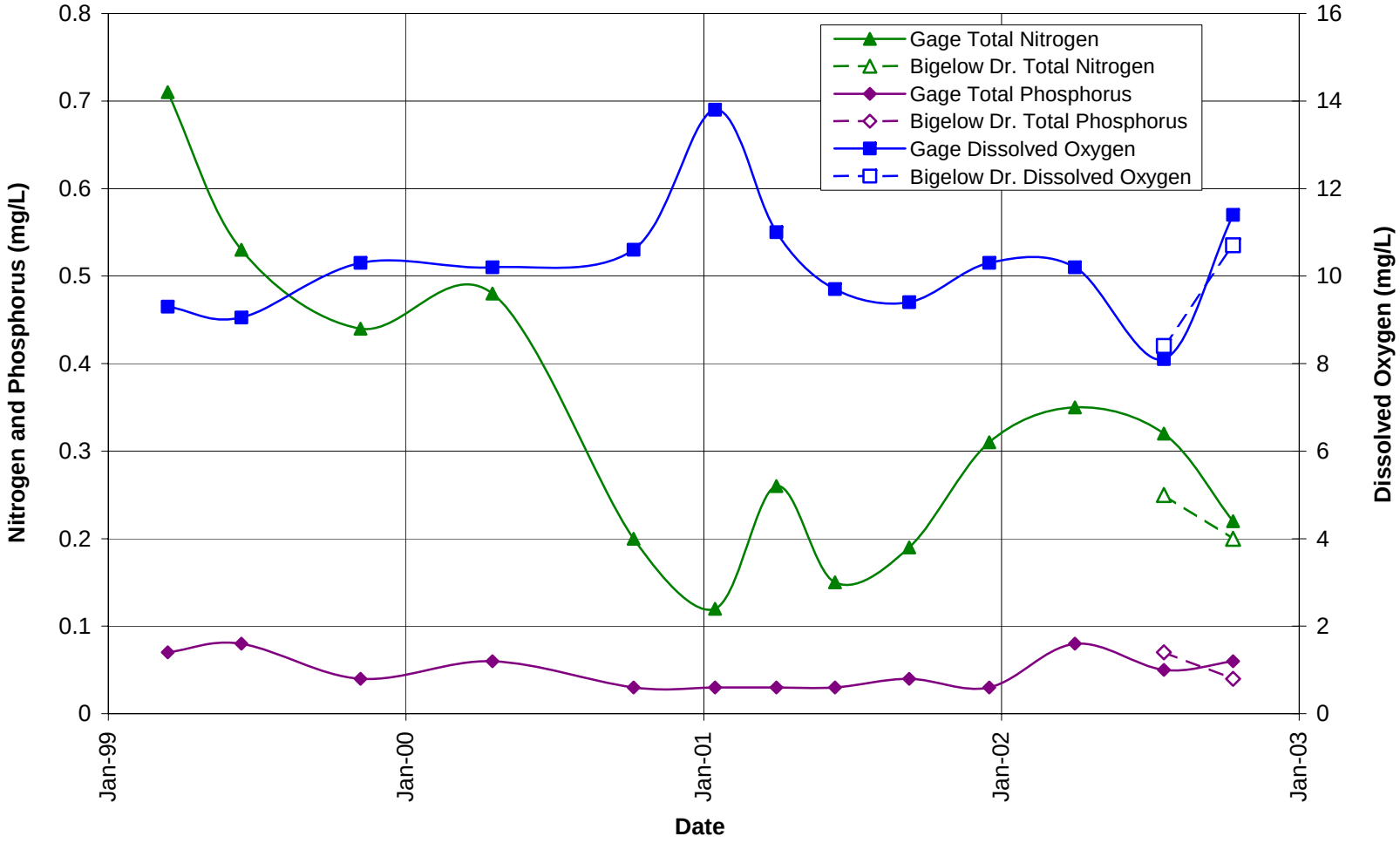


**Figure 2.31 Variations in concentrations of nutrients and dissolved oxygen in Clear Creek (data from NDEP, 2003).**

# Chapter III

## EXPERIMENTAL MATERIALS AND METHODS

A variety of rolled erosion control products (RECPs) were evaluated using a combination of laboratory testing and field testing. Representative soil and sediment samples from the Clear Creek watershed along U.S. Highway 50 were characterized. Bulk quantities of soil and sediment were obtained by the Nevada Department of Transportation (NDOT) and transported to the University of Nevada, Reno (UNR) for laboratory flume testing.

The performance of six erosion control products was evaluated by monitoring reductions in the erosion of soil and the resuspension of sediments during flume studies. These studies were conducted using the recirculating tilting flume in the hydraulics laboratory in the Department of Civil Engineering at UNR. The studies were conducted in a manner that simulated the field conditions of soils and sediments as closely as possible. The results of the laboratory studies were helpful in the selection of suitable products for further study during field testing.

During field testing, test plots were to be constructed at a channel experiencing severe erosion within the Clear Creek watershed. The purpose of the field testing was to monitor the performance of several RECPs during the winter and spring months when the majority of the runoff events causing erosion occur.

### Test Materials

A characteristic sample of native soils from the Clear Creek watershed area was utilized in all laboratory experiments. Areas with existing erosion problems along Clear Creek Road and areas between Clear Creek Road and Highway 50 were identified and categorized according to the type and severity of the erosion. Previous erosion studies were reviewed and extensive site inspections were conducted to locate the areas of significant erosion.

Information from product vendors and manufacturers relating to commercial erosion control products were collected and evaluated. Samples of rolled erosion control products (RECPs) that were evaluated during laboratory studies and field testing were also obtained.

Collection and Characterization of Soil Samples. The locations within the project area where substantial erosion is occurring were identified from site inspections and from watershed assessments performed by others (PBS&J, 2003; and Stevenson, 1989).

Representative samples of the soil and sediment from the most severely eroded areas of the watershed were obtained and were characterized with respect to grain size

and particle size distribution. The gradations from the samples were averaged to obtain a characteristic grain size. As shown in Figure 3.1, the soil consisted mostly of decomposed granite and was light brown in color. The soil had a median particle size ($d_{50}$) of approximately 1.5 mm as shown in Figure 3.2.

Using Equation 2-4 and the $d_{10}$ and $d_{60}$ particle sizes from the gradation curve shown in Figure 3.2, the uniformity coefficient $C_u$ is calculated as follows:

$$C_u = \frac{d_{60}}{d_{10}} = \frac{2.0}{0.5} = 4.0$$

A $C_u$ of 4 classifies the sediment as slightly well sorted (Fetter, 2001).

Using the geometric standard for grain size distribution yields very different results in the soil classification. From Figure 3.3, the grain size distribution results in a $d_{15.9}$ and $d_{84.1}$ of 0.66 mm and 3.30 mm, respectively. Utilizing Equation 2-5, the geometric standard deviation of the grain size distribution $\sigma_g$ is:

$$\sigma_g = \sqrt{\frac{d_{84.1}}{d_{15.9}}} = \sqrt{\frac{3.30}{0.66}} = 2.24$$

The $\sigma_g$ of 2.24 indicates that the generally considered to be poorly sorted (Diplas and Southerland, 1988).

In terms of cohesiveness, it can be seen from Figure 3.2, approximately 5% of the particles are less than 400 microns, and only a trace is less than 40 microns. Therefore, based on earlier discussions, the sediment is classified as slightly non-cohesive (Caywood, 1999; Miller et al., 1977).

**Figure 3.1 Soil sample (Dennett et al., 2002).**

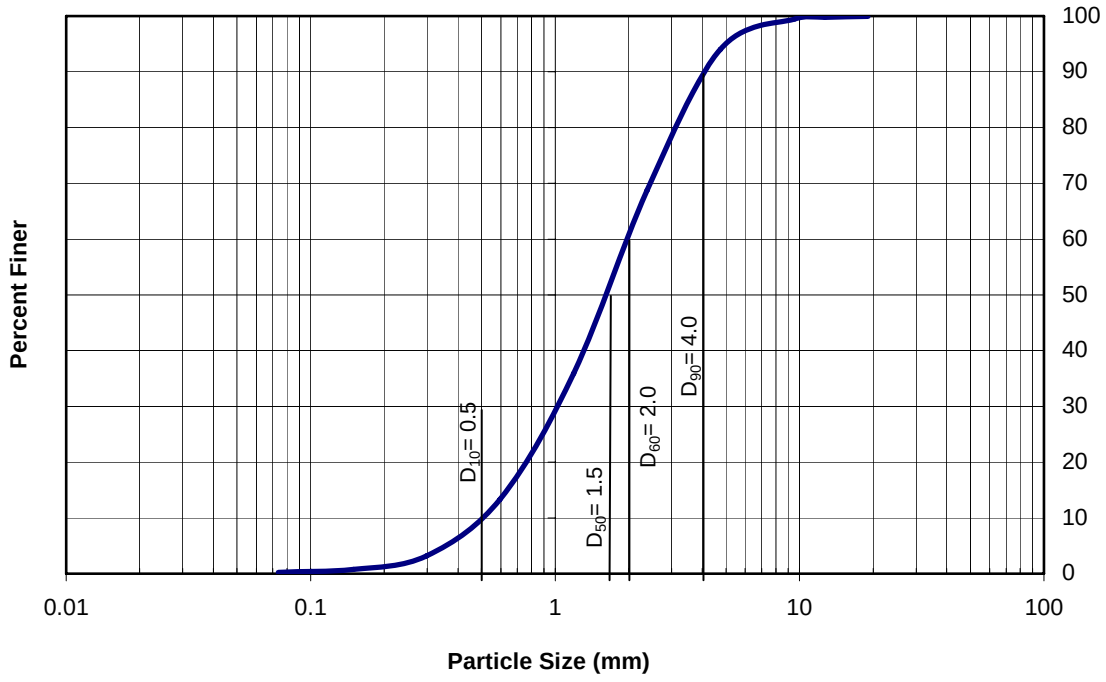


**Figure 3.2 Soil gradation curve (modified from Dennett et al., 2002).**

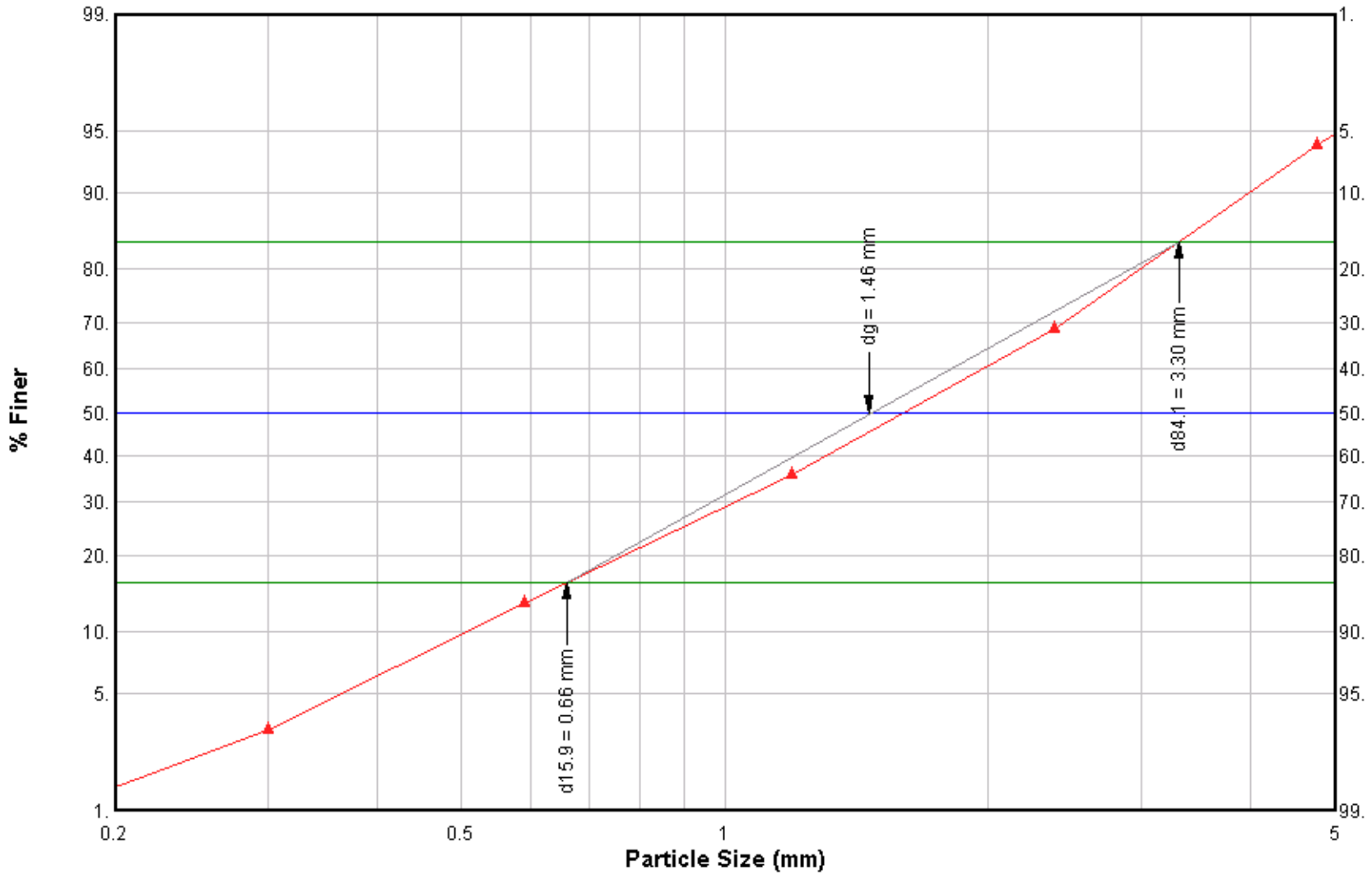


**Figure 3.3 Grain size distribution using a log/probability graph.**

Descriptions of Rolled Erosion Control Products (RECPs). Several mats and one blanket were selected for laboratory testing. These products covered a moderate to high range in quality from two manufacturers, SI Geosolutions (SIG) and North American Green (NAG). As shown in Table 3.1, the products tested included fabrics with straw, coconut fibers, polyolefin fibers, and polypropylene filaments. Photographs of the tested materials are shown in Figure 3.4, with further descriptions from the manufacturers' literature as follows:

- **SIG Landlok C2**, a coconut fiber blanket, is recommended for use in channels with moderate flows and slope protection on extreme slopes. Typical applications include grassed waterways, drainage ditch linings, bank rehabilitation, and slope protection. The netting on both sides is long lasting UV stabilized and photodegradable (less than 3 years).

- **SIG Landlok 450**, a polyolefin fiber mat, is recommended for use in channels with high velocity flows, slope protection on steep slopes and channel bank protection. The three dimensional web of green polyolefin fibers is bonded between two nets and is designed to be non-soil filled. The mat is generally placed above a seeded surface and relies on sediment capture rather than soil filling for increased stability. All components are stabilized against ultraviolet degradation (UV resistance at 1000 hours is 80% per ASTM D-4355) and inert to chemicals normally found in the natural soil environment.

- **SIG Landlok 435**, a polyolefin fiber mat, is also recommended for use in channels with high velocity flows, slope protection on steep slopes and channel bank protection. It is a lighter-weight version of SIG Landlok 450 and has a thickness of 0.35 inches (verses 0.50 inches for Landlok 450).

- **SIG Pyramat**, composed of a polypropylene pyramidal matrix mat, is recommended for use on steep slopes, high flow channels, channel bank stabilization, and inlet/outlet protection from culverts and drainage structures. Its three dimensional pyramid-like matrix helps stabilize soils and reinforce vegetation. Upward and downward protruding "pyra-cells" capture and contain soil. The matrix performs best when installed beneath the soil surface. When used as a vegetative reinforcement matrix, the product should be installed first, seeded, then a ½ inch to 1 inch veneer of soil placed and compacted into the pyra-cells. UV resistance at 3000 hours is 80% per ASTM D-4355.

- **NAG SC250**, a straw/coconut fiber mat, is recommended for medium to high flow channels such as roadside ditches and golf course swales and is also used to protect stream banks and slopes. The straw/coconut fiber is stitch bonded between permanent UV stabilized top and bottom nets. A super heavy duty UV stabilized, dramatically corrugated (crimped)

intermediate netting forms closely spaced ridges across the mat width. The fiber is considered degradable, with a functional longevity of 24 months. No soil in-filling is required and the mat is placed above a seeded surface.

- **NAG P550**, a polypropylene matrix mat, is recommended for applications with extremely high flows such as spillways, channels, and swales as well as shorelines and steep slopes. The 100% UV stabilized polypropylene fiber matrix is stitch bonded between three super heavy duty UV stabilized nets. The middle, dramatically corrugated (crimped) netting forms closely spaced ridges across the mat width. UV resistance per ASTM D-4355 is 100%.

When installed in the field, RECPs are laid down in shingle fashion with 4-inch to 6-inch overlaps. Anchor trenches that are 6-inches to 12-inches deep are typically provided at the beginning and end of the installation sections. Along the length of channels, continuous longitudinal anchor trenches are also installed. More detailed installation instructions are available from the product manufacturers.

RECPs are typically installed with metal or wood anchors (stakes or wire staples) at spacings that vary with the type of application. Slope protection applications typically have the widest anchor spacings ranging from 1.5 anchors per square yard (sy) to 2.5 anchors per sy. Anchors are typically staggered from row to row. Recommended anchor spacings are decreased for channels and usually range from 2.5 anchors per sy to 4 anchors per sy.

**Table 3.1 Properties of Rolled Erosion Control Products (Dennett et al., 2002)***

| Product Name | Product Description | Thickness (inches) | Mass Per Unit Area (oz/sy) | Tensile Strength (lb/ft) | Velocity Rating (ft/s)** | Shear Stress Rating (lb/sf)** | Total Cost*** ($/sy) |
|---|---|---|---|---|---|---|---|
| **SI Geosolutions, Inc., Chattanooga, Tennessee, USA** | | | | | | | |
| | Erosion Control Blanket. For use as a channel liner with moderate flows. Also used as an erosion control blanket on steep slopes. 100% natural coir (coconut) fiber, long lasting UV stabilized photodegradable netting on both sides. | 0.30 | 10.5 | 150 x 150 | (6) | (2) | 3.60 |
| Landlok 435 | Turf Reinforcement Mat. For use on slopes and channels. Composed of a three dimensional web of green polyolefin fibers bonded between two nets. Considered non-biodegradable. | 0.35 | 8 | 145 x 110 | 16 (16) | 5 (5) | 6.70 |
| Landlok 450 | Turf Reinforcement Mat. Thicker design than the LL 435. For use on slopes and channels. Composed of a three dimensional web of green polyolefin fibers bonded between two nets. Considered non-biodegradable. | 0.50 | 10 | 170 x 130 | 18 (18) | 7 (7) | 7.60 |
| Pyramat | Turf Reinforcement Mat. For use on steep slopes, water containment structures and high flow channels. Composed of polypropylene monofilament yarns woven in a configuration of pyramid-like projections. Considered non-biodegradable. | 0.50 | 14 | 3200 x 2200 | 20 (25) | 8 (10) | 13.50 |
| **North American Green, Inc., Evansville, Indiana, USA** | | | | | | | |
| SC250 | Turf Reinforcement Mat. Machine produced mat consisting of 70% straw and 30% coconut fiber matrix. Incorporated into a permanent three-dimensional 100% UV stabilized netting structure. Designed for medium to high flow channels with slopes of 1:1 and greater. | 0.73 | 16.21 | 700 x 500 | 9.5 (15) | 3 (6) | 5.70 |
| P550 | Turf Reinforcement Mat. Machine produced mat consisting of 100% UV stabilized polypropylene fiber matrix. Incorporated into a permanent three-dimensional netting structure. Designed for extremely high flow channels with a slope of 1:1 and greater. Considered non-biodegradable. | 0.76 | 20.28 | 1500 x 1300 | 12.5 (22) | 3.5 (10) | 8.70 |

*Information and performance data obtained from product literature or representative. ** Ratings are shown for unvegetated and vegetated ( ) conditions over a 30 minute duration. ***Costs include $3/sy for installation and are approximate and subject to change.

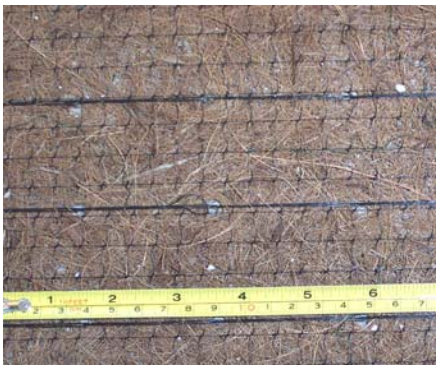

(a) Landlok C2

(b) NAG SC250

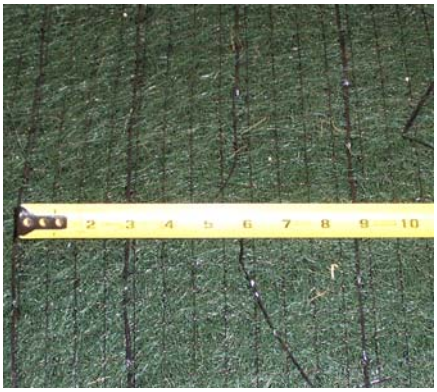

(c) Landlok 435

(d) Landlok 450

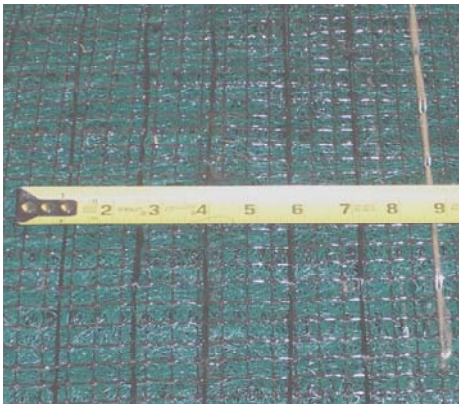

(f) NAG P550

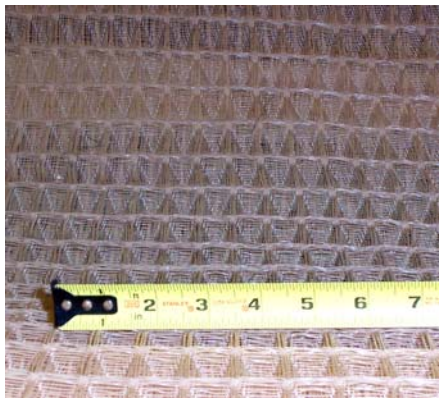

(e) Pyramat

**Figure 3.4 RECP photographs.**

**Laboratory Flume Studies**

Laboratory flume studies were conducted in order to evaluate the performance of various RECP products by comparing the sediment yield without erosion control (bare soil surface) to the sediment yield with erosion control (RECP cover).

Specific objectives of the laboratory studies were: (1) to estimate the critical shear stresses required to initiate the erosion of soil and/or the resuspension of sediment; (2) to estimate the erosion rates of soils and the rates of resuspension and/or deposition of sediments under varying flow conditions; and (3) to monitor the reduction in erosion due to various RECPs.

The laboratory studies were conducted in a manner that simulated the field conditions of the soils and sediments and the flow induced shear stresses as closely as possible. Field compaction methods typically used in remote, mountainous areas were used during the placement of soil and sediment samples within the flume.

Laboratory Facilities. The laboratory flume studies were conducted in the hydraulics laboratory at UNR. This laboratory is equipped with a rectangular, recirculating, tilting flume that is 80 feet (24 meters) long and 3 feet (0.9 meters wide). Plan and profile views of the flume are shown in Figure 3.5.

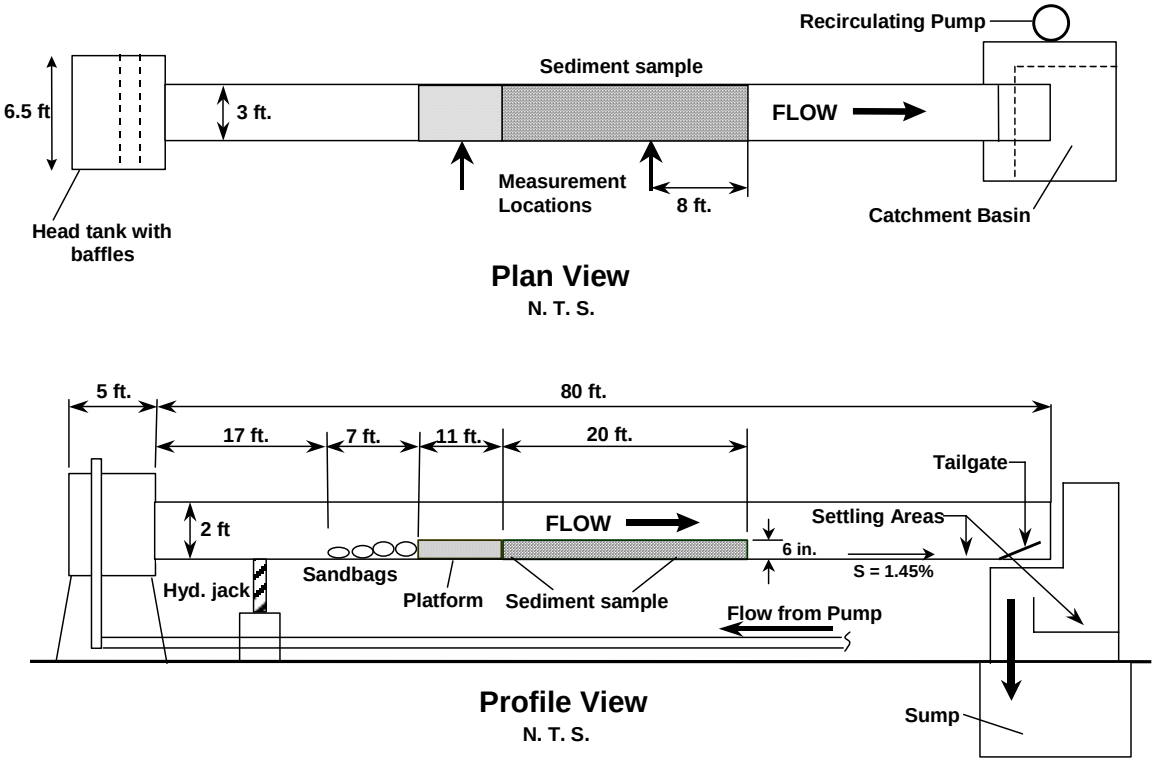


**Figure 3.5 Laboratory flume plan and profile (Modified from Dennett et al., 2002).**

Water at approximately 65 $^{o}$F is pumped from the sump and discharged to the head tank, where it is released to the flume through a sluice gate. At the end of the flume, the flow discharges into the catchment basin prior to returning to the sump. For these studies, the flume slope was set at its maximum slope of 1.45%. The recirculation and regulation of the flow was accomplished with the use of three pumps, used individually, or in combination to yield the desired flow. When the pumps were run simultaneously, the water level dropped in the sump, which increases the lift and causes a reduction in the overall pumping capacity of the system. As can be seen in Table 3.2, the sum of the maximum flow output, with all three pumps running is 4880 gpm. However, due to the lowering of the sump water level, the actual observed maximum discharge was approximately to 4600 gpm.

**Table 3.2 Pump Characteristics**

| Pump | Maximum Discharge | Flow Meter |
|---|---|---|
| Berkeley Model B3Z PM with 10 HP motor | 700 gpm | Hayward FloSite 2100 |
| Berkeley Model B6J PBM with 40 HP motor | 1580 gpm | Orifice meter |
| Worthington vertical turbine with 30 HP motor | 2600 gpm | Orifice meter |

Velocities were monitored in the flume during the tests utilizing a Marsh-McBirney Flo-Mate Model 2000 velocity probe. The velocity probe was attached to a top-setting measuring rod to assure a proper measuring depth.

Flume Test Section. A soil test section was constructed within the middle one third of the flume. As shown in Figures 3.5 and 3.6, it was framed 20 feet long by 3 feet wide by 6 inches deep. The frame, which was constructed of 2 by 6 dimensional lumber, encased the soil bed on all sides. Besides controlling the thickness of the soil bed, the frame was useful in providing a firm surface for anchoring the RECPs. Immediately upstream of the test section, a platform and a section of sandbags were installed to transition the flow to the surface elevation of the soil bed (Figures 3.5 and 3.6). The platform was framed to the same height of the test section and was surfaced with Plexiglas. Soil particles, of the characteristic size, were adhered to the Plexiglas surface to match the roughness of the soil.

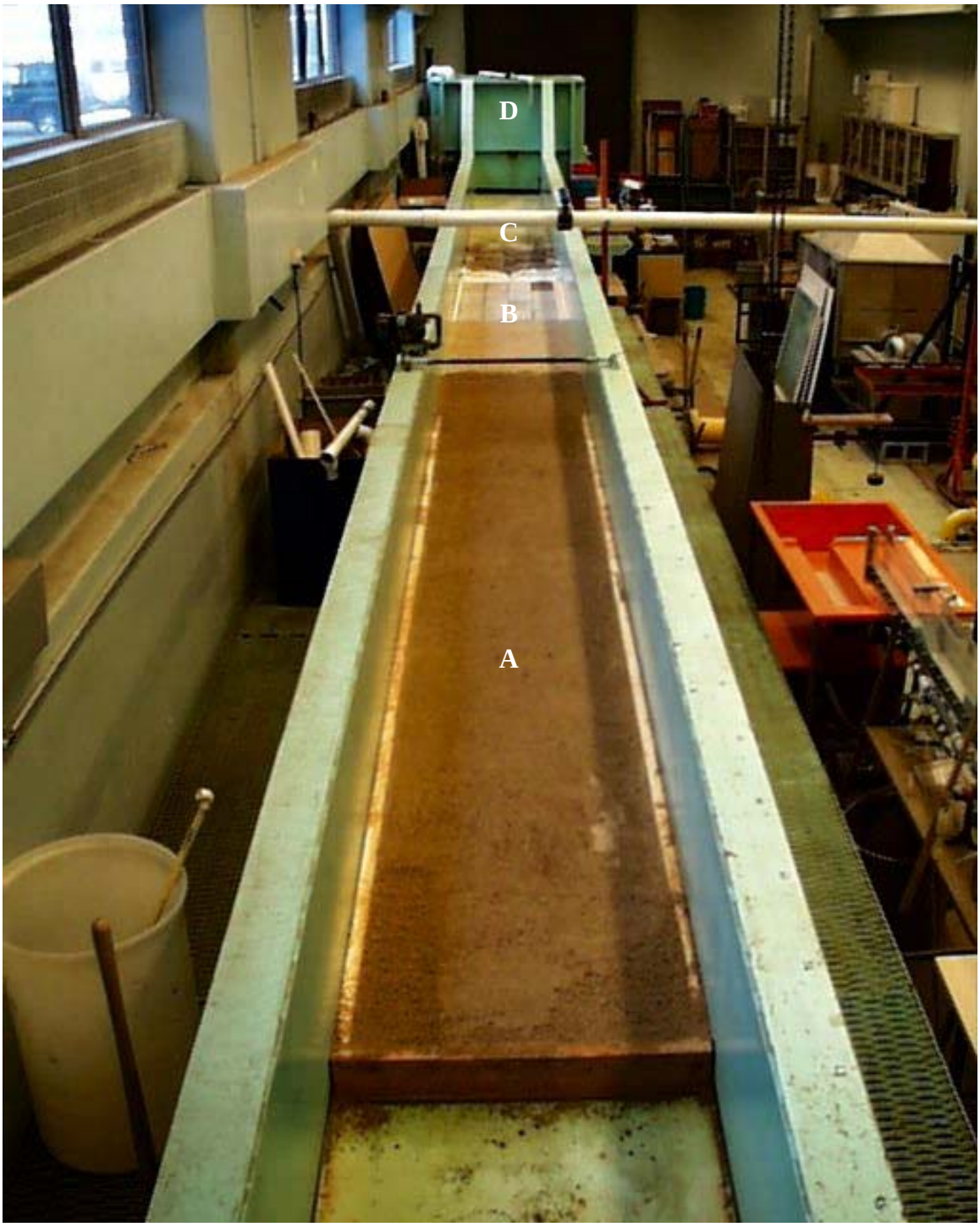


**Figure 3.6 Laboratory flume and test section assembly (looking upstream).**
A – Test Section
B – Platform
C – Sandbags
D – Head Tank

Laboratory Testing Procedure. As with the ASTM Standard Test Method D 6460 (ASTM, 2000), the objective of the flume testing was to provide a comparative evaluation of RECPs to baseline soil conditions under controlled and documented conditions. However, due to equipment constraints (e. g., maximum slope and flow capacity), the testing varied from procedures used by ASTM, USU, and TTI as described below:

At the beginning of each flow test, the soil was moisture-conditioned and compacted with a hand-tamper to approximately the same density. The following procedure was consistently used to prepare the soil prior to each test.

1. Soil scarifying and conditioning: The soil surface was raked and reconditioned with water, as necessary.
2. Initial leveling and compaction: The soil was redistributed to low areas and then leveled to the top of the soil box frame using a wood screed. A hand-held tamper was then used with maximum tamping force to compact the lower soil levels.
3. Final leveling and compaction: Step 2 was repeated with only minimal tamping force to compact the surface layer that was disturbed during the second leveling. At this stage, the soil bed was ready for bare soil testing.
4. RECP installation: A pre-cut section of RECP was placed over the test section and anchored to the soil box frame with screws located at 3-ft intervals. Since the flume is 3 feet wide, the resultant anchoring pattern was approximately 3 feet by 3 feet. This pattern results in approximately 2 anchors per sy, which is slightly less than the manufacturers recommendations of 2.5 anchors per sy. $1^1/_2$ -inch diameter washers were used with the screws to prevent tearing of the RECP and loss of the anchor support (Figures 3.7a and 3.7c). To simulate a worst-case scenario in the field, all tests were performed bare-mat, with no vegetation or veneer soil.

Each flume test consisted of one surface condition and one flow condition. Each surface condition (e.g., bare soil or different RECP product) was tested for a duration of 30 minutes at several subsequent flow conditions (e.g., 500 gpm, 1000 gpm, etc.). For example, the bare soil was tested consecutively in increments at flows increasing from 100 gpm to 1000 gpm. Measurements for quantifying the transported material and mapping of the soil surface were also obtained between each test. Each RECP was similarly tested. The soil was drained, reconditioned, and recompacted prior to each subsequent test.

Flow data was collected during each test by monitoring the average velocity and depth of flow. This data was then used to estimate the bed shear stress. As shown in Figure 3.5, depth and velocity were monitored at two locations: (1) at the midpoint of the approach platform upstream from the test section; and (2) eight feet upstream from the end of the test section. The depth measurements were obtained using a mechanical rod device with an accuracy of $^+$/- 0.001 ft. This accuracy was more than adequate due to the

irregularity of the water surface. Two depth measurements, at the third points across the flume, were obtained and averaged.

Average velocities were then calculated using the discharge indicated by the electronic flow meters and the continuity equation. The Flo-Mate velocity probe was also used to monitor the average velocity. Two velocity measurements at 60% of the depth of flow were made at each location and then averaged. The average readings obtained with the velocity probe were on the average about 15% higher than the velocities calculated using depth and the continuity equation.

After each test, soil that was transported from the test section was recovered in the settling area downstream from the test section and the catchment basin (Figure 3.5). The transported soil was then dried and weighed. Prior to the beginning of a subsequent test, the soil surface was roughly mapped to identify areas of aggradation and erosion.

The bed shear stresses for each test were calculated using the relationship $\tau_o = \gamma y S$ (Equation 2-6). The data collected during each test was immediately recorded for future analysis.

a) Anchoring TRM to Sideboard

b) TRM Leading Edge Anchoring

c) TRM Installed, Ready for Test

d) Flow Test Showing Hydraulic Jump

**Figure 3.7 RECP installation and testing in laboratory flume.**

**Field Testing**

Following the completion of the laboratory flume studies, four RECPs (i.e., Pyramat and Landlok 450 from SI Geosolutions and P550 and SC250 from North American Green) were evaluated further through the construction and monitoring of field plots along U.S. Highway 50. The field plots were routinely inspected over the period from October 2003 through June 2005.

Site Selection. Four field plots were constructed to test the better performing RECPs from the flume testing. The location and size of the field plots were determined in consultation with the Hydraulics Section and maintenance personnel from NDOT. Site selection was based on the severity of the existing erosion, ease of site access, and the compatibility in providing uniform testing conditions for all products.

The site selected for the field plots was located between U.S. Highway 50 and Clear Creek Road at Station 315+15 along U.S. Highway 50 which corresponds to point 103 on Figure 2.3. The drainageway is ephemeral and is approximately 400 feet long, with approximately 200 feet located within NDOT right-of-way. The field plots were constructed entirely within the NDOT right-of-way to avoid easement acquisition issues. Heavy equipment access to the field plot area was satisfactory from U.S. Highway 50.

Figures 3.8 shows photographs of existing conditions of the channel area prior to construction of the field plots. As shown in Figure 3.8a, the eroded channel had head-cut its way back to a point where it was adjacent to the edge of U.S. Highway 50. Due to the severe erosion, the outlet pipe is unsupported and on the verge of collapse. Figure 3.8b provides a view of the channel area downstream from the culvert outlet, which shows signs of moderate erosion. The existing channel side slopes ranged from approximately 3:1 to 2:1 (H:V) with sparse vegetation. According to the site assessment report (PBS&J, 2003), the flow capacity of the culvert was approximately 42 cfs.


a) Looking Upstream at the 24” CMP Culvert Outlet


b) Looking Downstream from the Culvert Outlet

**Figure 3.8 Initial conditions at field plot site.**

Field Plot Design. As shown in Figures 3.9 and 3.10, four field plots were designed for testing and monitoring. The channel section was trapezoidal with 2:1 (H:V) side slopes, covered with RECP material to an approximate length of 6 feet up-slope (Figure 3.11). Anchoring of the RECPs was in accordance with the manufacturers' recommendations. Due loose soil conditions in the field, 18 inch steel anchors fabricated from #3 rebar were installed.

Each field plot was 25-foot long and was preceded with 2-foot high drop structures to mitigate the extreme existing gradient. The drop structures were constructed of treated timber for ease of construction in remote areas (Figure 3.11). The timbers were keyed into the lower bank and anchored into the channel bottom with ½-inch diameter by 2-foot long steel stakes. A 5-foot long riprap apron was placed immediately below each drop structure in order to dissipate energy at the upstream end of each field plot section. The riprap aprons also acted as anchoring devices to secure the leading edge of the RECPs.

Four different RECP products were tested using field plots. The RECP products were installed in order of decreasing performance as determined by the laboratory flume studies (highest to lowest elevation). This was done in order to avoid having a weaker product fail upstream from a stronger one, thereby affecting the performance of the stronger product.

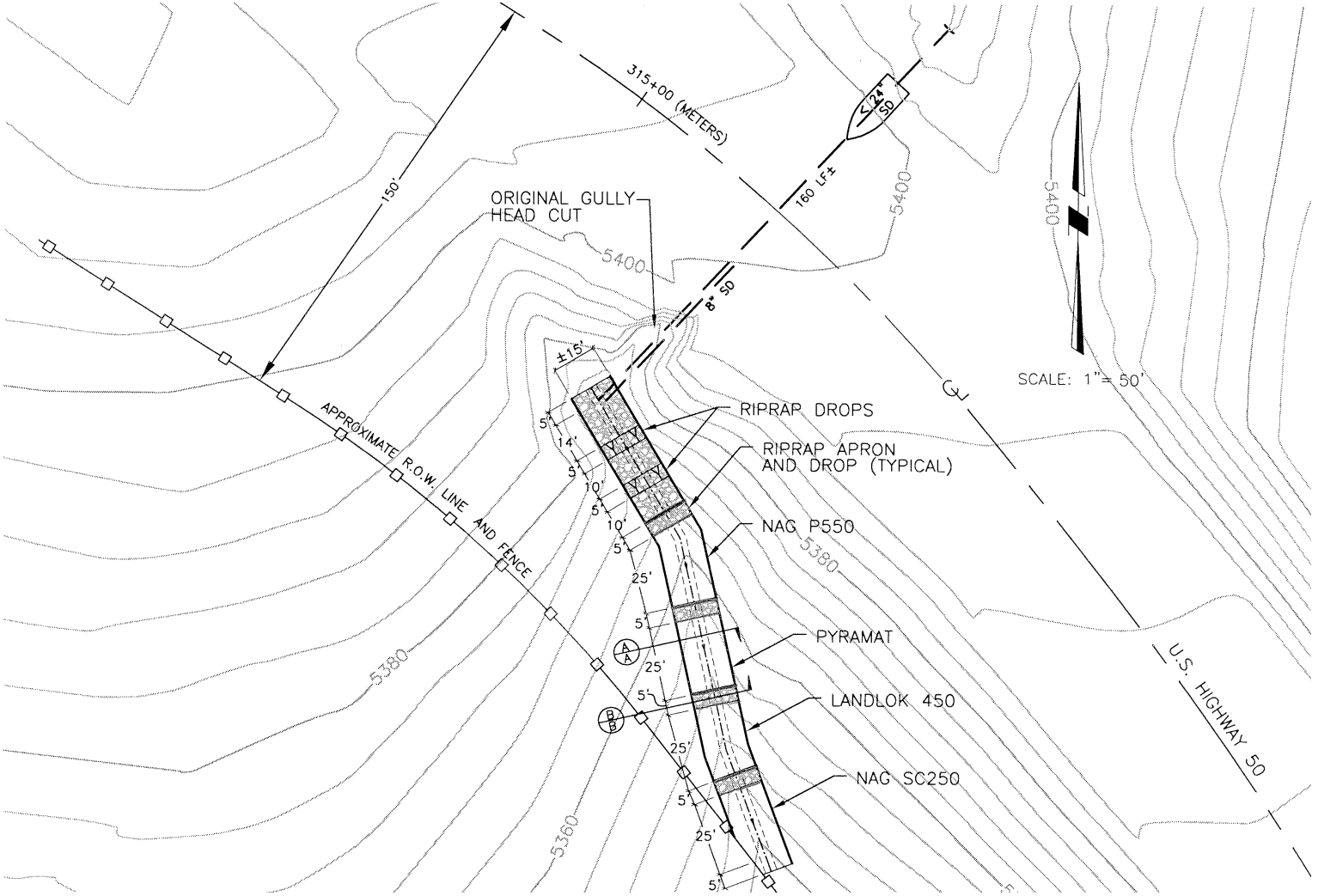


**Figure 3.9 Field plot plan.**

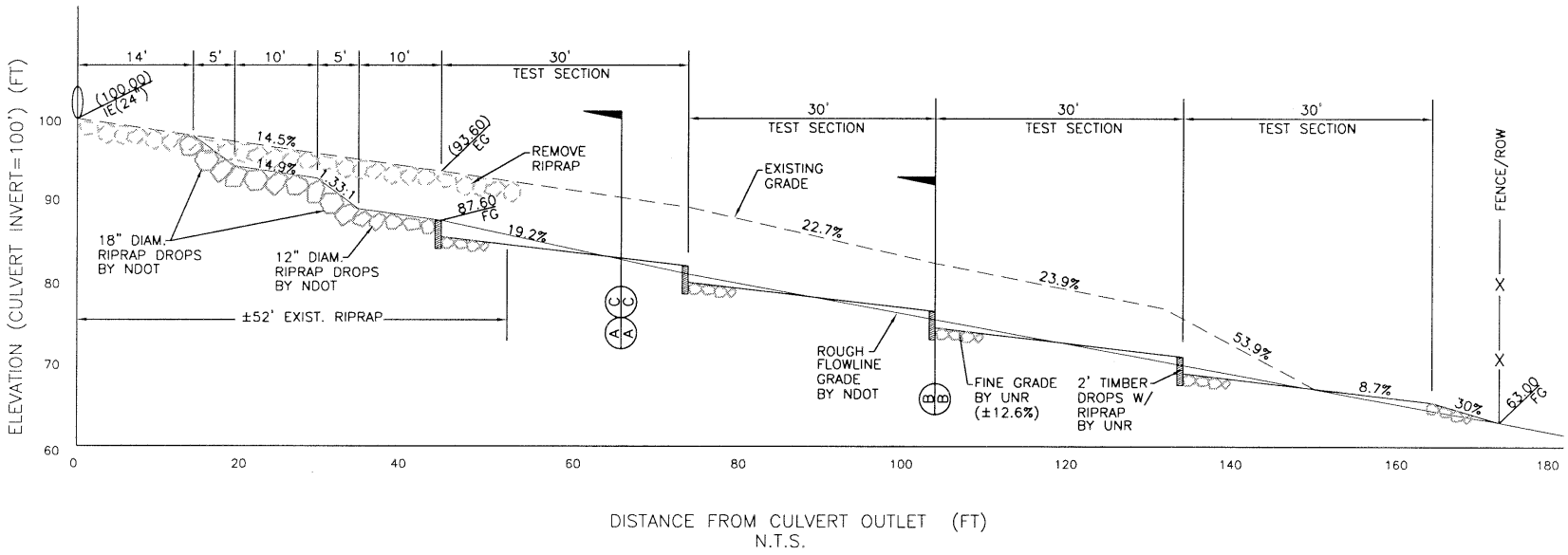


**Figure 3.10 Field plot profile.**

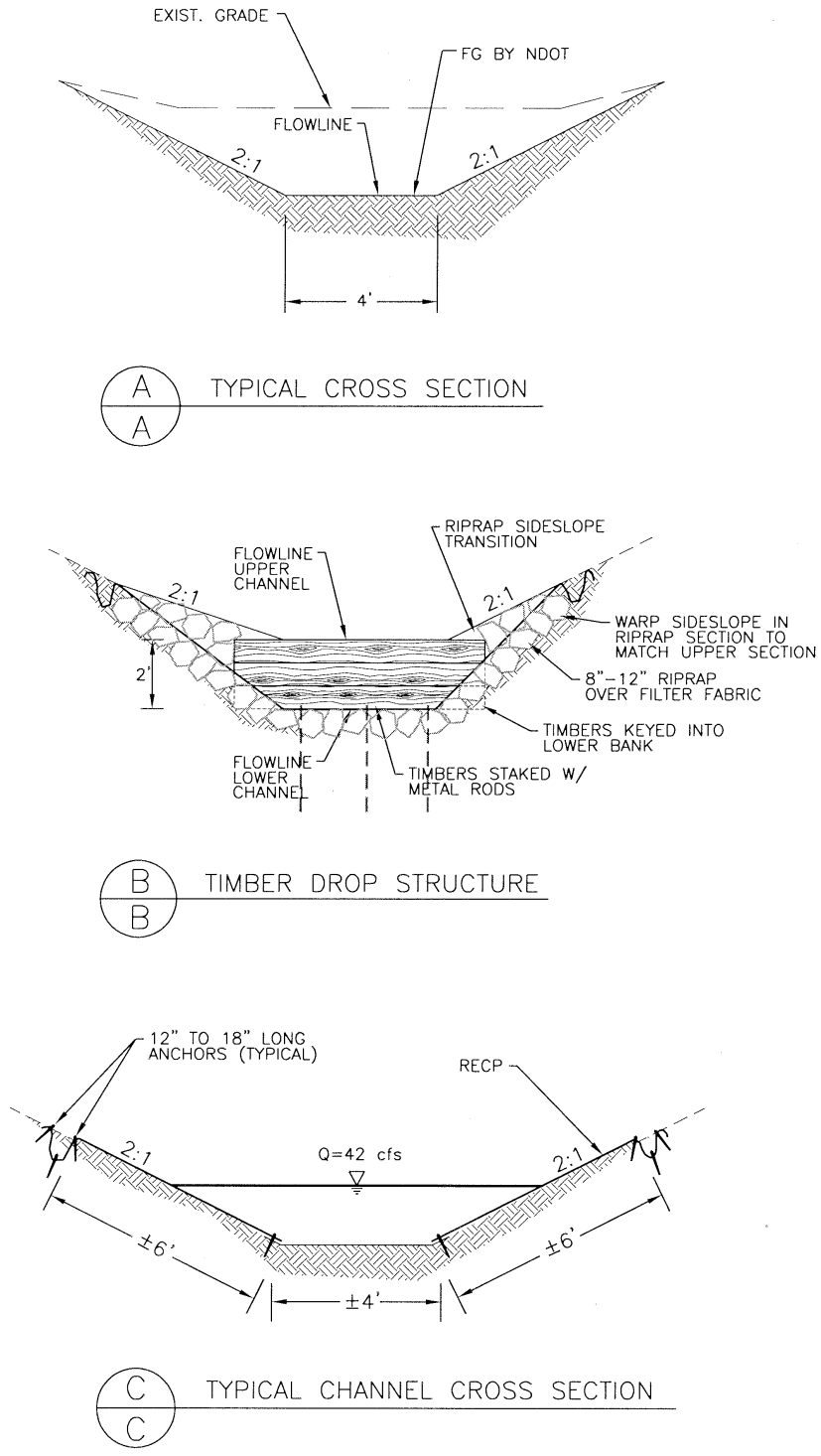


**Figure 3.11 Field plot cross sections.**

Hydraulic Analysis of Field Plot Sections. The US Army Corps of Engineers River Analysis System (HEC-RAS) version 3.0 computer model was used to analyze the hydraulic design of the field plots (Brunner, 2001). The program is capable of performing one-dimensional steady and unsteady flow hydraulic calculations by utilizing a computational method based on the solution of the energy equation:

$$y_2 + z_2 + \frac{\alpha_2 V_2}{2g} = y_1 + z_1 + \frac{\alpha_1 V_1}{2g} + h_e \qquad (3\text{-}1)$$

where:

$y_1, y_2$ = depth of water at cross sections
$z_1, z_2$ = elevation of the main channel inverts
$V_1, V_2$ = average velocities (total discharge / total flow area)
$\alpha$ = velocity weighting coefficients
$g$ = gravitational acceleration
$h_e$ = energy head loss

Water surface profiles are computed from one cross section to the next by solving the energy equation with an iterative procedure known as the standard step method.

The design flow of 42 cfs and the geometry information shown in Figure 3.11 were input to HEC-RAS to yield the results shown in Figures 3.12 through 3.13. Because of the steep slopes at the site, the predicted water surface profile is below the critical depth line indicating supercritical conditions (Figure 3.12, Hydraulic Profile). From this profile, the energy gradeline is very high compared to the water surface elevation, indicating that most of the energy comes from the velocity component of the energy equation. Figure 3.13a shows profile plots of the shear stress and velocity over the channel reach. As shown, the predicted shear stress ranges from approximately 3.7 to 6.6 lbs/sf across each of the test plots. The predicted velocities range from about 12.8 to 16.6 fps. Figure 3.13b shows the predicted water depth profile along the channel centerline with depths ranging from approximately 0.5 to 0.6 ft.

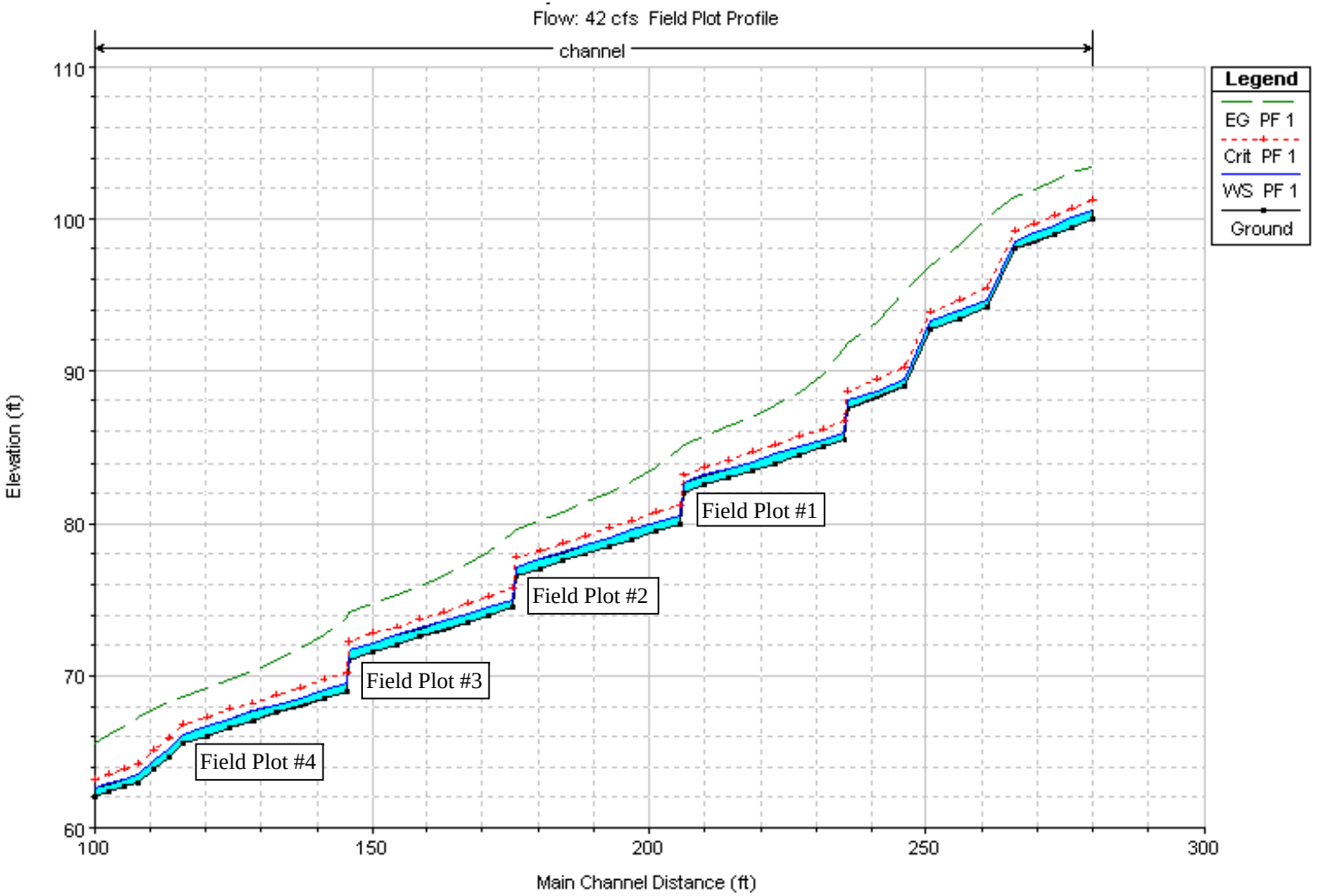


**Figure 3.12 HEC-RAS hydraulic profile.**

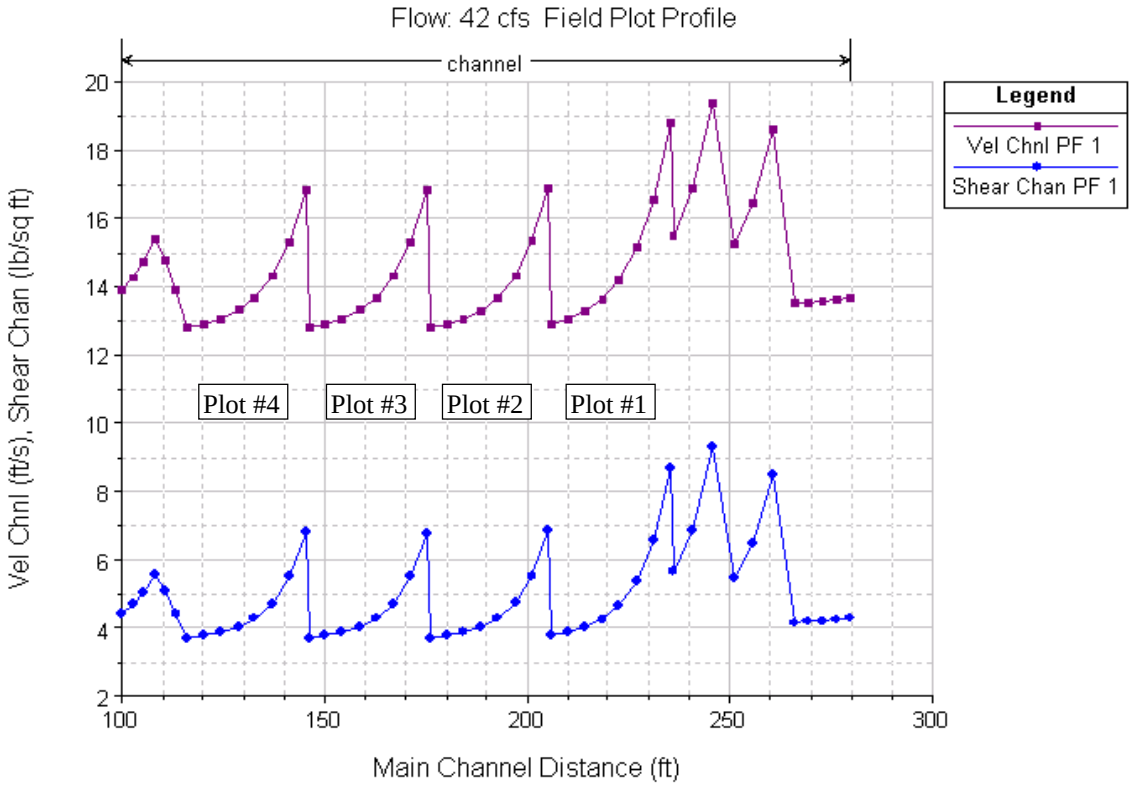


a) Velocity and Shear Stress Profile

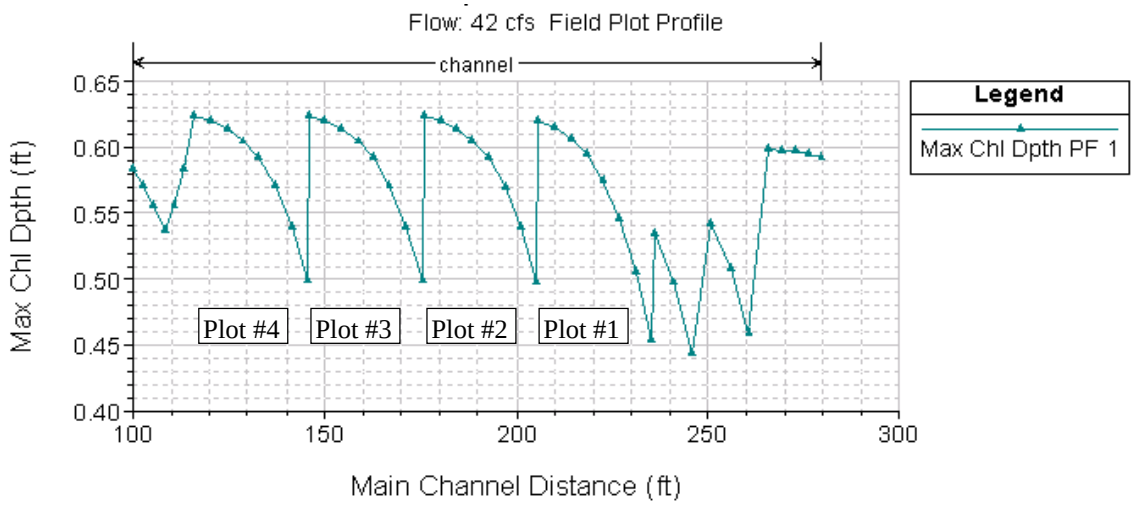


b) Depth of Flow Profile

**Figure 3.13 Velocity, shear stress, and depth of flow profiles.**

# Chapter IV

# RESULTS AND DISCUSSION

## Results of the Laboratory Flume Testing

As mentioned in Chapter III, the laboratory flume testing on the bare soil and RECPs was conducted to accomplish the following three objectives: (1) to estimate the critical shear stresses required to initiate the erosion of soil and/or the resuspension of sediment; (2) to estimate the erosion rates of soils and the rates of resuspension and/or deposition of sediments under varying flow conditions; and (3) to monitor the reduction in erosion due to various RECPs.

Bare Soil Testing. Flume tests using bare soil were performed to estimate the critical shear stress necessary to initiate erosion, to quantify the bare soil erosion rate, and to provide a relative benchmark to compare the performance of the RECP products. The soil was subjected to varying flow conditions from 100 gpm (0.2 cfs) up to 1000 gpm (2.2 cfs). Average velocities ranged from 0.8 to 3.4 feet per second (fps) and the depths of flow ranged from 0.06 to 0.32 feet at these flows. Under these conditions, the bed shear stresses ranged from about 0.05 to 0.29 lbs/square foot (lbs/sf).

Tests below 100 gpm were not performed due to the limitations of the equipment in accurately measuring flow characteristics (e.g., velocity and depth). Testing was halted at 1000 gpm due to the magnitude of erosion. At a flow of 500 gpm, soil had completely scoured to the flume bed at the leading edge of the soil test section.

From the onset of the 100-gpm test, soil particles were observed moving along the bed surface (Figure 4.1a). Over time, the bed scoured at the upstream half of the test section and deposited sediment in the lower half of the test section and below the test section (Figure 4.1b). The deposited sediment formed small sandbars (Figure 4.1c). As the flow was increased in subsequent tests, most of the sediment tended to be transported out of the test section with less being deposited in the test section (Figure 4.1d).

The mass of soil eroded (transported from the test section) was plotted as a function of the bed shear stress which showed a linear relationship, with $R^2 = 0.922$ (Figure 4.2). Extending the trendline to the x-axis (bed shear stress) yields an observed bed shear stress of approximately 0.018 lbs/sf, which may be considered as an estimate of the critical shear stress for this soil. To check the reasonableness of the test results, the theoretical critical bed shear stress was calculated utilizing the modified Shields diagram and associated Equations 2-10 through 2- 13. The theoretical critical bed shear stress was calculated as approximately 0.017 lbs/sf, a difference from the observed critical bed shear stress of only 0.001 lbs/sf.

a)

b)

c)

d)

**Figure 4.1 Bare soil flume testing photographs.**

Pictures a), b) and c) show flume testing at 500 gpm. Picture a) is looking upstream at the soil bed showing slightly turbulent flow. Picture b) is looking downstream from the test bed at the soil deposition during the test. Picture c) shows the soil bed condition and transported sediment after 30 minutes of flow. Picture d) is looking upstream at the increased erosion after a 1000 gpm / 30 minute flow test.

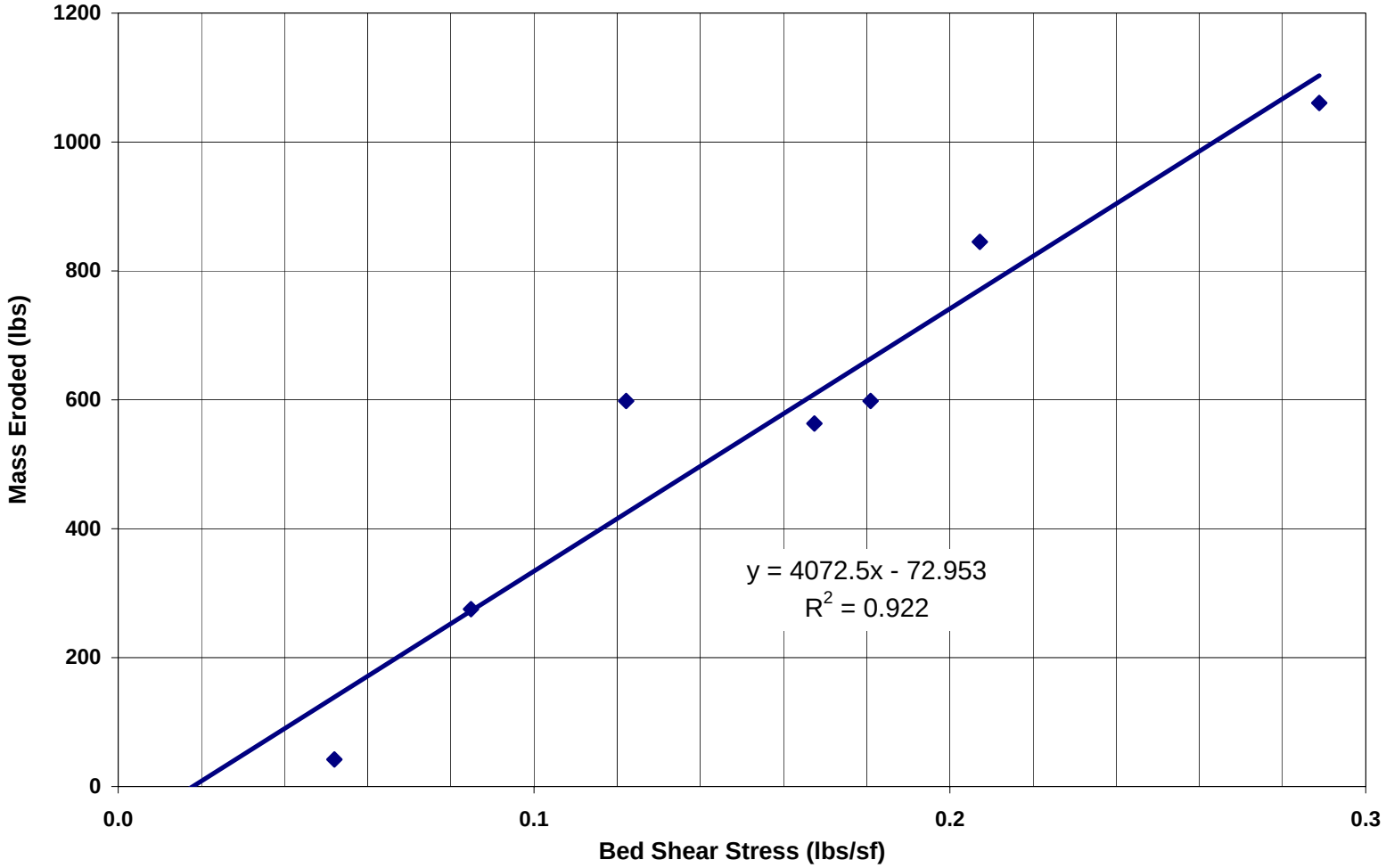


**Figure 4.2 Mass of bare soil eroded.**

RECP Testing. Flume testing of the RECP products was conducted under flow conditions varying from 250 gpm (0.6 cfs) to 4500 gpm (10.0 cfs). Average velocities ranged from 0.9 to 6.0 fps, depths of flow ranged from 0.18 to 0.77 feet, and bed shear stresses ranged from approximately 0.2 to 0.7 lbs/sf at these flows.

As shown in Figure 4.3, ridges typically formed under the blankets. The location of these ridges generally corresponded to the anchoring points at approximately 3 feet on-center. This pattern is consistent with a probable decrease in float across the anchor points (see Figure 2.28). However, in some tests of the stiffer NAG products (SC 250 and P 550), smaller ridges formed at more frequent intervals, which may have been caused by a reduction in the piping effect.

Figure 4.4 shows the mass of soil eroded as a function of bed shear stress for the various RECPs tested. In comparing the product performance, NAG P550 (North American Green) surpassed all other products since the mass of soil eroded was the lowest under all of the flow conditions that were tested. This product is constructed with a stiff corrugated netting which likely reduced the buoyancy effect and helped reduce the piping of water between the bed and liner. This may have contributed to less soil movement under the mat. Other top performers include Pyramat, Landlok 450, and NAG 250.

Landlok C2 and Landlok 435 did not perform as well as the other products in the flume tests. Due to the extensive loss of fibers in the Landlok C2, several holes developed causing excessive localized erosion of the soil bed (Figure 4.5). Tests for these products were halted prior to exceeding 3000 gpm (6.7 cfs).

a) Landlok C2

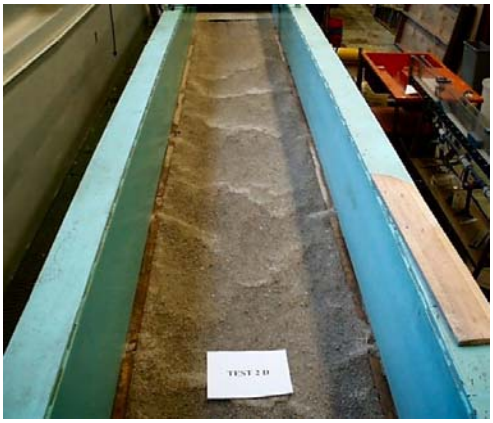

b) Landlok 435

c) Pyramat


d) NAG P550


d) NAG SC250

f) Landlok 450

**Figure 4.3 Typical bedforms under RECPs.**

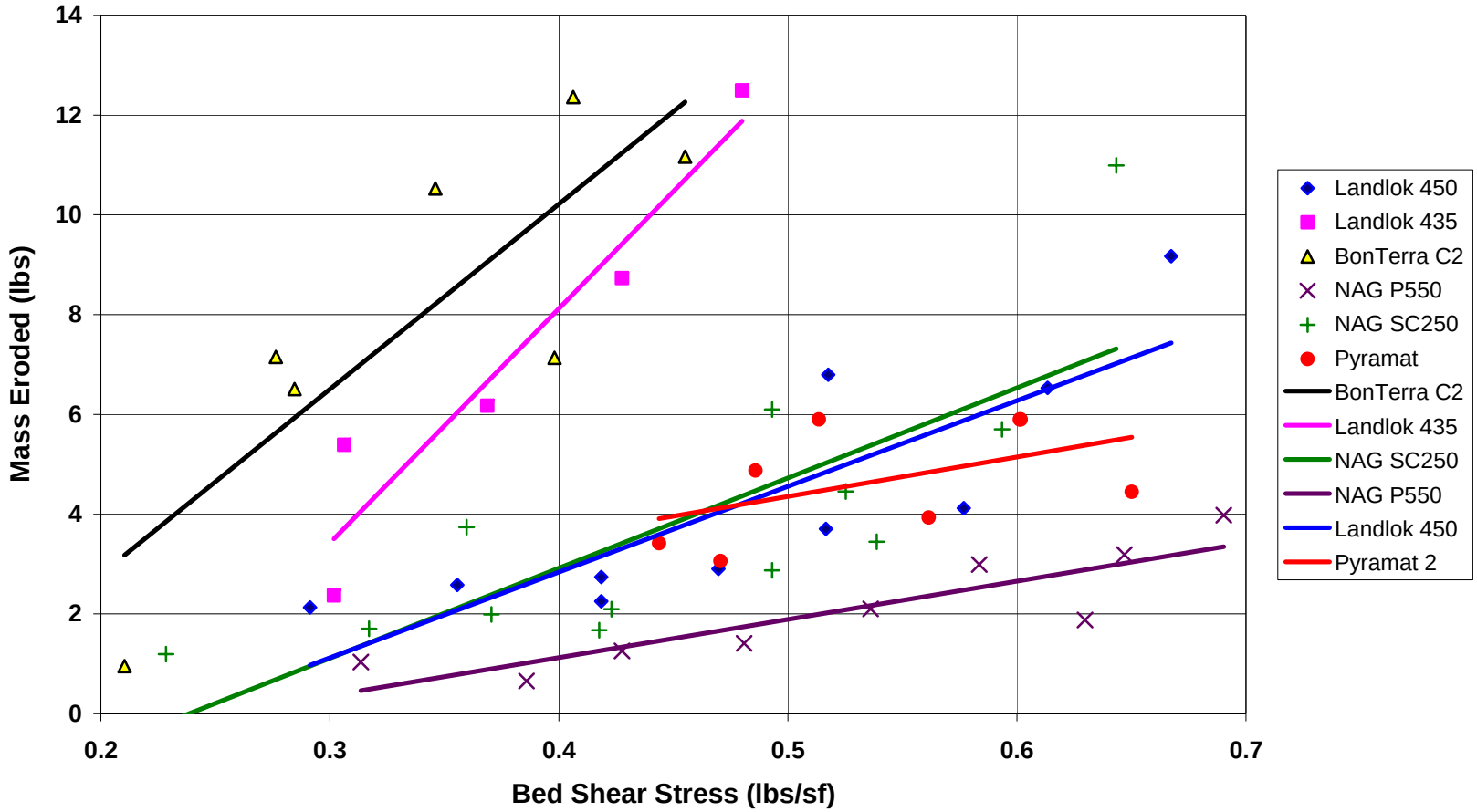


**Figure 4.4 Mass of soil eroded as a function of bed shear stress for various RECPs.**


a)


b)

**Figure 4.5 Examples of product failures.**
Picture a) shows excessive loss of coconut fibers from Landlok C2 after the 1500 gpm flow test. Picture b) shows excess erosion of the soil bed of over 1" for Landlok 435 after the 3000 gpm test.

Figure 4.6 illustrates the difference in magnitude between bare soil conditions and soil protected with RECPs. At a bed shear stress of approximately 0.3 lbs/sf, the order of magnitude difference in the mass of soil eroded is approximately three (bare soil = 1000 lbs. vs. RECP = 5 lbs.). Clearly, all of the RECPs tested offer significant protection against erosion.

The depths of erosion were measured and recorded after each flow test. Figures 4.7a and 4.7b are plots of the maximum depth of erosion for each flow. Figure 4.7a shows the maximum erosion depth that occurred over the entire length of the flume. Typically, the maximum erosion depth was observed within the first and last two feet of the soil test section. At the beginning of the test section, the flow transition from the approach platform to the test section may have caused increased turbulence and shear stress on the soil bed. Likewise, at the end of the test section, the bed frame may have induced increased turbulence on the soil bed.

As shown in Figure 4.7a, most of the products performed similarly with about 1 inch of maximum erosion occurring between 3000 and 4000 gpm. NAG P550 performed somewhat better at the lower flows. Landlok C2 reached a maximum of approximately 2.5 inches at only 2500 gpm. Landlok 435 performed well up to a flow of 3000 gpm.

Figure 4.7b considers the depth of erosion observed within the soil test section, excluding the first foot and the last two feet of length. This may eliminate some of the effects associated with the flow transitions discussed earlier and may be more representative of actual field conditions. Again, NAG P550 performed slightly better than the other products, with the most erosion still being observed with Landlock C2.

The average depths of erosion were plotted as a function of bed shear stress in Figure 4.8. These results indicate that the depths of erosion observed were insignificant when the bed shear stress was below approximately 0.7 lbs/sf.

All of the products tested during this project have also been tested at TTI under much greater shear stresses (i.e., 1 lb/sf to 8 lbs/sf). Figure 4.9 is a graph of results obtained at TTI, which indicates that all of the products meet their minimum shear stress performance standards except for Landlock C2 (above shear stresses of 6 lbs/sf). In these tests, Landlok 450 was the best performer overall. However, Pyramat, NAC P550, NAC SC250, and Landlok 435 performed quite well over the range of shear stresses.

As noted in Chapter III, the fabrics were all anchored with approximately 2 anchors per sy. This anchoring pattern, which was somewhat less than the manufacturer's recommendation (2.5 to 4.0 anchors per sy), likely resulted in increased erosion. Improved results would be anticipated with a closer anchoring pattern. Additionally, due to facility constraints, approach and end anchor trenches could not be constructed, which may have resulted in the increased erosion, which was observed at the beginning and end of the soil test section.

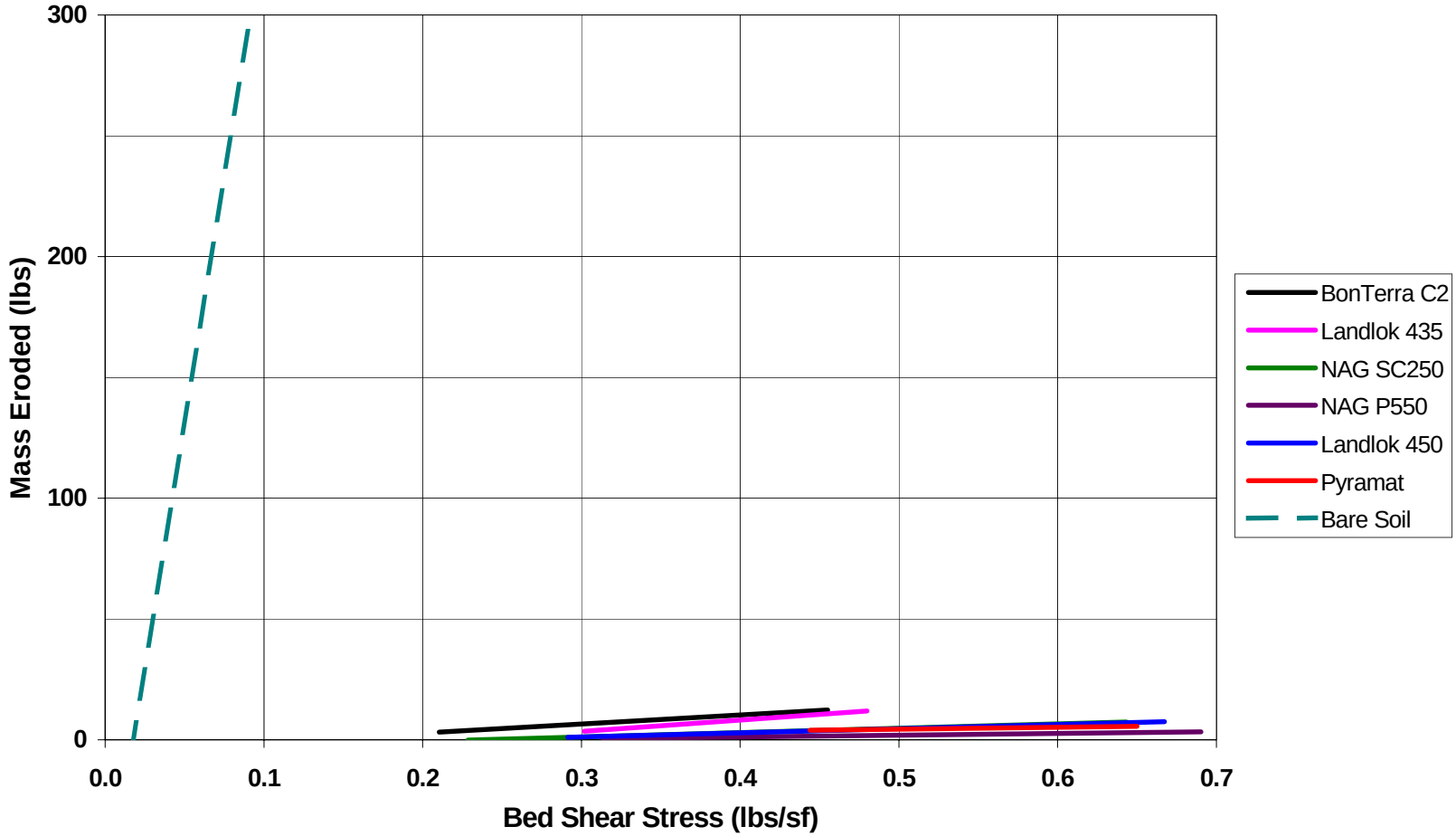


**Figure 4.6 Comparison of erosion observed for unprotected and protected soil test section.**

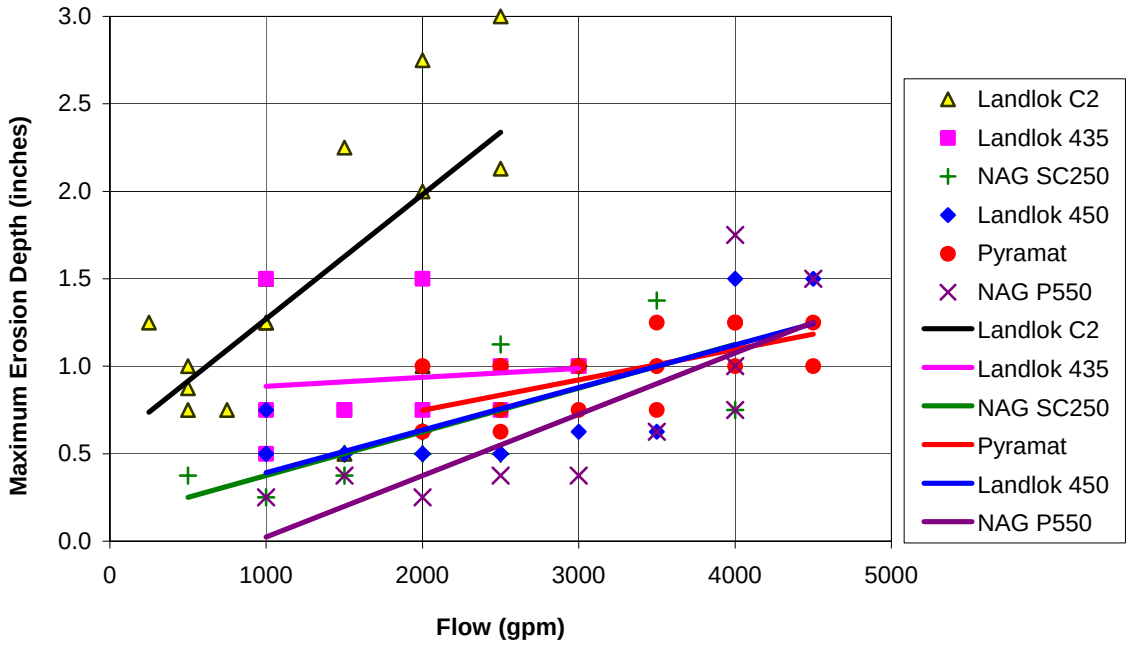


a) Data from entire test section.

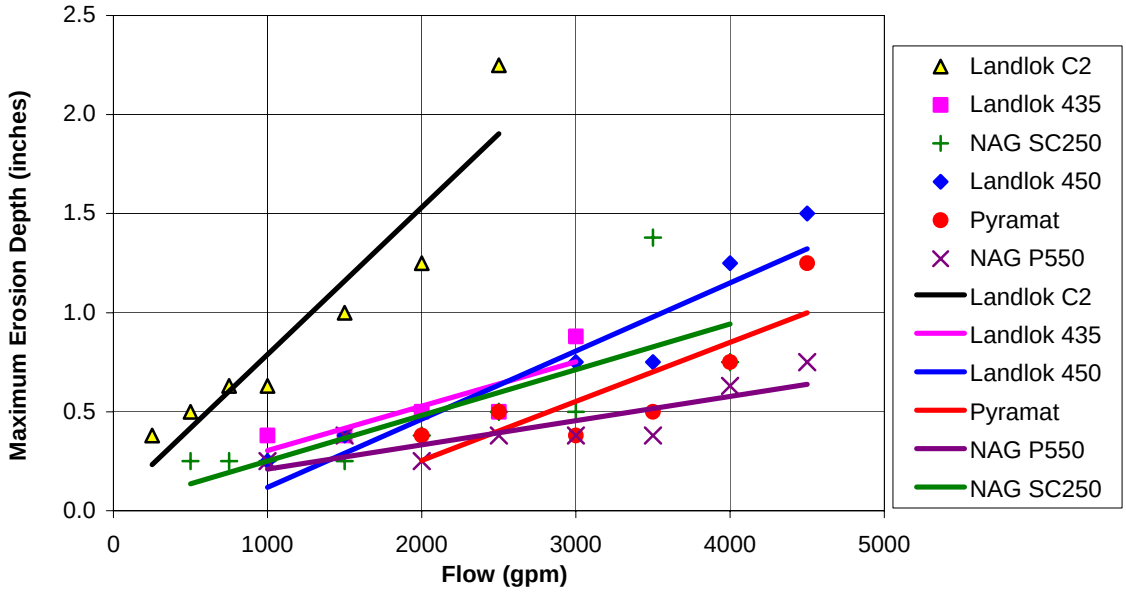


b) Data from middle 16 feet.

**Figure 4.7 Maximum depths of erosion.**

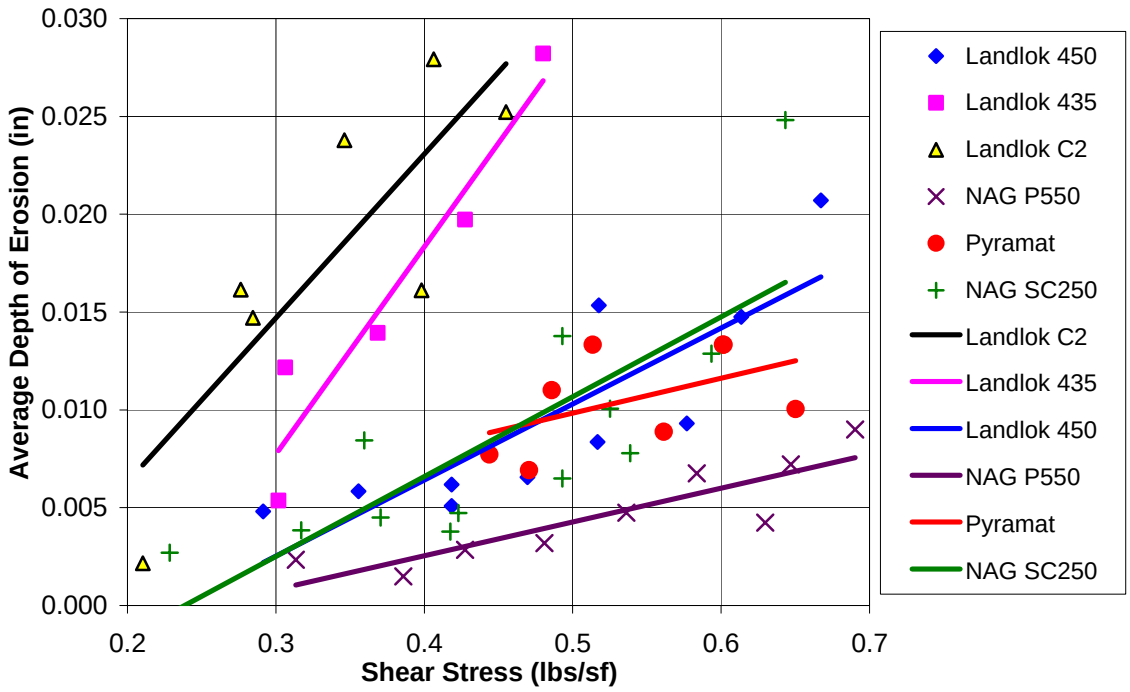


**Figure 4.8 Estimated depth of erosion over entire test section.**

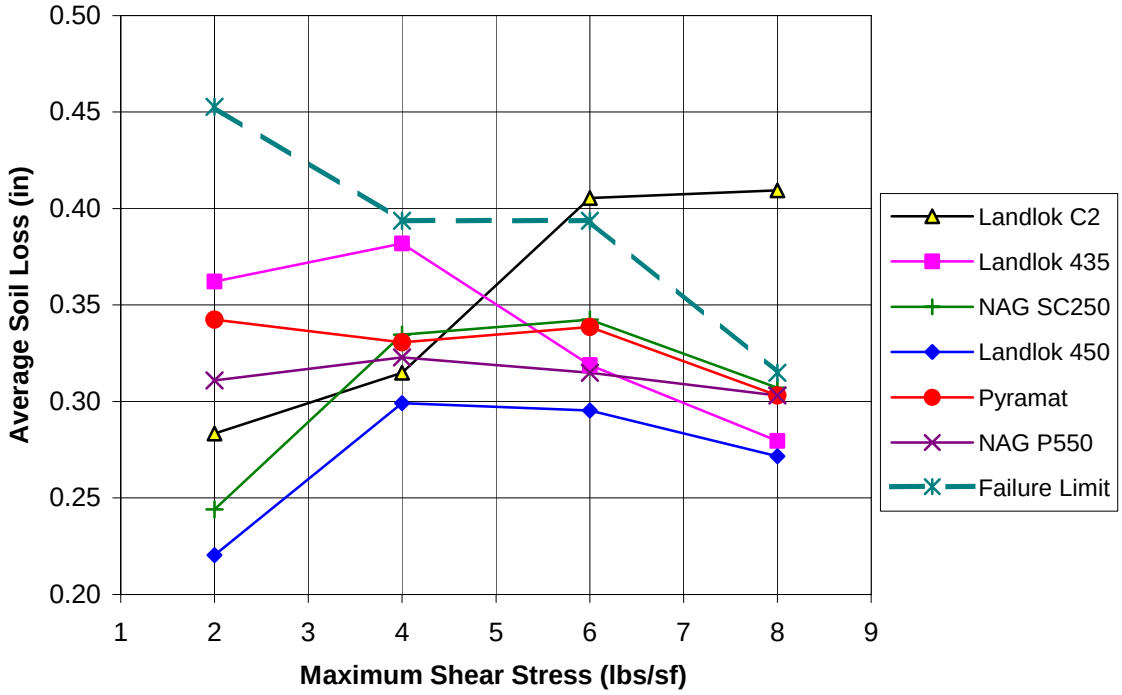


**Figure 4.9 Average depth of erosion (TxDOT/TTI, 2001).**

**Bedrock Testing and Classification**

Several exposed bedrock sites in the Clear Creek watershed were sampled to estimate the degree of granitic rock weathering. The sites chosen were distributed well across the watershed and were typically associated with roadway cut slopes and eroded gullies near culvert outfalls (Figure 2.3).

The classification method developed by Murphy (1985) was utilized in estimating the bedrock weathering grade classification (Table 2.4). The depths of the testing locations varied from 8 feet to 30 feet below the original ground surface elevation. A 3-lb rock hammer was used to test the weathering grade of in-place granite.

The test results revealed that fresh or slightly weathered rock is rare, while completely or highly weathered bedrock is ubiquitous in the watershed. This conclusion is supported by a visual inspection of the rock. At most of the roadway cut slopes along Highway 50, the rock has decomposed forming sediment 'fans' from the rock slope to the edge of the roadway.

**Field Plot Construction**

Figures 4.10 and 4.11 document the conditions at the culvert outlet prior to the site preparation for the field plots. Figure 4.12 shows some of the initial site preparation for the field plots by NDOT maintenance personnel in late summer of 2002. Because of the difficult site conditions, NDOT maintenance personnel also provided assistance with major earthwork for the channel subgrade preparation, which required earthmoving equipment. The majority of the work consisted of repairing the gully headcut that was threatening the stability of U.S. Highway 50 (Figure 3.8). The completed reconstruction of the culvert outlet is shown in Figure 4.13. Figure 4.14 shows the site following a minor storm event in October 2002.

Figure 4.15 shows photographs of the construction of a prototype drop structure by UNR personnel. The drop structures were readily constructed without the use of heavy equipment. The drop structures performed well after a storm event as shown in Figure 4.15d. These drop structures were incorporated into the design of the field plots at the upstream and downstream ends in order to reduce the bed slopes of the channel sections where the RECPs were installed (Figures 3.10 and 3.11).

In late summer of 2003, NDOT maintenance personnel return to the site and did additional grading and channel preparation. Figure 4.16 shows a typical channel section prior to the installation of the RECPs. The same channel section following the installation of the RECP is shown in Figure 4.17. Figures 4.18 and 4.19 shows the completed filed plot sections in October 2003.

**Figure 4.10 Uncontrolled erosion at culvert outlet before channel reconstruction and installation of field plots.**

**Figure 4.11 Original conditions at culvert outlet before channel reconstruction and installation of field plots.**

**Figure 4.12 Earthwork during initial site preparation at culvert outlet (August 2002).**

**Figure 4.13 Reconstructed culvert outlet (September 2002).**

**Figure 4.14  Initial site preparation after storm (October 2002).**

a) Key trench for timbers.

b) Steel rod anchoring of the timbers.

c) Completed timber drop structure.

d) Backfilled by erosion upstream.

**Figure 4.15 Prototype timber drop structure construction (September 2002).**

**Figure 4.16 Typical channel section of field plot before installation of RECP (August 2003).**

**Figure 4.17 Typical channel test section after installation of RECP (September 2003).**

**Figure 4.18  Completed installation of RECPs in upper field plots (October 2003).**

**Figure 4.19 Completed installation of rip rap and North American Green SC250 in lower field plot (October 2003).**

**Performance of the Field Plots**

The field performance of four rolled erosion control products (RECPs) was evaluated. These RECPs included Pyramat and Landlok 450 from SI Geosolutions and P550 and SC250 from North American Green. The performance of the field plots was monitored through routine inspections over the period from October 2003 through June 2005. The field plot site was visited every other month to examine the performance of the various RECPs. A series of photographs over this period of time is included in Figures 4.20 through 4.39. These photographs demonstrate that each of the products performed very well.

Monitoring of the surface profiles within each field plot section indicated that some localized scour of 2 to 3 inches in depth was initially observed at the leading edges of the channel sections immediately downstream from the rip rap. This may have been due to the reorientation of the surface layer of soil below the RECPs after installation. Every effort was made to uniformly compact the soil surface in the channel section prior to installation of the RECPs (Figure 4.16). However, due to the noncohesive characteristics of the soil in the watershed, some movement of the surface layer of the soil upon initial wetting was expected. Additional anchors were placed at the leading edges of each field plot section in order to minimize this scour. Some of the localized scour at the leading edge of each test section may also be attributed to the resuspension and transport of fine grained soils within each section. This fraction of the soil may have washed through the surface of the RECPs and been carried further downstream. It is likely that some of the soil that was resuspended was deposited further downstream within each test section. Some minor deposition of sediment was observed at the lower reaches of each field plot sections.

There is no evidence that any of the channel sections is experiencing severe erosion. Detailed profiles along the channel section were measured to confirm this. The gradual reorientation of soil particles below each of the RECPs and filling of void spaces with fine grained particles gradually increased the stability of the channel bed within each test section. Over time, the deposition and gradual accumulation of soil and sediment transported from the watershed and the roadway surface of Highway 50 is expected to further enhance the stability of the field plot sections.

As can been seen in the photographs of the field plot sections, the gradual emergence of vegetation within each channel section further enhanced channel stability. Figures 4.20 through 4.22 taken in July 2004 show the establishment of some vegetation. Figures 4.24 through 4.26 taken in November 2004 show the gradual increase in the density of the vegetation. Figures 4.31 through 4.37 show the vegetation present in the field plot sections in June 2005. The least amount of vegetation was consistently observed in the field plot lined with North American Green SC250 (Figures 4.23, 4.27, 4.38, and 4.39). This may be due to the accumulation of fine sediment at the channel surface as well as the fact that the lower field plot section received the least amount sunshine throughout the year.

**Figure 4.20 Field plot with North American Green P550 looking upstream (July 2004).**

**Figure 4.21 Field plot with SI Geosolutions Pyramat looking upstream (July 2004).**

**Figure 4.22 Field plot with SI Geosolutions Landlok 450 looking upstream (July 2004).**

**Figure 4.23 Field plot with North American Green SC250 looking downstream (July 2004).**

**Figure 4.24 Field plot with North American Green P550 looking upstream (November 2004).**

**Figure 4.25 Field plot with SI Geosolutions Pyramat looking upstream (November 2004).**

**Figure 4.26 Field plot with SI Geosolutions Landlok 450 looking upstream (November 2004).**

**Figure 4.27 Field plot with North American Green SC250 looking downstream (November 2004).**

**Figure 4.28  Culvert outlet (June 2005).**

**Figure 4.29 Channel section downstream from culvert outlet (June 2005).**

**Figure 4.30 Rip rap section upstream from field plots (June 2005).**

**Figure 4.31 Channel section with field plots looking downstream (June 2005).**

**Figure 4.32 Field plot lined with North American Green P550 looking upstream (June 2005).**

**Figure 4.33 Side view of field plot lined with North American Green P550 (June 2005).**

**Figure 4.34 Field plot lined with SI Geosolutions Pyramat looking upstream (June 2005).**

**Figure 4.35 Side view of field plot lined with SI Geosolutions Pyramat (June 2005).**

**Figure 4.36 Field plot lined with SI Geosolutions Landlok 450 looking upstream (June 2005).**

**Figure 4.37 Side view of field plot lined with SI Geosolutions Landlok 450 (June 2005).**

**Figure 4.38 Field plot lined with North American Green SC250 looking upstream (June 2005).**

**Figure 4.39 Field plot lined with North American Green SC250 looking downstream (June 2005).**

# Chapter V

## CONCLUSIONS AND RECOMMENDATIONS

The physical characteristics of the upper Clear Creek watershed consisting primarily of steep slopes, thin soil sections, and highly weathered bedrock allow for erosion to proceed almost unchecked. The erosion has manifested itself in the form of deep gullies and rilled slopes in many locations. In the gullies, most of the erosion appears to be from bedrock scouring because of the thin soil layer. Decomposed granite transported downstream of the gullies is also evidence that active rock scouring is occurring. Some of this decomposed granite may also be sourced back to the rilling of the roadway cut and fill slopes. Despite the clear evidence of active erosion, the water quality in Clear Creek appears to be very good for a mountain stream. This is an indication that a large portion of the sediment is relatively coarse (e.g., decomposed granite) and is not being transported long distances before it settles out of the water column.

The flume testing procedure used in this study presented a unique way of evaluating RECP products. In contrast with testing protocol in other previous studies, the testing procedure in this study evaluated the erosion for each subsequent incremental flow on a reconditioned soil bed. In the previous studies by others (e.g., ASTM, 2000; Chirbas and Urroz, 1999; and TxDOT/TTI, 2001), the soil was not re-leveled and reconditioned between subsequent flow tests.

The application of RECPs as channel liners was found to be an effective strategy to minimize erosion in both laboratory flume studies and field plot studies. RECPs will offer an economical solution to substantially reduce the erosion in both slope and channel applications in the Clear Creek watershed. The results of laboratory flume studies demonstrated that five RECP products (i.e., Landlok 435, Landlok 450, NAG SC250, NAG P550, and Pyramat) were very effective in reducing the erosion over bare soil by a magnitude of approximately three. Overall, NAG P550 performed slightly better than the other products. This was probably due to its stiffer corrugated construction, which apparently reduced the effects of water “piping” between the soil and the liner.

In performance testing by TTI, where the shear stresses ranged from 1 lb/sf to 8 lbs/sf, the same five products performed well in channel protection applications. However, under these higher stresses and under a different testing procedure, Landlok 450 performed slightly better than the other products.

Any of the five RECP products that were tested in the flume studies (i.e., Landlok 435, Landlok 450, NAG SC250, NAG P550, and Pyramat), or their equal, should perform well in channel applications within their published shear stress and velocity limitations. Each of these products, except NAG SC250, are fully UV resistant and are considered permanent linings. NAG SC250 has a degradable straw/coconut matrix and should primarily be used in locations where revegetation efforts will be successful.

Landlok C2, a degradable ECB composed of coconut fiber, should be considered for slope protection and low flow swales where revegetation efforts will be successful.

To more fully evaluate the effectiveness of the RECPs tested in the laboratory, field plots were constructed and the conditions of the field plot sections were routinely monitored over the period from October 2003 to June 2005. Even though the RECPs were installed in channel sections with bed slopes that were slightly higher than those recommended by the product manufacturers, each of the products performed well. Each of the RECPs that was tested effectively minimized channel erosion and dramatically improved channel stability.

There is no evidence that any of the channel sections is experiencing severe erosion. Monitoring of the surface profiles within each field plot section indicated that some localized scour of 2 to 3 inches in depth was initially observed at the leading edges of the channel sections immediately downstream from the rip rap. This may have been due to the reorientation of the surface layer of soil below the RECPs after installation. Additional anchors were placed at the leading edges of each field plot section in order to minimize this scour. Some minor deposition of sediment was observed at the lower reaches of each field plot sections. Over time, the deposition and gradual accumulation of soil and sediment transported from the watershed and the roadway surface of Highway 50 is expected to further enhance the stability of the field plot sections. In addition, the gradual emergence of vegetation within each channel section will further enhance channel stability.

## REFERENCES

Allan, J.R.L (1993) Sedimentary structures: Sorby and the last decade, *J. Geol. Soc.* (London) **150**, 417-425.

Allan, J.R.L. (1994) Fundamental properties of fluids and their relation to sediment transport processes, *Sediment Transport*, Pye, K. (Ed.), Blackwell, 25-60.

Allen, S.R. (1996) Evaluation and standardization of rolled erosion control products, *Geotextiles and Geomembranes*, **14**, 207-221.

Allen, S.R. (2001) *A Technical Guidance Manual: Terminology and Index Testing Procedures for Rolled Erosion Control Products*, Erosion Control Technology Council, St. Paul, MN.

American Society of Civil Engineers (1966) Nomenclature for bed forms in alluvial channels, by the Task Force on Bed Forms in Alluvial Channels, John F. Kennedy, Chmn., *Journal of the Hydraulics Division*, ASCE, Vol 92., No. HY3, Proc. Paper 4823, 51-64.

American Society of Civil Engineers (1975) *Sedimentation Engineering*, Manuals and Reports on Engineering Practice – No. 54, New York, NY, 91-107.

American Society for Testing and Materials (2000a) *Standard Test Method for determination of Erosion Control Blanket (ECB) Performance in Protecting Earthen Channels from Stormwater-induced Erosion*, designation D 6460-99, ASTM Committee D-18 on Soil and Rock, ASTM, West Conshohocken, PA.

American Society for Testing and Materials (2000b) *Standard Practice for Classification of Soils for Engineering Purposed (Unified Soil Classification System)*, D2487-00, ASTM Committee D-18 on Soil and Rock, ASTM, West Conshohocken, PA.

Annandale, G.W., and Parkhill, D.L. (1995) Stream bank erosion: application of the erodibility index method, *International Water Resources Egnineering Conference-Proceedings*, Proceedings of the 1st International Conference on Water Resources, Part 2, **2**, 1570-1574.

Annandale, G.W. (1995) Erodibility, *Journal of Hydraulic Research*, **33**, 471-494.

Annandale, G.W., Smith, S.P., Nairns, R., and Jones, J.S. (1996) Scour power, *Civil Engineering*, **66** (7), 58-60.

Annandale, G.W., Wittler, R.J., Ruff, J.F., and Lewis, T.M. (1998) Prototype validation of erodibility index for scour in fractured rock media, *International Water Resources*

*Engineering Conference-Proceedings*, Proceedings of the 1998 International Water Resources Engineering Conference, Part 2, **2**, 1096-1101.

Arteaga, F.E., and Durbin, T.J. (1978) Development of a relation for steady-state pumping rate for Eagle Valley groundwater basin, Nevada. *USGS Open-File Report 79-261*, 44pp.

Banerjee, S. (1992) Turbulence structures, *Chem. Eng. Sci*. **47**, 1793-1817.

Bateman, P.C. (1974) Model for the origin of Sierran granites. *Calif. Geol*. **7**, 3-7.

Bell, F.G. (1999) Soil erosion and desertification", *Geological Hazards: Their Assessment, Avoidance, and Mitigation*, E and FN Spon, Routledge, New York, 390-451.

Bennett, S.J., Bridge, J.S., and Best, J.L. (1998) Fluid and sediment dynamics of upper-stage plane beds, *J. Geophys. Res*. 103, 1239-1274.d

Best, J.L. (1993) On the interactions between turbulent flow structure, sediment transport and bedform development: some considerations from recent experimental research, *Turbulence: Perspectives on Flow and Sediment Transport*, (Clifford, N.J., Ed.), 61-92.

Best, J.L. (1996) The fluid dynamics of small scale alluvial bedforms, *Advances in Fluvial Dynamics and Stratigraphy*, Carling P.A., Dawson, M. (Eds) Wiley, Chichester, 67-125.

Bhandari, G., Sarkar, S.S., and Rao, G.V. (1998) Erosion Control with Geosynthetics", *Geohorizon: State of the Art in Geosynthetics Technology*, edited by S.S. Sarkar, A.A. Balkema Publishers, Brookfield, Vermont, 151-169.

Boone, R.L. (1983) Groundwater recharge and subsurface flow processes on a hillslope in the Clear Creek Watershed, eastern Sierra Nevada, *Mines Thesis 1772*, University of Nevada, Reno.

British Standards Institute (1981) *Code of Practice for Site Investigation (BS5930)*, London Section 44.

Brunner, G.W. (2001) HEC-RAS, *River Analysis System Hydraulic Reference Manual*, US Army Corps of Engineers, Hydrologic Engineering Center (HEC), Davis, CA.

Burkins, D.L. Blum, J.D., Brown, K., Reynolds, R.C., and Erel, Y. (1999) Chemistry and mineralogy of a granitic, glacial soil chronosequence, Sierra Nevada Mountains, California. *Chemical Geology* **162**, 1-14.

Brooke, J.W., Kontomaris, K., Hanratty, T.J., and Mclaughin, J.B. (1992) Turbulent deposition and trapping of aerosols at a wall, *Phys. Fluids* **A4**, 825-835.

Candland, D.M. (1979) *Soil Survey of Carson City Area, Nevada*, Soil Conservation Service, U.S. Department of Agriculture, 1-7.

Carey, W.C., and Keller, M.D. (1957) Systematic changes in the beds of alluvial rivers, J. of the Hydraulics Div., ASCE, Vol. 83, No. HY4.

Caywood, C.L. (1999) *Determination of Erosion Rates of Cohesive Sediments in the Carson and Truckee Rivers*, Master's Thesis, University of Nevada, Reno.

Chakrabrorty, C., and Bose, P.K. (1992) Ripple/dune to upper-stage bed transitions: some observations from the ancient record, *Geol. J.* 27, 349-359.

Chirbas, K., and Urroz, G. (1999) Performance evaluation of rolled erosion control products, *Land and Water* **43**, 39-42.

Chow, V.E. (1959) *Open-Channel Hydraulics*, McGraw-Hill Book Company, Boston, Massachusetts.

Clopper, P.E., and Byars, M.S. (1998*) A Review and Summary of Methods Used in the Performance Testing of RECPs,* Ovens Ayres & Associates, Fort Collins, CO.

Cook, R.U., and Smalley (1968) Salt weathering in deserts, *Nature*, **220**, 1226-1227.

Cruden, D.M. (1991) A simple definition of a landslide, *Bulletin of the International Association of Engineering Geology* **43**, 27-29.

Dahlgren, R.A., Boettinger, J.L., Huntington, G.L., and Amundson, R.G. (1997) Soil development along an elevational transect in the western Sierra Nevada, California. *Geoderma* **78**, 207-236.

Dai, F.C., Lee, C.F., and Ngai, Y.Y. (2002) Landslide risk assessment and management: an overview, *Engineering Geology* **64**, 65-87.

Dearman, W.R. (1974) Weathering classification in the characterization of rock for engineering purposes in British practice. *Bull. Int. Assoc. Eng. Geol.* **9**, 33-42.

Dearman, W.R., Baynes, F.J., and Irfan, Y. (1978) Engineering grading of weathered granite, *Eng. Geol.* **12**, 345-374.

Dennett, K.E. (1995) *Flume Studies on the Erosion of Cohesive Sediments*, Ph.D. Dissertation, Georgia Institute of Technology, December 1995.

Dennett, K.E., Sturm, T.W., Amirtharajah, A., and Mahmood, T. (1998) Effects of adsorbed natural organic matter on the erosion of kaolinite sediments, *Water Environment Research*, Vol. 70, No. 3, May/June 1998, 268-275.

Dennett, K., Fritchel, P., Siddharthan, R., and Soltani, A. (2002) Evaluation of strategies to control erosion along U.S. Highway 50 between Carson City and Lake Tahoe, *Proceeding of the First International Conference on Scour of Foundations*, Texas A&M University College Station, Texas, 642-655.

Dennison, M.S. (1996) *Storm Water Discharges: Regulatory Compliance and Best Management Practices*, CRC Lewis Publishers, Boca Raton, Florida.

Dey, S. (1999) Sediment threshold, *Applied Mathematical Modeling*, **23**, 399-417.

Diplas, P., and Sutherland, A.J. (1988) Sampling techniques for gravel sized sediments, *Journal of Hydraulic Engineering*, **114**, 484-501.

Egiazaroff, J.V. (1965) Calculation of nonuniform sediment concentrations, *J. Hydr. Div.* ASCE **91**, 225-247.

Environmental Protection Agency (2002) *Current Drinking Water Standards*, EPA 816-F-02-013, Washington, D.C.

Ehlen, J. (2002) Some effects of weathering on joints in granitic rocks, *Catena* **49,** 91-109.

Elliot, W.J., and Ward, A.D. (1995) Soil erosion and control practices, *Environmental Hydrology*, edited by A.D. Ward and W.J. Elliot, CRC Press, Boca Raton, Florida, 177-204.

Feth, J.H., Roberson, C.E., and Polzen, W.L. (1964) *U.S. Geol. Surv. Water Supply Paper 1535-I*, 170.

Fetter, C.W. (2001) *Applied Hydrogeology, Fourth Edition*, Prentice-Hall, Inc., Upper Saddle River, New Jersey, 66-75.

Fiorotto, V., and Rinaldo, A. (1992) Turbulent pressure fluctuations under hydraulic jumps, *Journal of Hydraulic Research*, **30**, 499-520.

Fisher, J.B. (1978) Flume development for a study of bedload and suspended sediment in Clear Creek Drainage, Eastern Sierra Nevada, *Mines Thesis 1246*, University of Nevada, Reno.

Friedman, G.M., and Sanders, J.E. (1978) *Principles of Sedimentology*, John Wiley, NY, NY.

Ffolliott, P.F., Brooks, K.N., Gregersen, H.M., and Lundgren, A.L. (1995) *Dryland Forestry: Planning and Management*, John Wiley and Sons, New York, 344-364.

Garrels, R.M., and MacKenzie, F.T. (1967) Origin of the chemical composition of some springs and lakes. In *Equilibrium Concepts in Natural Water Systems*, Advance Chemical Series (ed. W. Stumm), Vol. 67, 222-242.

Gharabahgi, B., Dickinson, W.T., Rudra, R.P., Snodgrass, W.J., and Krishnappan, B.G. (1999) Performance analysis of reinforced vegetative channel lining systems, *Computers and Structures*, **72**, 149-164.

Goldman, S.J., Jackson, K., and Bursztynsky, T.A. (1986) *Erosion and Sediment Control Handbook*, McGraw-Hill, New York.

Granger, D.E., Riebe, C.S., Kirchner, J.W., and Finkel, R.C. (2001) Modulation of erosion on steep granitic slopes by boulder armoring, as revealed by cosmogenic $^{26}$Al and $^{10}$Be, *Earth and Planetary Science Letters* **186**, 269-281.

Haigh, M.J. (2000) Erosion Control: Principles and Some Technical Options, *Reclaimed Land: Erosion Control, Soils, and Ecology*, edited by M.J. Haigh, A.A. Balkema Publishers, Brookfield, Vermont, 75-110.

Harden, D.R. (1998) *California Geology*, Prentice-Hall, Inc., 157.

Hyndman, D.W. (1972) *Petrology of Igneous and Metamorphic Rocks*. McGraw Hill, New York, 1975.

Highway Research Board (1970) *Tentative Design Procedure for Riprap-lined Channels, Report No. 108*, Washington, D.C.: National Academy of Sciences, National Cooperative Highway Research Program.

Hough, B.K. (1969) *Basic Soils Engineering*, John Wiley and Sons, New York, 12-58.

Iwagaki, Y. (1956) Fundamental study on critical tractive force, *Trans. JSCE* **41**, 1-21.

Jeffries, H. (1929) Transport of sediment by streams, *Proc. Cambridge Philosoph. Society*, Cambridge, U.K. **25**, 72.

Julien, P.Y. (1995) *Erosion and Sedimentation*, Cambridge University Press, New York, NY, 112-133.

Kaftori, D., Hetsroni, G., and Banerjee, S. (1994) Funnel-shaped vortical structures in wall-turbulence, *Phys. Fluids* **6**, 3035-3045.

Kaftori, D., Hetsroni, G., and Banerjee, S. (1995) Particle behavior in turbulent boundary layer: incipient motion, deposition, entrainment, *Phys. Fluids* **7**, 1095-1106.

Kehew, A.E. (2002) *Applied Chemical Hydrogeology*, Prentice-Hall, Inc., Upper Saddle River, New Jersey.

Kirkbride, A. (1993) Observations of the Influence of Bed Roughness on Turbulence Structure in Depth Limited Flows Over Gravel Beds, *Turbulence: Perspectives on Flow and Sediment Transport*, edited by N.J. Clifford, J.R. French, and J. Hardisty, John Wiley and Sons Ltd. Chichester, 185-196.

Kirsten, H.A.D. (1982) A classification system for excavation in natural materials, *The Civil Engineer in South Africa*, **25**, 292-308.

Kirsten, H.A.D. (1988) Case histories of groundmass characterization for excavatability, *Rock Classification Systems for Engineering Purposes*, ASTM, STP 984, L. Kirkaldie, (Ed.), 102-120.

Klaassen, G.J., Ribberink, J.S., and De Ruiter, J.C.C. (1987) On the transport of mixtures in the dune phase, *Euromech 215 Colloquium*, Genova, Italy, 15-19 Sept 1987, also *Delft Hydraulics Publication 394*, Delft, The Netherlands.

Kleinhans, M.G. (2001) The key role of fluvial dunes in transport and deposition of sand-gravel mixtures, a preliminary note, *Sedimentary Geology*, **143**, 7-13.

Krank, K.D. (1980) The effects of weathering on the engineering properties of Sierra Nevada granodiorites, *Mines Thesis 1394*, University of Nevada, Reno, 15-33.

Kurihara, M. (1948) On the critical tractive force, Report No. 3 (Vol 4), *Res. Inst. for Hydr. Eng.*

Lal, R., and Elliot, W. (1994) Erodibility and Erosivity, *Soil Erosion Research Methods*, second edition, edited by R. Lal, Soil and Water Conservation Society and Saint Lucie Press, Delray Beach Florida, 181-208.

Lane, E.W. (1955) Design of stable channels, *Transactions*, ASCE, Vol. 120, Paper No. 2776, 1234-1279.

Lau, Y.L., and Engel, P. (1999) Inception of sediment on steep slopes, *Journal of Hydraulic Engineering*, **125**, No. 5, 544-547.

Lewin, S. (1990) Susceptibility of calcareous stones to salt weathering, *Proceedings of the 1st International Symposium, Conference on Conservation of Monuments in the Mediteranean Basin, Bari*, Bari Grato. Bresica, 59-63.

Ling, C.H. (1995) Criteria for incipient motion of spherical sediment particles, *J. Hydr. Eng.* ASCE **121**, 472-478.

Maidment, D.R. (1993) *Handbook of Hydrology*, McGraw-Hill, Inc., New York, NY, 11.1-11.73.

Mantz, P.A. (1977) Incipient transport of fine grains and flanks by fluids-extended Shields diagram, *J. Hydr. Div.,* ASCE **103**, 601-615.

Mazumder, R. (2000) Turbulence – particle interactions and their implications for sediment transport and bedform mechanics under unidirectional current: some recent developments, *Earth Science Reviews* **50**, 113-124.

McLaughin, J.B. (1989) Aerosol particle deposition in numerically simulated channel flow, *Phys. Fluids* **A1**, 1211.

Middleton, G.V. and Southard, J.B. (1984) *Mechanics of Sediment Movement*, Society of Economic Paleontologists and Mineralogists, 165-239.

Miller, M.C., McCave, I.N., and Lomar, P.D. (1977) Threshold of sediment motion under unidirectional currents, Sedimentology, **24**, 507-528.

Moore, J.C. (1969) *Geology and Mineral Resources of Lyon, Douglas and Ormsby Counties, Nevada*, Bureau of Mines and Geology.

Murphy, W.L. (1985) *Geotechnical Descriptions of Rock and Rock Masses*, US Army Engineer Waterways Experiment Station, Vicksburg, MS GL-85-3.

Mutchler, C.K., Murphree, C.E., and McGregor, K.C. (1994) Laboratory and field plots for erosion research, *Soil Erosion Research Methods*, second edition, edited by R. Lal, Soil and Water Conservation Society and Saint Lucie Press, Delray Beach Florida, 11-37.

Nettleton, W.D., Flach, K.W., and Borst, G. (1968) A toposequence of soils in tonalite grus in the southern California Peninsular Range. *Soil Surv. Invest. Rep. 21*, USDA, Soil Conservation Service, Washington, D.C. 41pp.

Nevada Division of Environmental Protection (2003) Unpublished water quality data from Clear Creek, Nevada.

Ollier, C.D. (1965) *Weathering*. American Elsevier Publishing Company, Inc. New York.

Ollier, C.D. (1984) *Weathering*, Oliver and Boyd, Edinburgh, 2nd Ed., 270 pp.

Oost, A.P., and Baas, J.H. (1994) The developments of small scale bedforms in tidal environments: an empiricalmodel for unsteady flow and its applications, *Sedimentology* 41, 883-904.

Parker, W.R. (1993) Cohesive sediment-scientific background, *Coastal, Estuarial and Harbour Engineers Reference Book*, Ed. Abbott, M.R. and Price, W.A. Chapman Hall, London, 571-576.

Pease, R.C. (1980) Geological map of Carson City Area, map #1Ag, Nevada Bureau of Mines and Geology, University of Nevada, Reno.

PBS&J Consultants (2003) *Clear Creek Erosion Assessment* prepared for the Nevada Department of Transportation.

Rademacher, L.K., Clark, J.F., Hudson, G.B., Erman, D.C., and Erman, N.A. (2001) Chemical evolution of shallow groundwater as recorded by springs, Sagehen basin; Nevada County, California. *Chemical Geology* **179**, 37-51.

Raudkivi, A.J. (1990) *Loose Boundary Hydraulics*, Third Edition, Pergamon Press, Oxford.

Ravisangar, V., Dennett, K.E., Sturm, T.W., and Amirtharajah, A., Effect of sediment pH resuspension of kaolinite sediments, *Journal of Environmental Engineering*, American Society of Civil Engineers, Vol. 127, No. 6, June 2001, 531-538.

Rickson, R.J. (1995) Simulated Vegetation and Geotextiles, *Slope Stabilization and Erosion Control: A Bioengineering Approach*, edited by R.P.C. Morgan and R.J. Rickson, E and FN Spon, London, 95-132.

Roberts, B.C. (1995) *Best Management Practices for Erosion and Sediment Control*, Report No. FHWA-FLP-94-005, Federal Highway Administration, Washington, D.C.

Rubey, W.W. (1933) Settling velocities of gravel, sand, and silt particles, *Am. J. Sci.* **25**, 325-338.

Rubey, W.W. (1938) The forces required to move particles on a stream bed, *Professional Paper 189 E*, United States Geological Survey, Washington, D.C.

Sarker, S., Mazumder, R., and Bose, P.K. (1999) Changing bed form dynamics: some observations from Protoproterozoic Chaibasa Formation, India, *J. Indian Assoc. Sediment* **18** (1), 31-40.

Selby, M.J. (1980) A rock mass strength classification for geomorphic purposes: with tests from Antarctica and New Zealand, Z. *Geomorphol*. **24**, 31-51.

Shields, A. (1936) Application of similarity principles and turbulence research to bed-load movement, *Mitteilunger der Preussischen Versuchsan Stalt fur Wasserbau and Schiffbau* **26**, 5-24.

Simons, D.B., and Richardson, E.V. (1965) A study of variables affecting flow characteristics and sediment transport in alluvial channels, *Proceeding, Agriculture Research Service* **970**, 193-207.

Simons, D.B., and Richardson, E.V. (1966) *Resistance to Flow in Alluvial Channels*, Professional Paper 422-J, US Geological Survey, Washington, D.C.

Simons, D.B., and Senturk, F. (1977) *Sediment Transport Technology*, Water Resources Publications, Fort Collins, CO, Chap. 5.

Small, E.E., Anderson, R.S., Repka, J.L., and Finkel, R. (1997) Erosion rates of alpine bedrock surfaces deduced from in situ $^{10}$Be and $^{26}$Al., *Earth and Planetary Science Letters* **150**, 413-425.

Southard, J.B., and Boguchwal, L.A. (1990) Bed configurations in steady unidirectional water flow: Part 2. synthesis of flume data, *J. Sediment Petrol*. 60, 458-479.

Stauffer, R.E. (1990) Granite weathering and sensitivity of alpine lakes to acid depositioin, *Limonol. Oceanogr*. **35**, 1112-1134.

Stevenson, T. K. (1989) *Clear Creek Erosion – Sedimentation Evaluation, Carson – Walker RC and D*, Soil Conservation Service, U.S. Department of Agriculture, Washington, D.C.

Tison, L.J. (1953) Studies of the critical tractive force for the entrainment of bed materials, *Proc. Minnestota Int. Hydr. Conf.*, International Association for Hydraulics Research, Delft, The Netherlands, 21-35.

TxDOT/TTI (2001) *Flexible Channel Liner Installation and Evaluation Procedures*, Texas Department of Transportation / Texas Transportation Institute Hydraulics and Erosion Control Laboratory, Texas A&M University, Bryan, Texas.

United States Geological Survey (1903), Chemical Analysis of Igneous Rocks. *Professional Paper 99*.

Van Ash, T.W.J., Buma, J., and Van Beck, L.P.H. (1990) A view on some hydrological triggering systems in landslides, *Geomorphology* **30**, 25-32.

Wahrhaftig, C. (1965) Stepped topography of the southern Sierra Nevada, California. *Geol. Soc. Am. Bull*. **76**, 1165-1190.

Warke, P.A. and Smith, B.J. (1998) Effects of direct and indirect heating on the validity of rock weathering simulation studies and durability tests, *Geomorphology*, **22**, 347-357.

White, A.F., Bullen, T.D., Davison, V.V., Schulz, M.S., and Clow, D.W. (1999a) The role of disseminated calcite in chemical weathering of Granitoid rocks. *Geochimica et Cosmochimica Acta* **63**, 1939-1953.

White, A.F., Blum, A.E., Bullen, T.D., Davison, V.V., Schulz, M., and Fitzpatrick, J. (1999b) The effect of temperature on experimental and natural weathering rates of granitoid rocks. *Geochimica et Cosmochimica Acta* **63**, 3277-3291.

White, C.M. (1940) The equilibrium of grains on the bed of a stream, *Proc., Royal Society of London, Series A*, London **174** (958), 322-338.

Wiberg, P.L., and Smith, J.D. (1987) Calculations of the critical shear stress for motion of uniform heterogeneous sediments, *Water Resour. Res.* **23(8)**, 1471-1480.

Williams, (1967) Flume experiments on the transport of coarse sand, *U.S. Geol. Sur. Prof. Paper* 562-B, 31.

Wischmeier, W., and Smith, D. (1965) Universal soil loss equation, *Agriculture Handbook No. 537*, United States Department of Agriculture, Washington, D.C.

Yalin, M.S., and Karahan, E. (1979) Inception of sediment transport, *J. Hydr. Div.* ASCE **105**, HY 11, 1433-1443.

Yang, C.T., and Molinas, A. (1982) Sediment transport and unit stream power function, *Journal of the Hydraulics Division*, ASCE, **108**, 774-793.

Yatsu, E. (1988) *The Nature of Weathering*, Sozosha, Tokyo, 624 pp.


**Kenny C. Guinn, Governor**

Jeff Fontaine, P.E. Director
Prepared by Research Division
Tie He, Research Division Chief
(775) 888-7803
the@dot.state.nv.us
1263 South Stewart Street
Carson City, Nevada 89712